

The role of conventional dendritic cell subsets in T-cell activation in Ebola virus infection

Dissertation

Submitted by

Linda Rita Niemetz

for the attainment of the degree *Doctor rerum naturalium*
from the Faculty of Mathematics, Informatics, and Natural Sciences

Department of Biology

University of Hamburg



Hamburg
2024



The present work was performed under the guidance of Prof. Dr. César Muñoz-Fontela, Dr. Estefania Rodríguez-Burgos, and Dr. Lisa Oestereich at the Bernhard Nocht Institute for Tropical Medicine (BNITM) in Hamburg.

1st Reviewer: **Prof. Dr. Esther Schnettler**
Bernhard Nocht Institute for Tropical Medicine
Research Group Mosquito-Virus Interaction
Bernhard-Nocht-Straße 74, 20359 Hamburg

2nd Reviewer: **Prof. Dr. César Muñoz-Fontela**
Bernhard Nocht Institute for Tropical Medicine
Research Group Virus Immunology
Bernhard-Nocht-Straße 74, 20359 Hamburg

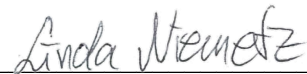
Oral defense: 28.06.2024

Eidesstattliche Versicherung – Declaration on oath

Hiermit erkläre ich an Eides statt, dass ich die vorliegende Dissertationsschrift selbst verfasst und keine anderen als die angegebenen Quellen und Hilfsmittel benutzt habe.

I hereby declare, on oath, that I have written the present dissertation by my own and have not used other than the acknowledged resources and aids.

Hamburg, den 16.05.2024



Acknowledgements

I would like to thank the following people without whom I would not have been able to complete this dissertation. Firstly, I would like to thank all members of the virus immunology, the Lassa virus immunology and the preclinical models research group at the BNITM for all the rewarding discussions, team work and fun.

I owe special thanks to my supervisors, Prof. César Muñoz-Fontela, who guided me through the project with his expertise and supporting mentorship, and taught me to not lose sight of the bigger picture, Dr. Lisa Oestereich, who motivated me to strengthen my skills beyond the everyday lab work and inspired me to question the details, and Dr. Estefania Rodríguez-Burgos, whose encouraging support helped me to focus on the achievements. Special thanks also to Prof. Esther Schnettler and Dr. Wiebke Hartmann for their (co-)supervision.

I would like to especially thank Dr. Beatriz Escudero-Pérez for the BSL4 training and her motivating words throughout the years. I would also like to thank Molly Vickers for sharing the fascination for dendritic cells, great team work and for carrying the project forward. Many thanks to all the PhD students of the 'Landesforschungsförderung LFF-FV74' for the support on the extracellular vesicle topic. Special thanks also to Dr. Katharina Hoehn for the electron microscopy, to the animal facility and to the FACS facility at the BNITM and at the LIV.

Finally, I would like to thank my parents Petra and Andreas. Ich danke euch dafür, dass ihr mir ermöglicht habt einen selbstbestimmten Weg zu gehen und für eure liebevolle Unterstützung über all die Jahre. Jag vill också tacka Elliot, som inte bara är min pojkvän utan även min bästa vän och som har stått mig närmast genom de senaste årens upp- och nedgångar. Tack för din kärlek och det stöd du ger mig.

Table of Contents

Eidesstattliche Versicherung – Declaration on oath.....	I
Acknowledgements.....	II
Table of Contents.....	III
Abbreviations.....	VI
Summary.....	1
Zusammenfassung.....	2
1. Introduction.....	3
1.1. The <i>Orthoebolavirus</i> genus.....	3
1.1.1. Ecology of Ebola virus.....	4
1.2. Clinical manifestation of Ebola virus disease.....	5
1.2.1. Treatment and Vaccines.....	5
1.3. Molecular biology of Ebola virus.....	6
1.4. Ebola virus disease pathogenesis.....	9
1.5. The immune response against Ebola virus – a constant battle.....	9
1.5.1. Innate immunity – the role of dendritic cells and macrophages.....	10
1.5.2. Adaptive immunity against Ebola virus.....	11
1.6. The dendritic cell lineage.....	12
1.6.1. Dendritic cell ontogeny.....	13
1.6.1.1. <i>In vitro</i> differentiation of dendritic cells.....	15
1.6.2. Phenotypical characterization of dendritic cells.....	15
1.6.3. Dendritic cell function.....	18
1.7. Dendritic cell – T-cell interaction.....	19
1.7.1. Antigen sources for antigen-presentation – the role of extracellular vesicles.....	22
1.7.2. Ovalbumin as a model antigen to study DC-T cell interactions.....	24
1.8. Aim of the study.....	25
2. Materials.....	26
2.1. Cell lines.....	26
2.2. Viruses.....	26
2.3. Mouse strains.....	26
2.4. Reagents.....	27
2.5. Consumables.....	28
2.6. Buffers and Media.....	28
2.7. Antibodies.....	29
2.7.1. Antibodies for Flow Cytometry and FACS.....	29
2.7.2. Antibodies for Immunofocus assay.....	30
2.7.3. Antibodies for Western Blot.....	30
2.8. Kits.....	30
2.9. Machines and equipment.....	31
2.10. Software.....	32

3. Methods	33
3.1. Immune cell isolation and differentiation.....	33
3.1.1. <i>In vitro</i> generation of Dendritic cells	33
3.1.1.1. Isolation of bone marrow progenitor cells.....	33
3.1.1.2. Differentiation of Dendritic cells from bone marrow progenitor cells.....	34
3.1.2. CD8 T cells	34
3.1.2.1. CD8 T-cell isolation from mouse spleen	34
3.1.2.2. CellTrace Violet staining of CD8 T cells.....	35
3.2. Dendritic cell-T cell co-cultures	35
3.3. Infections	36
3.3.1. Infection of Dendritic cells (suspension cells).....	36
3.3.2. Infection of Vero E6 (adherent cells)	37
3.3.3. Virus inactivation methods.....	37
3.3.3.1. Inactivation with Paraformaldehyde or Formaldehyde	37
3.3.3.2. Inactivation by UV-irradiation.....	38
3.4. Isolation of cell debris	38
3.5. Isolation of extracellular vesicles (EVs).....	38
3.6. Analytical methods	39
3.6.1. Flow cytometry	39
3.6.2. Antibody labeling.....	40
3.6.3. Fluorescence-activated cell sorting (FACS).....	41
3.6.4. Nanoparticle tracking analysis (NTA)	41
3.6.5. Transmission electron microscopy (TEM).....	42
3.6.6. Immunofocus assay (virus titration)	42
3.6.7. Bead-based cytokine assay (Luminex).....	43
3.6.8. Newcastle disease virus (NDV)-based interferon bioassay	43
3.6.9. BCA protein assay.....	44
3.6.10. SDS-PAGE and Western Blot	44
3.7. Statistics.....	45
4. Results	46
4.1. Deriving murine conventional dendritic cells <i>in vitro</i>	46
4.1.1. Differentiation of murine conventional dendritic cells from bone marrow progenitor cells.....	46
4.1.2. Extended characterization of the mixed dendritic cell culture.....	48
4.2. Infection of dendritic cells with EBOV-OVA.....	50
4.2.1. EBOV cell tropism for different dendritic cell subsets <i>in vitro</i>	50
4.2.2. Activation of dendritic cells upon EBOV infection.....	54
4.3. An <i>in vitro</i> DC-T cell co-culture model to study T-cell activation.....	57
4.4. T-cell activation by EBOV-OVA-infected dendritic cell cultures	61
4.5. The role of cross-presentation in T-cell activation during EBOV infection	62

4.5.1. Isolation of cell debris and extracellular vesicles (EVs) from EBOV-OVA-infected epithelial cells.....	63
4.5.2. Dendritic cell maturation by stimulation with cell debris or EVs.....	67
4.5.3. Cross-presentation of antigens from cell debris or EVs.....	68
4.5.4. Cross-presentation of cell debris by cDC1 and cDC2	70
4.5.5. Effect of EBOV-infection on cross-presentation capacity of dendritic cells .	72
4.6. Contribution of cDC1 and cDC2 to T-cell activation	73
5. Discussion.....	77
5.1. A summary of the findings	77
5.2. The mixed dendritic cell culture – a good representation of <i>in vivo</i> dendritic cell subsets?	77
5.3. The recombinant EBOV-OVA – a key to a bigger toolbox	80
5.4. The difficulty of validating and comparing T-cell proliferation	80
5.5. Dendritic cell functionality in EBOV infections – not so impaired after all	81
5.5.1. EBOV-infection of dendritic cells – not every subset is susceptible	82
5.5.2. Conventional dendritic cells are activated upon EBOV infection and activate CD8 T cells.....	82
5.6. The role of cross-presentation in EBOV infections.....	84
5.6.1. Extracellular vesicles in cross-presentation – high potential with limitations	84
5.7. Direct presentation vs. cross-presentation – who is doing the job?.....	85
5.8. Conclusions about the role of conventional dendritic cells in EBOV infections	87
5.9. Outlook	88
References	89
List of Figures	103
List of Tables	104
List of Supplementary Data	105
Appendix	106
Publication	110

Abbreviations

ALR	absent in melanoma-2 (AIM2)-like receptors
APC	antigen presenting cell
BDBV	Bundibugyo virus (<i>Orthoebolavirus bundibugyoense</i>)
BOMV	Bombali virus (<i>Orthoebolavirus bombaliense</i>)
BSL	biosafety level
CD	cluster of differentiation
cDC	conventional dendritic cell
cDC1	conventional dendritic cell subtype 1
cDC2	conventional dendritic cell subtype 2
CDP	common lymphocyte progenitor
CFR	case fatality rate
CLR	C-type lectin receptors
cMoP	common monocyte progenitor
CMP	common myeloid progenitor
CTLA4	cytotoxic T-lymphocyte associated protein 4
DAMP	damage associated molecular pattern
DAMP	damage associated molecular pattern
DC	dendritic cell
dpi	day(s) post infection
DRC	Democratic Republic of the Congo
dsRNA	double-stranded RNA
EBOV	Ebola virus (<i>Orthoebolavirus zairense</i>)
EMA	European Medicines Agency
ESAM	endothelial cell adhesion molecule
EV	extracellular vesicle
EVD	Ebola virus disease
FACS	Fluorescence-activated cell sorting
FCM	Flow Cytometry
FDA	U.S. Food and Drug Administration
FFU	focus forming unit
Flt3L	fms-like tyrosine kinase 3 ligand
FSC	forward scatter
GM-CSF	granulocyte-macrophage colony-stimulating factor
GMDP	granulocyte-monocyte-dendritic cell progenitors
GP	glycoprotein

HIS	human immune system
IFN-I	type I interferon
IFNAR -/-	interferon receptor knock-out
IL	interleukin
LCMV	lymphocytic choriomeningitis virus
LPS	lipopolysaccharides
mAB	monoclonal antibody
MACS	magnetic-activated cell sorting
MARV	Marburg virus
MHC	Major histocompatibility complex
moDC	monocyte-derived dendritic cell
MOI	multiplicity of infection
MVA	modified Vaccinia virus Ankara
NHP	non-human primate
NK	natural killer (cell)
NLR	nucleotide oligomerization domain (NOD)-like receptors
NPC1	Niemann-Pick C1
OVA	ovalbumin
PAMP	pathogen associated molecular pattern
PAMP	pathogen associated molecular pattern
PBS	phosphate buffered saline
PD-1	programmed cell death-1
pDC	plasmacytoid dendritic cell
PRR	pattern recognition receptor
PRR	pattern recognition receptor
RBC	red blood cell
RESTV	Reston virus (<i>Orthoebolavirus restonense</i>)
RLR	retinoic acid-inducible gene-I (RIG-I)-like receptors
RNA	ribonucleic acid
RSV	respiratory syncytial virus
SDS-PAGE	sodium dodecyl sulfate polyacrylamide gel electrophoresis
SSC	side scatter
SUDV	Sudan virus (<i>Orthoebolavirus sudanense</i>)
SV	Sendai virus
SVD	Sudan virus disease
TAFV	Tai Forest virus (<i>Orthoebolavirus taiense</i>)
TCR	T-cell receptor

Tfh	T follicular helper (cell)
Th	T helper (cell)
TIM-1	T-cell immunoglobulin mucin domain-1
TLR	toll-like receptor
TLR	toll-like receptor
TNF	tumor necrosis factor
UV	ultraviolet
VSV	vesicular stomatitis virus
wt	wildtype

Summary

Severe Ebola virus disease (EVD) is characterized by high levels of inflammation, virus dissemination and excessive, dysregulated T-cell activation. As important initiators of T-cell immunity, dendritic cells (DCs) came into the focus of EVD research. In contrast to the immune activation observed in EVD patients, it has been described that *in vitro* Ebola virus (EBOV) infection of monocyte-derived DCs (moDCs) inhibits DC maturation resulting in suppression of T-cell activation. However, DCs are highly heterogenous and it is unknown how other DC subsets, namely conventional DCs (cDCs) and plasmacytoid DCs (pDCs), respond to EBOV infection. In fact, it was recently found that not all DC subsets in mice are equally infected by EBOV, suggesting that not all DC subsets are functionally impaired by EBOV infection.

To better understand how DCs initiate T-cell activation during EBOV infection, we assessed the response of FMS-like tyrosine kinase 3 (Flt3)-dependent, mouse cDCs and pDCs to EBOV infection and developed a novel DC-T cell co-culture system utilizing a recombinant EBOV expressing the model antigen ovalbumin.

Our findings suggest that in contrast to moDCs, cDCs were poorly infected with EBOV, but displayed high levels of activation. DCs were able to activate EBOV-specific CD8 T cells via cross-presentation of EBOV antigens obtained from cell debris of EBOV-infected cells. Additionally, the cross-presentation capacity of DCs was further enhanced by infection. Finally, we showed evidence that cross-presentation is the main driver of T-cell proliferation observed in EBOV infections.

Our data indicate that EBOV infection of Flt3-dependent cDCs results in their activation rather than inhibition leading to high levels of CD8 T-cell activation. With that, we propose a mechanistic explanation for the excess T-cell activation observed in severe human EVD.

Zusammenfassung

Das schwere Ebolafieber (engl. Ebola virus disease, kurz: EVD) ist gekennzeichnet durch starke Inflammation, die Ausbreitung des Ebolavirus (EBOV) im gesamten Körper und eine überschießende, dysregulierte T-Zell-Aktivierung. Als wichtige Initiatoren der T-Zell-Immunität rückten dendritische Zellen (DCs) in den Fokus der EVD-Forschung. Im Gegensatz zu der bei EVD-Patienten beobachteten Immunaktivierung haben Zellkulturstudien gezeigt, dass die *in-vitro*-Infektion von aus Monozyten gewonnenen DCs (moDCs) mit EBOV die DC-Aktivierung hemmt, was zu einer Unterdrückung der T-Zell-Aktivierung führt. DCs sind jedoch sehr heterogen und es ist unbekannt, wie andere DC-Untergruppen abseits von moDCs, nämlich konventionelle DCs (cDCs) und plasmazytoide DCs (pDCs), auf eine EBOV-Infektion reagieren. Tatsächlich wurde festgestellt, dass nicht alle DC-Subtypen in Mäusen gleichermaßen von EBOV infiziert werden, was darauf hindeutet, dass möglicherweise nicht alle DC-Subtypen durch eine EBOV-Infektion funktionell beeinträchtigt werden.

Um besser zu verstehen, wie DCs die T-Zellen während einer EBOV-Infektion aktivieren, haben wir untersucht wie FMS-ähnlichen Tyrosinkinase 3 (Flt3) -abhängige, murine cDCs und pDCs auf eine EBOV-Infektion reagieren. Dafür haben wir ein DC-T Zell Co-Kultursystem entwickelt, das ein rekombinantes EBOV verwendet, welches das Modellantigen Ovalbumin exprimiert.

Unsere Ergebnisse deuteten darauf hin, dass cDCs im Gegensatz zu moDCs kaum mit EBOV infiziert, aber im Falle einer Infektion stark aktiviert waren. DCs waren in der Lage, EBOV-spezifische CD8 T-Zellen über die Kreuzpräsentation von EBOV-Antigenen zu aktivieren, die aus Zelltrümmern von EBOV-infizierten Zellen gewonnen wurden. Darüber hinaus wurde diese Fähigkeit zur Kreuzpräsentation durch eine EBOV-Infektion der DCs weiter gesteigert. Schließlich gaben unsere Daten Hinweise darauf, dass die T-Zell-Proliferation in EBOV-Infektionen hauptsächlich auf die Kreuzpräsentation zurückzuführen ist.

Damit deuten unsere Daten darauf hin, dass eine EBOV-Infektion von Flt3-abhängigen cDCs eher zu einer Aktivierung als zu einer Hemmung führt, was wiederum ein hohes Maß an CD8 T-Zellaktivierung zur Folge hat. Hiermit schlagen wir eine mechanistische Erklärung für die überschießende T-Zell-Aktivierung vor, die bei schwerem Ebolafieber beobachtet wird.

1. Introduction

1.1. The *Orthoebolavirus* genus

Orthoebolaviruses belong to the *Filoviridae* family together with seven other genera, namely *Cuevavirus*, *Dianlovirus*, *Oblavirus*, *Orthomarburgvirus*, *Striavirus*, *Tapjovirus* and *Thamnovirus*. The genus *Orthoebolavirus* comprises 6 virus species, which are listed in Table 1.^{1,2}

Table 1 Species of the *Orthoebolavirus* genus

Species	Virus name	Abbreviation
<i>Orthoebolavirus bombaliense</i>	Bombali virus	BOMV
<i>Orthoebolavirus bundibugyoense</i>	Bundibugyo virus	BDBV
<i>Orthoebolavirus restonense</i>	Reston virus	RESTV
<i>Orthoebolavirus sudanense</i>	Sudan virus	SUDV
<i>Orthoebolavirus taiense</i>	Taï Forest virus	TAFV
<i>Orthoebolavirus zairense</i>	Ebola virus	EBOV

Orthoebolaviruses can cause viral haemorrhagic fever. The first outbreaks of Ebola virus disease (EVD) caused by infection with Ebola virus (EBOV) and Sudan virus disease (SVD) caused by Sudan virus (SUDV), occurred simultaneously in 1976 in the Democratic Republic of the Congo (DRC, formerly Zaire) and South Sudan (formerly Sudan), respectively.^{3,4} Since then, infections with Orthoebolaviruses have caused multiple sporadic outbreaks in Central and Western Africa with high case-fatality rates (CFR). Most of them were attributed to infections with EBOV (Figure 1). The largest EVD outbreak occurred between 2014 and 2016 in West Africa, with approximately 28,600 reported cases and 11,300 deaths.⁵ High CFR have also been reported for outbreaks caused by SUDV.⁵ Bundibugyo virus (BUDV) and Taï Forest virus (TAFV) are also pathogenic for humans. To date, BUDV has caused only two outbreaks, the first one in 2007 in Uganda⁶ and another in the DRC in 2012.⁷ Only a single case has been recorded for Taï Forest virus infection in Cote d'Ivoire, which led to severe but non-fatal disease.⁸ Less is known about the putative pathogenicity of Reston virus (RESTV) and Bombali virus (BOMV). RESTV appears to infect humans only asymptotically⁹ while BOMV currently has only been detected in bats.^{10,11}

Due to its high pathogenicity and frequency of causing outbreaks, the present study focuses exclusively on EBOV.

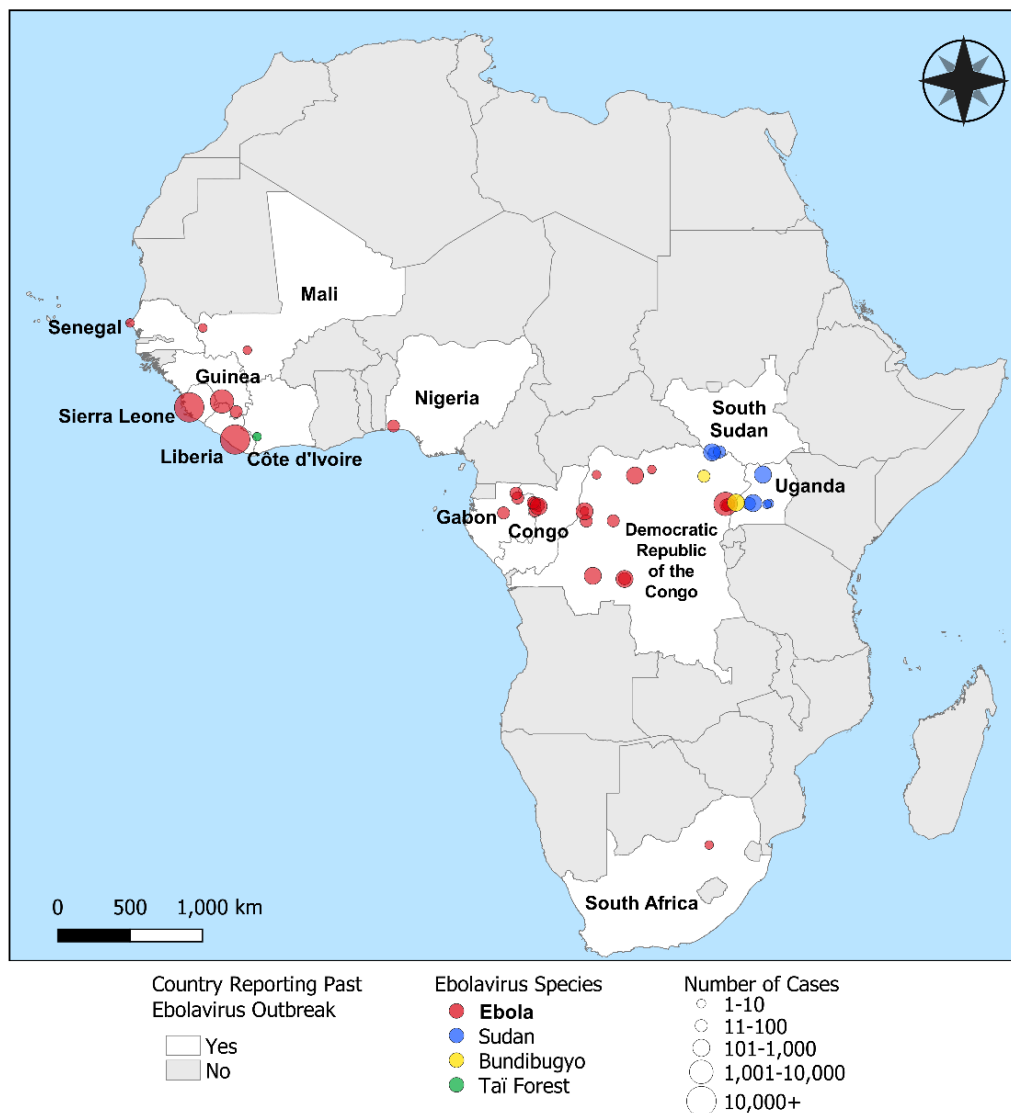


Figure 1 Outbreaks caused by viruses within the *Orthoebolavirus* genus since 1976. Orthoebolaviruses cause sporadic outbreaks in central and western Africa. Different colors represent different species: Ebola virus (red), Sudan virus (blue), Bundibugyo virus (yellow), Taï Forest virus (green). The size of the dot reflects the approximate number of cases. adapted from CDC¹²

1.1.1. Ecology of Ebola virus

The natural reservoir of EBOV has not yet been identified, but several pieces of evidence point to bats as primary hosts. EBOV-specific antibodies and EBOV-RNA have been detected in several bat species such as *Hypsignathus monstrosus*, *Epomops franqueti* and *Myonycteris torquata*.¹³ Additionally, experimental EBOV infections of certain bat species such as Angolan free-tailed bats (*Mops condylurus*), resulted in virus replication, viral shedding in urine and feces and vertical virus transmission to offspring.^{14,15} In fact, an EVD outbreak in 2007 was

suspected to be linked to direct contact of human with potentially infected bats.¹⁶ However, to date no infectious EBOV or a complete EBOV-genome has been isolated from bats. In contrast, studies in 2016 isolated a complete genome of BOMV, a new *Orthoebolavirus* at that time, from bats in Sierra Leone¹⁰ (also 2019 in Kenya¹¹). Furthermore, the Egyptian Rousette (*Rousettus aegyptiacus*) bat has been identified as a natural reservoir of Marburg virus (MARV), a filovirus closely related to EBOV.¹⁷

EBOV also infects non-human primates such as great apes and presumably other animals, including forest antelopes and pigs. Great apes, like human, develop severe disease.^{18,19} Transmission to humans occurs via direct contact with infected animals during hunting or handling of animal carcasses. However, recent studies suggested that EBOV can also persist in EVD survivors, which is a concerning potential source for future outbreaks. EBOV RNA was detected in semen, vaginal fluids, breast milk and urine of survivors of the 2014-2016 West African EVD outbreak and the 2021 SDV outbreak long after recovery.²⁰ In fact, the EBOV outbreak in Guinea in 2021 was suggested to originate from such a persistent infection source.²¹ In an outbreak setting, human to human transmission via contact with infectious body fluids is the main transmission route.

1.2. Clinical manifestation of Ebola virus disease

EBOV enters the human body via skin or mucosal surfaces. After an incubation time of about 1 to 3 weeks, first non-specific febrile symptoms, such as anorexia, arthralgia, headache, malaise, myalgia, and rash occur. In a matter of days, the disease progresses with often persistent fever and severe gastrointestinal symptoms, including nausea, vomiting, and diarrhea, which result in severe dehydration and electrolyte disbalance. About 7-12 days after disease onset, patients present with tissue hypoperfusion and coagulopathy, which lead to multiple organ dysfunction including acute kidney and hepatic injury. Some patients also develop central nervous system manifestations and encephalopathy. Despite the fact that EVD is considered a viral haemorrhagic fever, hemorrhages are only observed in about 40 % of the patients. EVD is fatal in 40 – 90 % of the cases, and the outcome highly depends on the time passed between disease onset and start of treatment. Survival is often connected to long recovery times and severe sequelae that are summarized as post-EVD syndrome. Those symptoms include arthralgia, myalgia, neurological symptoms and abdominal pain.^{22,23}

1.2.1. Treatment and Vaccines

For a long time, patients depended solely on supportive care such as the administration of fluids and electrolytes, and medication to reduce vomiting, diarrhea, coagulation, fever and pain.

Efforts were put on the development of therapeutics to further improve the treatment of patients. The first experimental drug ZMapp, a combination of three monoclonal antibodies (mAB), was tested during the EVD outbreak in West Africa in 2015. The ZMapp treatment improved EVD survival but it did not reach the prespecified threshold for efficacy.²⁴ In another trial that was performed during the EVD outbreak in the DRC in 2018, two new experimental treatment regimens were tested with Inmazeb™ – a combination of three monoclonal antibodies (mAB), and Ebanga™, a single mAB. Both drugs improved survival significantly over ZMapp²⁵ and were approved by the U.S. Food and Drug Administration (FDA) in 2020.²⁶ However, 34 % of all EVD patients and 67 % of patients with high viral loads died despite receiving one of the tested drugs²⁵, demonstrating that the necessity for development of new treatment strategies persists.

The first EBOV-vaccine ERVEBO®, also called rVSV-ZEBOV or V920, was approved by the FDA and the European Medicines Agency (EMA) in 2019 and has shown very high efficacy to reduce mortality when applied in outbreak settings. It is a replication-competent, live, attenuated recombinant vesicular stomatitis virus (rVSV) vaccine, encoding the EBOV glycoprotein (GP). An additional vaccine regimen was used under a research protocol during the EVD outbreak in DRC in 2019 and has been approved by the EMA for use under ‘exceptional circumstances’ in 2020. This vaccine consists of two distinct components – Ad26.ZeBOV (Zabdeno), an adenovirus-based vaccine, and MVA-BN-Filo (Mvabea), a modified Vaccinia Ankara virus (MVA)-based vaccine.²⁷

All of the above-mentioned drugs and vaccines are specific to EBOV and have not been tested clinically for their efficacy against other Orthoebolaviruses or MARV. However, vaccine and treatment development directed against EBOV, other Orthoebolaviruses and MARV are ongoing. Efforts have been particularly directed towards the development of universal Orthoebolavirus vaccines and treatments.^{26–29}

1.3. Molecular biology of Ebola virus

EBOV has an envelope, which the virus acquires from the host membrane during viral budding.³⁰ The virions are filamentous in shape with a length of approximately 980 nm and a diameter of 96-98 nm.³¹ The EBOV genome is a linear, non-segmented, single-strand, negative-sensed RNA of about 18.9 kb. It comprises 7 genes, encoding the nucleoprotein (NP), the glycoprotein in its different forms (GP_{1,2}, sGP and ssGP), the polymerase (L), the viral protein (VP)35, VP24, VP30 and VP40 (Figure 2).

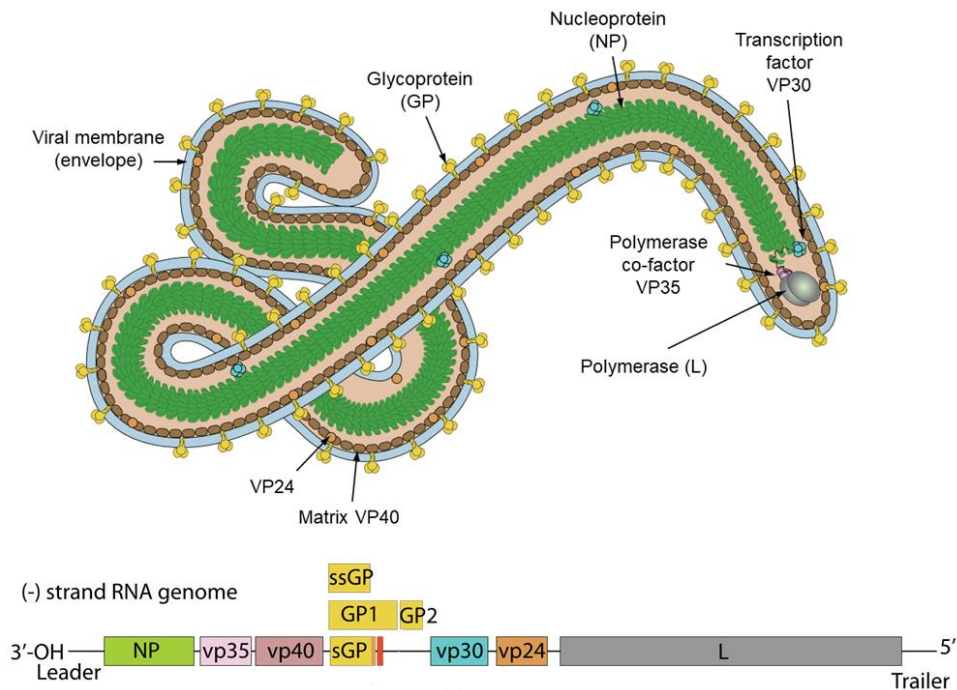


Figure 2 Ebola virus particle and genome organization. (top) The EBOV particle is surrounded by the viral membrane or envelope (light blue). The virion further consists of the glycoprotein (GP, yellow), the nucleoprotein (NP, green), VP30 (turquoise), VP35 (purple), VP40 (brown), VP24 (orange), and the polymerase, encoded by the L-gene (grey). (bottom) Organization of the negative-strand RNA genome. (adapted after ViralZone SIB Swiss Institute of Bioinformatics, 2023)

The GP is located within the viral membrane and is the only viral surface protein. It is composed of the receptor-binding subunit GP₁, and the fusion subunit GP₂.³³ The surface GP is essential for viral entry as it serves as an attachment factor to host cell surface molecules, including C-type lectins such as DC-SIGN and L-SIGN³⁴, and sialoadhesins such as Siglec-1.³⁵ Furthermore, EBOV can bind to T-cell immunoglobulin mucin domain-1 (TIM-1) via phosphatidylserines incorporated in the viral envelope.³⁶ After initial attachment, EBOV is taken up into endosomes mainly via macropinocytosis, but also clathrin-dependent endocytosis.³⁷ In late endosomes, the low pH-dependent cysteine proteases cathepsin B and L change the conformation of the GP. Hereby, new binding sites of the GP₁ subunit are exposed, which subsequently interact with Niemann-Pick C1 (NPC-1). This interaction leads to GP₂-dependent fusion of the viral envelope with the endosomal membrane, releasing the viral ribonucleoprotein complex including the viral RNA, viral polymerase L, NP, and polymerase co-factors into the cytosol.³⁸ The L protein is an RNA-dependent RNA-polymerase, a multifunctional protein required for transcription and genome replication. Viral replication is facilitated by the formation of viral factories, also called inclusion bodies.³⁹ VP35, also a component of the nucleocapsid, serves as a co-factor for the polymerase and is involved in the blocking of innate intracellular immune responses. VP30 is involved in transcription initiation and regulation (Figure 3).⁴⁰

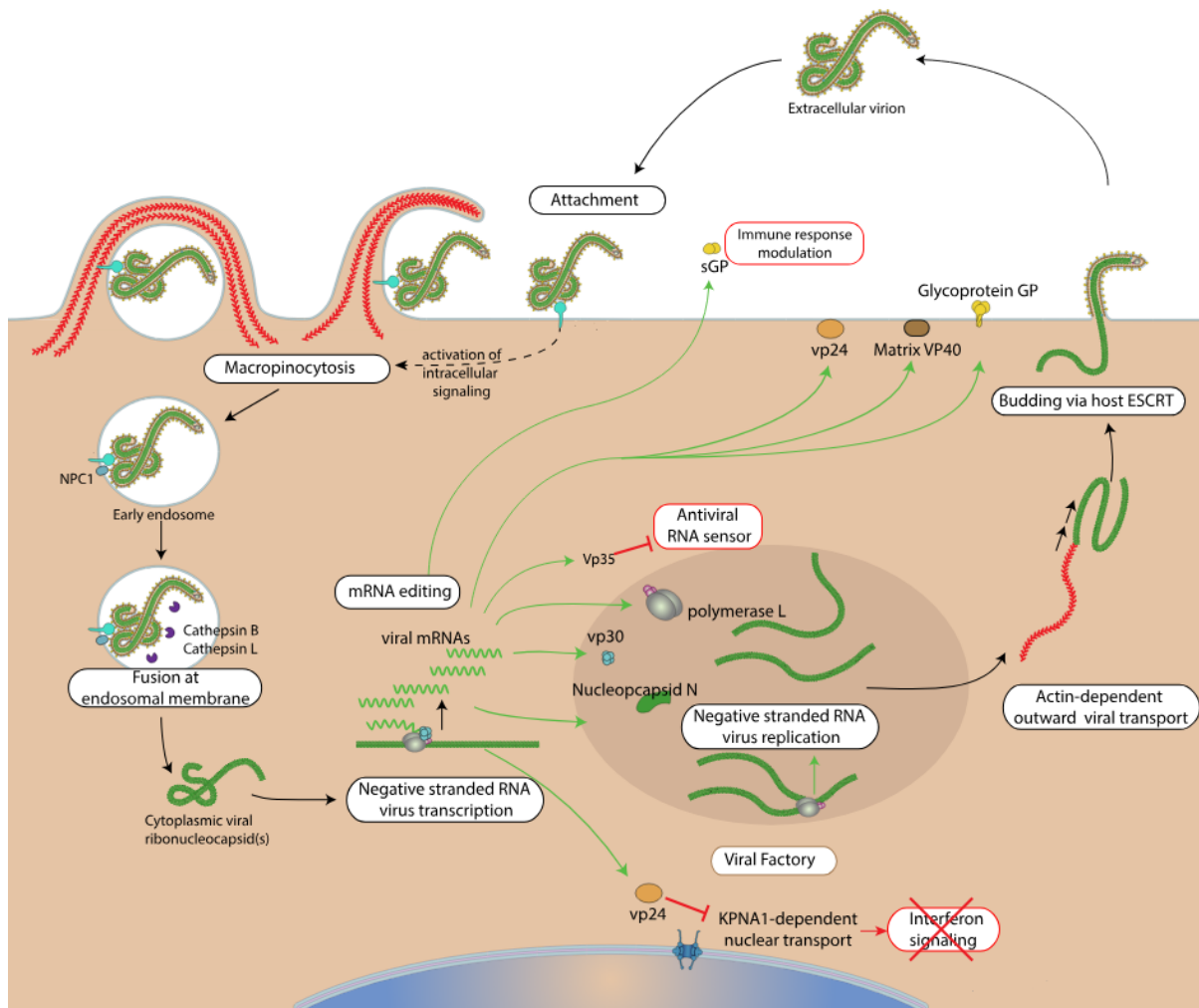


Figure 3 Ebola virus life cycle. EBOV-GP binds to cellular attachment factors and mediates uptake via macropinocytosis. Within the late endosome, GP is cleaved by cellular cathepsin B and cathepsin L, exposing GP₂, which mediates fusion with the endosomal membrane via NPC1. The viral nucleocapsid is released into the cytosol. Here, viral RNA is transcribed by the L protein (polymerase) to mRNA for the translation of proteins and amplified for the assembly of new nucleocomplexes, which are transported to the cell surface for viral budding. VP35 and VP24 inhibit intracellular innate immune responses. ViralZone SIB Swiss Institute of Bioinformatics, 2023

Viral proteins are translated from mRNA by the host cell translation machinery. Besides the membrane-bound GP, a soluble GP (sGP) is produced in large amounts. sGP is not incorporated in the viral particle but is secreted by infected cells and has been attributed to anti-inflammatory functions.⁴¹ An additional small sGP (ssGP), shows structural similarity to sGP but does not seem to share the same functional properties.⁴² These forms of GP are not to be confused with another soluble GP that is shed from the surface of infected cells by cleavage of membrane-bound GP.⁴³ NP forms the nucleocapsid, surrounding the genomic RNA. VP24 is a matrix protein which is involved in nucleocapsid formation and assembly. Moreover, it is considered an important virulence factor as it inhibits type I interferon (IFN-I) responses. VP40 coats the

inside of the viral membrane and thereby maintains structural integrity. Even more important, it facilitates viral budding^{44,45} (Figure 3).

1.4. Ebola virus disease pathogenesis

EBOV has a wide tissue and cell tropism, including but not limited to, epithelial and endothelial cells.⁴⁶ Mononuclear phagocytes, such as dendritic cells (DCs) and macrophages, are considered primary targets upon initial virus entry. Due to their migratory characteristics, especially DCs are suspected to contribute to virus dissemination.⁴⁷ As the virus is released into the circulation, EBOV disseminates throughout the whole body. Levels of viremia at the time of hospitalization correlate with the disease outcome.⁴⁸ Besides virus replication in different organs, disease severity is associated with the host immune response to infection. High inflammation, hypercytokinemia ('cytokine storm') and coagulopathy are associated with clinical disease signs such as hypovolemic shock and multiorgan failure. Immune activation may even persist during convalescence and has been suggested to contribute to sequelae.^{23,49} How EBOV interacts with the immune system and how immune responses contribute to EVD pathogenesis is discussed in the next chapter.

1.5. The immune response against Ebola virus – a constant battle

The immune system has many different tools to fight viral infections, which can be divided in two branches – innate and adaptive immunity. Innate immune responses are the first line of defense that act non-specifically against all invading pathogens. Adaptive immunity on the other hand, is highly specific. Precise coordination of the different responses is essential to efficiently suppress viral replication and simultaneously avoid detrimental effects from immunological overreaction. While the immune system has evolved sophisticated strategies against pathogens, also viruses have evolved different strategies to evade these immune responses.

Our knowledge regarding immune responses in the context of EVD is partly based on human clinical data, but also largely depends on data obtained from experimental infections of different animal models. Non-human primates (NHPs) show the best representation of human EVD with similar symptoms and case-fatality rates.⁴⁷ However, limited availability, high experimental difficulty and strong ethical concerns have kept experiments with NHPs to a minimum. Experiments with mice generally have certain advantages, such as easy handling and maintenance, fast and high reproduction rates, abundance of experimental tools and a large number of genetically modified strains. Nonetheless, a problematic feature in the context of studying EVD in inbred laboratory mice is that they do not develop disease upon EBOV

infection, despite supporting high levels of viral replication. This resistance has been linked to a strong IFN-I response. Consequently, genetically modified mouse strains, in which the IFN-I response is suppressed by knocking out the IFN-I receptor (IFNAR $-/-$), develop disease and succumb to infection.⁵⁰ However, the high lethality of this model and the immunosuppressed background impede studies focused on the immune response to EBOV. This problem is circumvented by the development of chimeric mice, harboring a competent hematopoietic system in the IFNAR $-/-$ background. These chimeric mice allow EBOV replication and a competent, hematopoietic-driven immunological response, and show a fatality rate of about 50%.⁵¹ This concept can be expanded to mouse models harboring a human immune system (HIS), allowing for closer resemblance to human immune responses.⁵²

Besides different animal models, cell culture experiments investigating very specific immunological pathways have also contributed to our understanding of EVD. Data on the immune response to EBOV infections from clinical studies, as well as animal and cell culture experiments, will be summarized on the following paragraphs.

1.5.1. Innate immunity – the role of dendritic cells and macrophages

The skin is the first barrier for viruses to overcome. Small skin lesions or viral particle contact with mucus membranes in the eye, mouth or nose facilitate virus entry into the body. At mucosal sites, DCs and macrophages are initial infection targets of EBOV.^{47,53} *In vitro* studies have shown that DCs and macrophages support viral replication to high titers.^{52,54}

Macrophages become activated upon EBOV-infection and release large amounts of inflammatory cytokines such as IL-1 β and tumor necrosis factor (TNF)- α , chemokines including MIP-1 α , and nitric oxide (NO). These mediators induce monocyte, macrophage, and neutrophil migration to the site of infection and cause vasodilation and increased endothelial permeability. While these responses are initially beneficial for viral clearance, they become detrimental if they occur prolonged or systemically. EBOV-infection of macrophages has also been linked to the coagulopathy observed in EVD patients.^{53,55}

In contrast to what has been shown for macrophages, previous studies suggest that DCs are not activated upon EBOV infection. The ability of EBOV to suppress DC activation results from the function of VP35 and VP24 to suppress IFN-I responses in infected cells. In these studies, it was suggested that the lack of DC activation upon EBOV-infection leads to poor T-cell activation and immunosuppression.^{53,54,56–58} However, a recent study showed that not all DC subsets are equally infected in mice. Here, CD103 $^+$ DCs showed lower infection rates than CD11b $^+$ DCs, suggesting that not all DC subsets may respond equally to EBOV infection.⁵¹

DCs, in opposition to macrophages, have migratory capability and thus are suggested to contribute to viral dissemination.⁵¹ The importance of mononuclear phagocytes for the suppression of viral dissemination is underscored when comparing lethal, mouse-adapted and non-lethal, non-adapted EBOV infection in mice. As described above, wildtype mice are resistant to EBOV infection and do not develop disease. While non-adapted EBOV only replicates in mononuclear phagocytes in these mice, mouse-adapted EBOV successfully overcomes innate immune barriers and spreads to different organs.⁴⁹ This suggests that DCs in particular form an important check point in EBOV dissemination.

Besides DCs, also migratory monocytes are suggested to contribute to EBOV dissemination. Despite the fact that monocytes are initially refractory to infection, EBOV can associate with undifferentiated monocytes and complete the entry process upon differentiation into macrophages or DCs.^{51,59}

IFN-I is a key antiviral cytokine that is produced by all cells – especially macrophages and DCs can release IFN-I in high concentrations. IFN-I production in EBOV-infected cells is induced by the recognition of viral RNA by pattern recognition receptors (PRRs), mainly RIG-I and MDA-5, with viral RNA (for details see chapter 1.6.3). Simultaneously, EBOV inhibits IFN-I responses by the action of VP35 and VP24. Most cells are able to detect IFN-I with IFN-I receptors. Thereby, IFN-I acts in an autocrine and paracrine manner in infected and uninfected bystander cells and leads to transcription of numerous IFN-stimulated genes (ISGs). The new transcription profile transfers the cells into an antiviral state that blocks viral replication.^{60,61} These mechanisms are especially important for controlling viral replication at early time points after EBOV infection. Again, regulated levels of IFN-I are required for viral clearance, but a systemic overshooting of the IFN-I response leads to immunopathology.²³

1.5.2. Adaptive immunity against Ebola virus

Adaptive immunity includes humoral and cellular immune responses that are both required for EVD survival.⁶² T cells are required for the elimination of virus-infected cells. To facilitate T-cell-mediated killing, infected cells present viral antigens on major histocompatibility complex class I (MHC-I) molecules on the cell surface. MHC-peptide complexes are recognized by the T-cell receptor (TCR) of cognate CD8 T cells, which subsequently release granzyme B and perforin that induce apoptosis of the infected cell.⁶³ Besides these cytotoxic T cells, CD4 T cells are important regulators of the immune response and exert diverse T-helper functions. In the context of viral infections, naïve CD4 T cells may differentiate for example into T-helper 1 (Th1) effector cells that help CD8 T cells to lyse infected cells, and into T follicular helper cells (Tfh) that help B cells in antibody generation. CD4 T cells are further

involved in the recruitment of innate immune cells, such as macrophages and natural killer (NK) cells, to the sites of infection.⁶⁴

Clinical investigations have shown that EVD patients mount robust adaptive immune responses with high numbers of activated, EBOV-specific CD8 and CD4 T cells in survivors as well as fatal cases.⁶⁵⁻⁶⁷ However, T cells of patients with fatal outcome showed lower TCR diversity, and higher expression of the inhibitory molecules cytotoxic T-lymphocyte-associated protein 4 (CTLA-4) and programmed cell death-1 (PD-1), which suggested a dysregulation of the T-cell response.⁶⁵⁻⁶⁷ This early T-cell proliferation is followed by severe lymphopenia, which was suggested to result from an abortive infection of T cells.⁶⁸ Moreover, other studies demonstrated that, *in vitro*, T cells release high levels of TNF α upon contact with EBOV particles, which was associated with the death of bystander T cells and is suggested to contribute to the high levels of inflammation seen in EVD patients.^{69,70}

Moreover, adaptive immunity includes antibody production by activated B cells. The functions of antibodies are diverse and can include direct neutralization of viruses by blocking viral entry receptors, activation of the complement system and cellular cytotoxicity, and to facilitate phagocytosis.⁷¹ A robust antibody response has been associated with viral clearance and EVD survival.⁶⁵⁻⁶⁷ Conversely, often patients with fatal outcomes do not mount virus-specific antibody responses. However, there are also studies reporting fatal cases in which high levels of antibodies were detected and survivors in which EBOV-specific antibodies were not detectable for weeks after recovery. Thus, the contribution of humoral immune responses to EVD pathogenesis and disease outcome are still poorly understood.²³

In order to pursue their function T- and B cells depend on activation signals from professional antigen-presenting cells (APCs). DCs play a pivotal role in the activation of T cells, while B cells are primarily activated by macrophages and follicular DCs, which reside in B-cell follicles. However, recently other types of DCs have been suggested to also contribute to B-cell activation.⁷² Thus, DCs build an important bridge between innate and adaptive immunity. To further understand the mechanisms initiating adaptive immunity in EVD we need to take a closer look at the complex DC lineage.

1.6. The dendritic cell lineage

In 2011 Ralph Steinman received the Nobel Prize in Physiology or Medicine for the discovery of DCs, which he and his colleagues first described in 1976.⁷³ Since then, the field of DC research has expanded tremendously. Today, we know that DCs form a highly heterogenous class of immune cells with distinct developmental pathways. Generally, DCs can be divided in

conventional DCs (cDCs), plasmacytoid DCs (pDCs) and monocyte-derived DCs (moDCs). The development and characterization of the different DC subsets is a highly debated topic and under constant revision. DC subsets can be characterized by the expression of diverse marker proteins. While some markers are unique to a certain subset, similar subsets can only be distinguished by a combination of markers or their absence. Possible phenotypical transition of one subset to another and location-specific differences further complicate the characterization. For most human DC subsets equivalent cells have been identified in mice. However, protein markers are not always conserved between human and mice, and functionality may differ. The current knowledge on the DC lineage is summarized on the following pages.

1.6.1. Dendritic cell ontogeny

All DC subsets arise in the bone marrow from common myeloid progenitors (CMP), which further differentiate into granulocyte-monocyte-dendritic cell progenitors (GMDP). From here, DC development can be divided into two main pathways dependent on the expression level of the transcription factor IRF8. Cells with high levels of IRF8 develop into the common dendritic cell progenitor (CDP). Meanwhile, cells with low IRF8 expression levels progress towards the monocyte or DC type 3 (DC3) lineage.^{74,75} (Figure 4)

CDP differentiate into pre-cDC or pre-pDC, which migrate from the bone marrow into the blood and further into the periphery. The driving forces for pre-DC migration and homing to different tissues are still under investigation, but different homing receptors like CCR2 or CX₃CR1 are suggested to be involved.⁷⁶ In the tissue, pre-cDCs and pre-pDCs finally give rise to cDC type 1 (cDC1) and type 2 (cDC2), or pDCs, respectively. The microenvironment of different organs further shapes the phenotypical and functional characteristics of the DCs, giving rise to even more diverse subtypes.^{77,78} This developmental pathway of the so-called 'bona fide' DCs depends on the stimulation of Fms-like tyrosine kinase 3 receptor (Flt3) by Flt3-ligand (Flt3L).^{79,80} Furthermore, the commitment of pre-cDC to cDC1 or cDC2 is determined by distinct transcriptional profiles.⁸¹ Additional pathways of pDC development from lymphoid progenitors have been identified in mice, but whether similar pathways exist in humans is currently unknown.⁸² For humans, the transition of pDCs into cDC2 via so-called transitional DCs (tDCs) is currently discussed.⁸³

Monocytes originate from common monocyte progenitors (cMoP) in the bone marrow and migrate into the blood where they circulate in high numbers. Upon inflammatory stimulation, they migrate into tissue and differentiate into macrophages or monocyte-derived DCs (moDCs) and are dependent on GM-CSF stimulation.⁸⁴

DC3 is a newly described DC subset with a developmental pathway distinct from cDCs, pDCs or monocytes. Which stimulants are driving DC3 development is still under debate. Both Flt3L and GM-CSF have been proposed to support DC3 development at different stages. To date, DC3s have only been found in the human bone marrow and blood, their presence in tissue and whether an equivalent DC subset exists in mice is still unknown.^{75,85}

Fully differentiated cDCs are short-lived immune cells with limited proliferation capacity. As they only live for 10-14 days, they constantly must be replenished by pre-cDCs from the bone marrow, blood, or tissue.^{86,87}

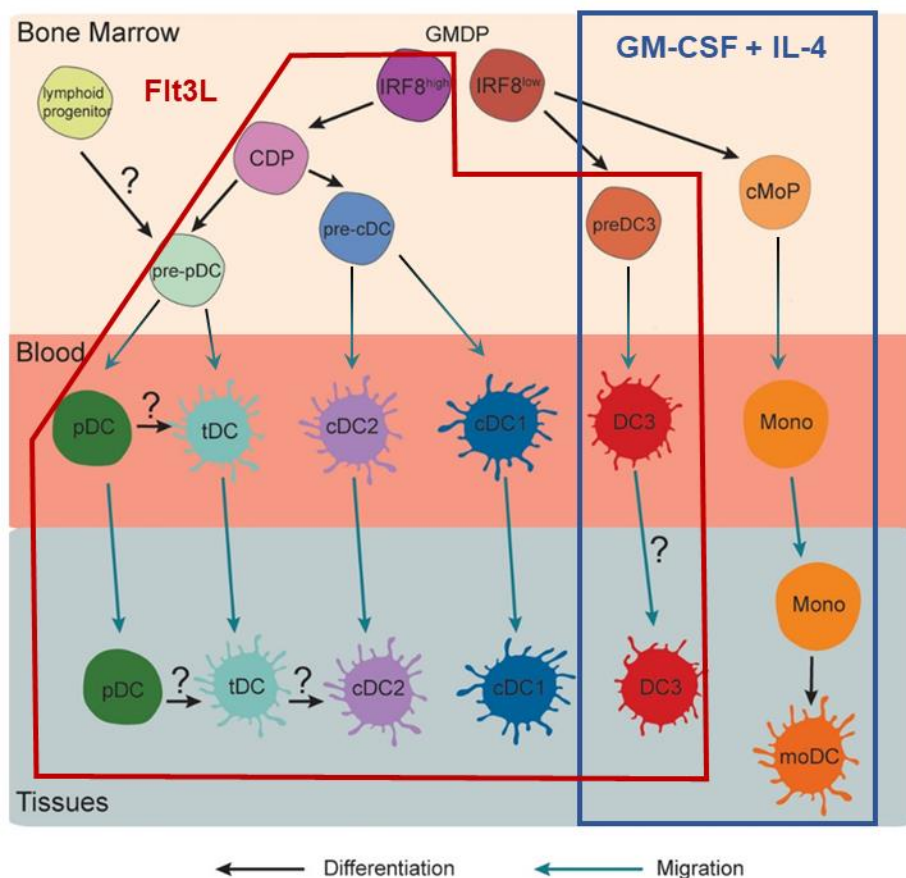


Figure 4 Human dendritic cell ontogeny. DCs develop from granulocyte-monocyte-dendritic cell progenitors (GMDP) in the bone marrow. Depending on the expression level of IRF8, GMDP differentiate into common DC progenitors (CDP) or common monocyte progenitors (cMoP). CDP give rise to pre-cDC and pre-pDC, which further differentiate to conventional DC type 1 (cDC1, blue) and type 2 (cDC2, purple), as well as plasmacytoid DCs (pDC, green), respectively. pDC and cDC development depends on Flt3 stimulation by Flt3-ligand (Flt3L, red box). pDC can also derive from lymphoid progenitors via different pathways. cMoPs differentiate into monocytes (orange). DC3 (red), a newly described subset, develop via separate pathways. Pre-DCs and monocytes migrate from the bone marrow into the blood and further into tissue, where they finalize their differentiation. In the tissue, monocytes differentiate into moDCs upon stimulation with GM-CSF and IL-4 (blue box). pDCs can transform into cDC2 via so-called transitional DCs (tDCs, turquoise). Black arrows indicate differentiation steps, blue arrows indicate migration. Adapted from (Segura, 2022)

1.6.1.1. *In vitro* differentiation of dendritic cells

Studying DCs in detail requires access to this rare cell type. Low numbers of DCs in the blood and tissues make it difficult to directly isolate them in sufficient numbers. Therefore, different developmental pathways are employed to generate DCs *in vitro*. Monocytes circulate in the blood in high numbers, and are therefore a well-accessible source to generate human moDCs *in vitro*. Monocytes and monocyte progenitors are also present in the bone marrow, which is often utilized to derive murine moDCs. For that, monocytes are isolated and cultured for 5-7 days in the presence of GM-CSF and IL-4.⁸⁸ Because they are easily accessible, most of our knowledge on DC functionality is based on studies using moDCs.

Other DC subsets, namely cDCs and pDCs, can only be derived from progenitors that mainly reside in the bone marrow. This makes it much more difficult to generate human bona fide DCs *in vitro*. However, in recent years innovative protocols have been developed to generate human cDCs and pDCs from stem cells.⁸⁹ Alternatively, murine cDCs and pDCs can be derived from murine bone marrow similar to moDCs. For that, DC progenitors are isolated and differentiated to cDCs and pDCs by stimulation with Flt3L for 8-9 days.^{90,91}

1.6.2. Phenotypical characterization of dendritic cells

DCs can form a variety of cell shapes with constantly extending and contracting cytoplasmic projections – the so-called dendrites. This morphology prompted Steinman and Cohn to name the newly discovered cell type dendritic cells.⁷³ (Figure 5)

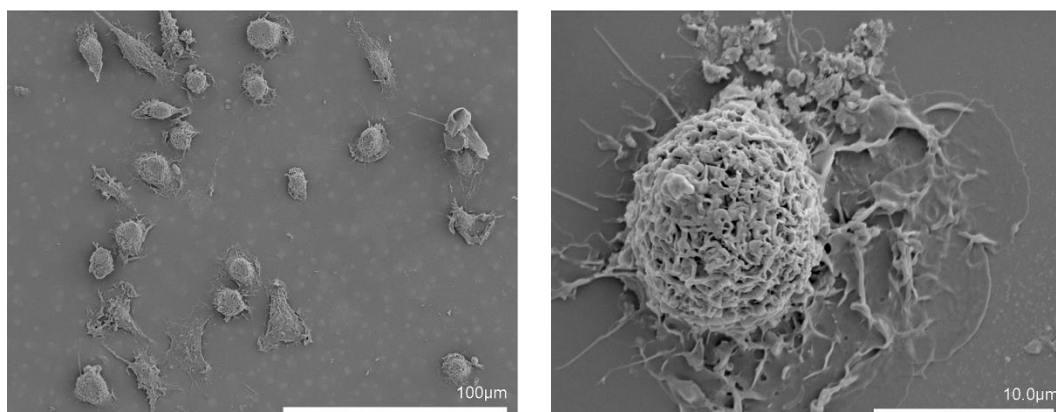


Figure 5 Murine dendritic cell morphology. Scanning electron microscopy images at 500x (left, bar = 100 μm) and 4000x magnification (right, bar = 10 μm) of moDCs derived from murine bone marrow by stimulation with GM-CSF, IL-4 and TNF-α for 8 days. Mature DCs develop a large surface area by the formation of extensive dendrites. Images from Ding et al. 2020

The detailed characterization of DC subsets requires the investigation of a set of protein markers. Relevant protein marker of murine DCs and their function in DCs are listed in Table 2.

CD11c, also known as integrin alpha X, is widely used as a defining marker for all human and murine DC subsets. However, CD11c has also been found on other cell types such as macrophages and neutrophils.^{93,94} As professional APCs, DCs express not only MHC-I, like all nucleated cells, but also MHC-II. Both are highly important for DC functionality as described in chapter 1.6.3.

Conventional DCs are divided in two main subsets – cDC1 and cDC2. In mice, these can be distinguished by the expression of XCR1 and CD8, or SIRP α and CD4, respectively.⁹⁵ However, another study has claimed that a XCR1⁺/SIRP α ⁺ double-positive intermediate subset exists in small numbers.⁹⁶ XCR1 expression on cDC1 has been linked to a fully differentiated phenotype and both XCR1 and SIRP α are conserved between human and mice.⁹⁷ Furthermore, murine cDC1 show higher expression of CD24 than other murine DC subsets. Other typical markers of cDC2 and moDCs described below are not present on cDC1.⁹⁸ Conventional DC1 can be further subclassified by the expression level of CD103. cDC1 in lymph nodes classically express lower levels of CD103 than equivalent cells in non-lymphoid tissues such as liver, intestine and lung.⁹⁹ Human cDC1 are specifically characterized by the expression of CD141 and CADM1.¹⁰⁰

The precise characterization and distinction of cDC2 from moDCs is more complicated due to overlapping marker expression. Both cDC2 and moDCs express high levels of SIRP α and CD11b, but cDC2 are most often missing typical moDC markers such as CD14, F4/80, Ly6C (only mouse) and CD64. However, this does not hold true for all cDC2 in all organs. In fact, studies suggested that cDC2 in lung and kidney partly express CD64 and cDC2 in skin-draining lymph nodes have been shown to express high levels of CD14.⁷⁸ While all the markers mentioned above are conserved between human and mice (except Ly6C), human cDC2 are additionally characterized by the expression of CD1c.¹⁰⁰

pDCs received their name “plasmacytoid” due to their morphology, that resembles plasma cells, rather than classical DCs. They show lower expression levels of CD11c compared to other DCs and additionally express CD45RA and Ly6C. Siglec-H is considered a specific murine pDC marker, which allows their distinction from other DC subsets.¹⁰¹ Important to note is that several cDC progenitors have been shown to also express Siglec-H.¹⁰² Human pDCs are characterized by the expression of CD123.¹⁰⁰

Table 2 Relevant murine DC markers and their functions

Marker	Function	DC subset
CD103	= Integrin alpha E Mediates cell adhesion to epithelial cells and is therefore involved in migration ¹⁰³	cDC1 (some cDC2 in intestine)

Introduction

CD11b	= Integrin alpha M Involved in cell adhesion and phagocytosis ¹⁰⁴	cDC2 moDC
CD11c	= Integrin alpha X Involved in cellular adhesion, migration, phagocytosis also: complement receptor 4 ¹⁰⁵	all DC subsets (and presumably some macrophages)
CD14	= a glycosyl-phosphatidylinositol anchored cell surface glycoprotein A pattern recognition receptor and co-receptor involved in cell activation ¹⁰⁶	moDC (monocytes and macrophages)
CD24	= a glycosyl-phosphatidylinositol anchored cell surface glycoprotein Required for optimal T-cell priming ¹⁰⁷	cDC1 (some cDC2 in lung)
CD45RA	= a protein tyrosine phosphatase receptor type C Leukocyte common antigen, function on DCs not described, mainly on DC progenitors ^{90,108}	pDC (and DC progenitors)
CD64	= Fc- γ -receptor 1 Binding of immunoglobulin G antibody (IgG)-antigen complexes ¹⁰⁹	moDC (macrophages, some cDC2)
F4/80	= part of the epidermal growth factor-seven transmembrane (EGF-TM7) family Involved in immune tolerance by activation of regulatory T cells ¹¹⁰	moDC (macrophages, some cDC2)
Ly6C	= lymphocyte antigen-6 complex Function uncertain, mainly monocyte and macrophage marker ¹¹¹	pDC moDC (monocytes)
MHC-I	= Major histocompatibility complex class I Antigen presentation (endogenous and exogenous antigen sources) ¹¹²	All nucleated cells
MHC-II	= Major histocompatibility complex class II Antigen presentation (exogenous antigen sources) ¹¹²	All DCs subsets (all APCs)
Siglec-H	= sialic acid binding Ig-like lectin H Involved in antigen recognition and uptake and control of IFN-I release ¹¹³	pDC (DC progenitors)
SIRP α	= Signal regulatory protein α	cDC2

	Inhibitory receptor: downregulation of cell growth and phagocytosis ¹¹⁴	moDC
XCR1	= X-C motif chemokine receptor 1 Involved in chemotaxis ¹¹⁵	cDC1

1.6.3. Dendritic cell function

DCs can be found in all organs, especially at the interface with the environment, in skin and mucosal surfaces. Here, patrolling DCs sample their surroundings for antigens which may originate from pathogens, damaged cells, or cancer cells. These antigens are recognized by their specific molecular structure through pattern recognition receptors (PRRs) that are expressed on the surface, in endosomal spaces and in the cytosol of DCs. The big group of PRRs includes the Toll-like receptors (TLRs), nucleotide oligomerization domain (NOD)-like receptors (NLRs), retinoic acid-inducible gene-I (RIG-I)-like receptors (RLRs), C-type lectin receptors (CLRs), and absent in melanoma-2 (AIM2)-like receptors (ALRs). Different PRRs recognize specific structures, so-called pathogen-associated molecular patterns (PAMPs) or damage-associated molecular patterns (DAMPs), with their ligand recognition domains. The diverse repertoire of these innate immune receptors allows DCs to respond to a broad range of pathogens and tissue damage. PAMPs or DAMPs include but are not limited to double-stranded (ds)RNA, bacterial lipopolysaccharides (LPS), or F-actin. Ligand binding induces downstream signaling pathways which ultimately leads to DC activation.¹¹⁶ DC activation can also be initiated by stimulation with pro-inflammatory cytokines like IL-1, TNF- α or IFN-I.⁸⁶

DC activation, which is also referred to as DC maturation, is the transition from a resting state to a functional state, which allows the DC to convey information to other cells. Activation involves phenotypical changes such as increased surface expression of MHC molecules and their co-stimulatory molecules CD80, CD86 and CD40, which are often summarized as DC activation markers. Moreover, activation includes the upregulation of chemokine receptor CCR7, which facilitates homing of the DC from the periphery to secondary lymphoid tissues such as lymph nodes, spleen, tonsils, or Peyer's patches in the intestine. Here, activated DCs interact with T cells, and stimulate their differentiation, activation, and proliferation. T-cell activation is the most important function of DCs, because with that they build a bridge between innate and adaptive immunity.⁸⁶

While all DCs are able to activate different types of T cells, different DC subsets have been linked to distinct functions in the immune response. The ability of pDCs to activate T cells is highly debated, but they are appreciated as IFN-I-secreting cells. In fact, pDCs are considered the primary source of IFN-I in viral infections.¹⁰¹ Conventional DCs, on the other hand, are

recognized as the main T-cell activating subsets. cDC1 and cDC2 have been associated with CD8 and CD4 T-cell activation respectively. However, this functional distinction is not fixed and is highly debated. Monocyte-derived DCs are suggested to contribute to T-cell activation, especially in an inflammatory setting, even though this has also been challenged in recent studies.^{86,117} The mechanisms of how DCs activate T cells are further described in the next chapter.

1.7. Dendritic cell – T-cell interaction

DCs belong to the group of professional APCs, together with macrophages and B cells. As such, they are able to present antigens in the context of MHC and thereby activate T cells.

As described in chapter 1.5.2., T cells can be divided in CD8 and CD4 T cells. While CD4 T cells orchestrate the immune response by interacting with other immune cells, CD8 T cells identify and kill virus-infected cells and therefore fulfil a pivotal role in viral clearance. However, before T cells can execute their function, they must be activated by professional APCs, mainly DCs.

First, DCs take up antigens from their surroundings by phagocytosis or endocytosis. Engulfed antigens are contained in the phagosome, which fuses with a lysosome. In the acidic endo-lysosome, the pH-sensitive protease Cathepsin S facilitates hydrolysis of the antigens into peptides, which are subsequently loaded onto MHC-II molecules. MHC-II molecules are initially formed in the endoplasmic reticulum (ER) and then trafficked to the endosome for peptide loading. MHC-II-peptide complexes are transported to the cell surface, where they can be recognized by cognate CD4 T cells.¹¹⁸

CD8 T cells, in contrast, depend on the antigen-presentation in the context of MHC-I. As part of homeostasis, all nucleated cells constantly present endogenous antigens that are cleaved by the proteasome and loaded onto MHC-I. This pathway is known as direct MHC-I presentation and facilitates a signal for CD8 T cells to detect intracellular pathogens, cell damage or cancer cells. In that sense, the presentation of pathogen-derived antigens on MHC-I by DCs would require infection of the DCs themselves. However, DCs have developed pathways that allow the presentation of exogenously acquired antigens, not only on MHC-II, but also on MHC-I. This process called cross-presentation of exogenous antigens on MHC-I has been considered a specific feature of DCs, but in recent years has also been shown to take place in macrophages.¹¹⁹

Exogenous antigens can be loaded onto MHC-I directly in the phagosome. This so-called vacuolar pathway is analogous to the loading of MHC-II. Additionally, exogenous antigens can be transported into the cytosol, where they are cleaved by the proteasome like endogenous

antigens, and then transported back into endosomes or the ER, where the peptides are loaded onto MHC-I. This cross-presentation pathway is termed cytosolic pathway.¹²⁰ MHC-I-antigen complexes are finally transported to the cell surface, where they provide the first activation signal to naïve CD8 T cells.

CD8 T cells recognize specific MHC-I-peptide complexes with a specific TCR. The TCR is tightly connected to the co-receptor CD3, which transduces the antigen recognition signal to downstream pathways. Successful T-cell activation further requires co-stimulation through the interaction of CD80 and CD86 on the DC surface with CD28 on the T-cell surface. As a third signal for T-cell activation, the DC releases cytokines, mainly IL-12 and IFN-I, which further promotes CD8 T-cell activation¹²¹ (Figure 6). These additional signals can only be provided by activated DCs. In the absence of co-stimulation DCs present antigens to T cells to induce tolerogenic responses, for example in response to self-peptides encountered in the periphery (peripheral tolerance).

Binding of CD80 or CD86 to CTLA-4 instead of CD28 gives an inhibitory signal to the T cell. The interaction of PD-1 on the T cell side with PD-1L on the DC side also contributes to this inhibition and induces T regulatory responses. With these inhibitory mechanisms, the immune system avoids overreaction and autoimmunity.

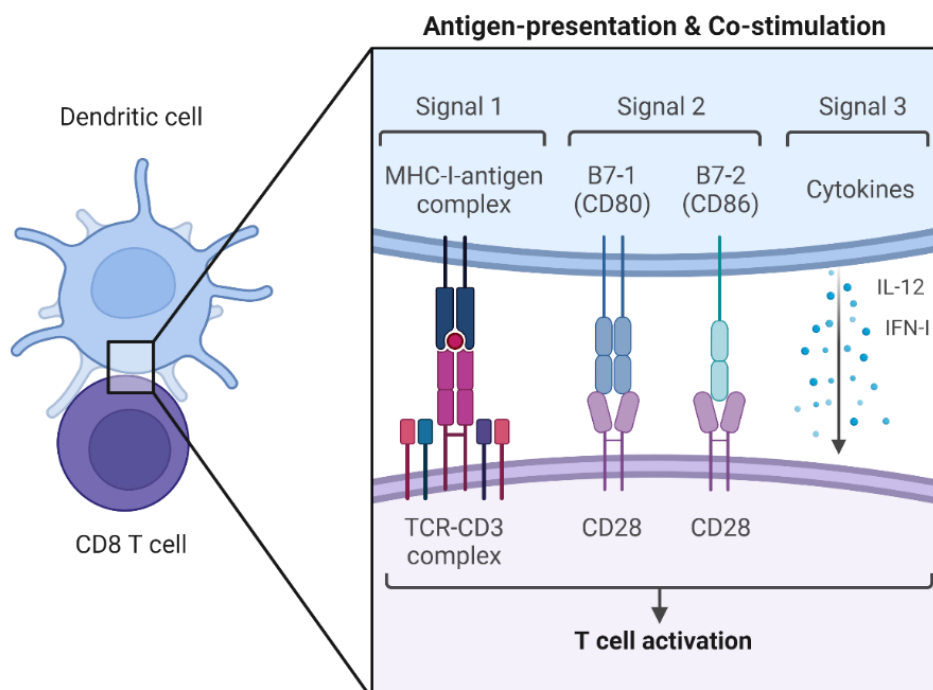


Figure 6 Dendritic cell – CD8 T-cell interaction. T-cell activation requires three signals from the DC. Signal 1: Antigens presented by DCs on MHC-I are recognized by the T-cell receptor (TCR)-CD3 complex of CD8 T cells. Signal 2: Co-stimulation is provided by the DC with B7-1 (CD80) and B7-2 (CD86) that bind to CD28 on the T cell. Signal 3: Cytokines, such as IL-12 and IFN-I, are released by the DC and promote T-cell proliferation and survival. Image created with BioRender

Activated T cells undergo phenotypical changes and differentiate into diverse effector and memory subtypes. Activated T cells migrate from the lymph node to the blood stream, from where they can enter different tissues. As early as 2-3 hours after activation, T cells upregulate CD69 and later also CD44, which are markers involved in homing and migration.¹²² In opposition, homing receptors that lead naïve T cells to re-circulate to lymph nodes, such as CD62L, are downregulated. After the initial activation phase, the T cells enter the expansion phase, in which especially CD8 T cells proliferate to high numbers with an estimated peak doubling time of around 4 hours.¹²³ They release high levels of IL-2 and IFN- γ . IL-2 again is detected by activated T cells with the upregulated IL-2 receptor (CD25), which further stimulates T-cell proliferation in a positive feedback loop. IFN- γ also acts in an autocrine or paracrine manner and enhances T-cell motility, and CD8 T-cell-mediated killing.¹²⁴ When the virus is cleared, T cells enter the contraction phase, in which most T cells undergo apoptosis. Only a small fraction of memory T cells persist over months or years and can be rapidly re-activated in case of re-infection.¹²⁵

Table 3 Relevant T-cell markers and their functions

Marker*	Function
CD25	= α -chain of the IL-2 receptor Involved in T-cell proliferation ¹²⁶
CD3	= TCR co-receptor Involved in signal transduction of the activation signal from the TCR ¹²⁷
CD4	= TCR co-receptor Closely associated with TCR and binds MHC-II and enhances antigen sensitivity ¹²⁸
CD44	= C-type lectin receptor binding hyaluronic acid Involved in T-cell migration ¹²⁹
CD62L	= L-selectin Homing of naïve T cells to lymph nodes and activated CD8 T cells to sites of virus infection ¹³⁰
CD69	= type II C-lectin receptor ¹²² Involved in cytokine release, homing, and migration
CD8	= TCR co-receptor Closely associated with TCR and binds MHC-I and enhances antigen sensitivity ¹²⁸

* All of the explained T-cell marker are conserved between human and mice

1.7.1. Antigen sources for antigen-presentation – the role of extracellular vesicles

DCs may acquire exogenous antigens for antigen-presentation and subsequent T-cell activation via different routes. Virus-infected cells often undergo apoptosis or necrosis, resulting in the production of cellular debris. Cell debris is rapidly taken up and degraded by scavenger cells, mainly macrophages. However, DCs also take up this cell debris and utilize it for antigen-presentation. As virus-infected cells produce viral proteins, these are also included in the debris and thus presented.

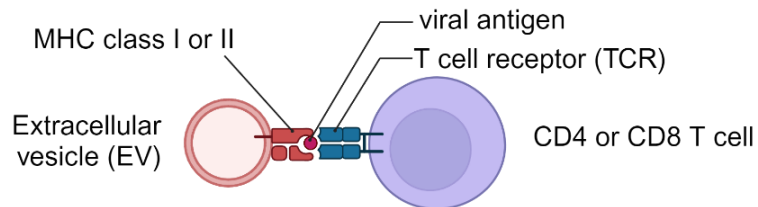
On the other hand, not all infected cells die rapidly upon infection. Instead, live cells have developed mechanisms to transfer antigens to DCs. Generally, antigens can be transferred between the same or different T cell types. Antigen transfer from one to another DC subset becomes especially important, considering that not all DC subsets harbor the same migration capacity. Thus, migrating DCs could potentially transfer antigens from the periphery to secondary lymphoid tissue and there, transfer antigens to resident DC subsets, which can contribute to T-cell activation and further orchestrate the immune response.

Antigen transfer between two living cells may occur via direct cell-to-cell contact. Hereby two cells form a synapsis that facilitates antigen transfer mainly via the exchange of intracellular vesicles.¹³¹ These vesicles formed in a cell can also be secreted as extracellular vesicles (EVs). EVs have become a hot topic in many different research fields as they are secreted by virtually all living cells in high numbers. They are nano-sized lipid-membrane enclosed particles that can incorporate proteins, lipids and nucleic acids of the host cell and can be taken up by seemingly all other cells. With that, they mediate cell-cell communication and we are just beginning to understand which effects EVs can have on the recipient cells.¹³²

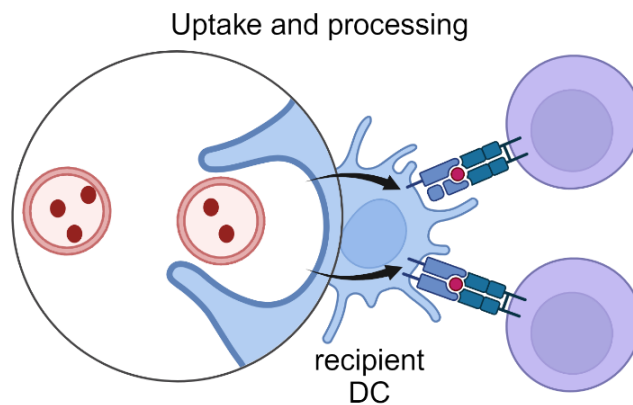
EVs can be involved in antigen-presentation in different ways (Figure 7). Secreted by virus-infected cells, EVs can incorporate viral antigens that are taken up by a DC and are subsequently processed and presented in the context of MHC similar to other exogenous antigens (Figure 7B). Additionally, EVs themselves can carry MHC-antigen complexes on the EV surface and, with that, directly contribute to T-cell activation as free EVs (Figure 7A) or coated on the DC surface. DCs can also recycle the acquired MHC-antigen complexes in a process called cross-dressing (Figure 7C). This opens the possibility that DC subsets, which are less efficient cross-presenting subsets, utilize pre-loaded MHC-I-antigen complexes, acquired from other cells, for T-cell activation.¹³²

These mechanisms become of particular interest considering that recent studies showed that EBOV-infected cells secrete extracellular vesicles, which contain different EBOV proteins, namely VP40, NP and GP.^{133,134}

A Direct antigen presentation by free EVs



B Antigen cross-presentation



C Antigen cross-presentation via cross-dressing

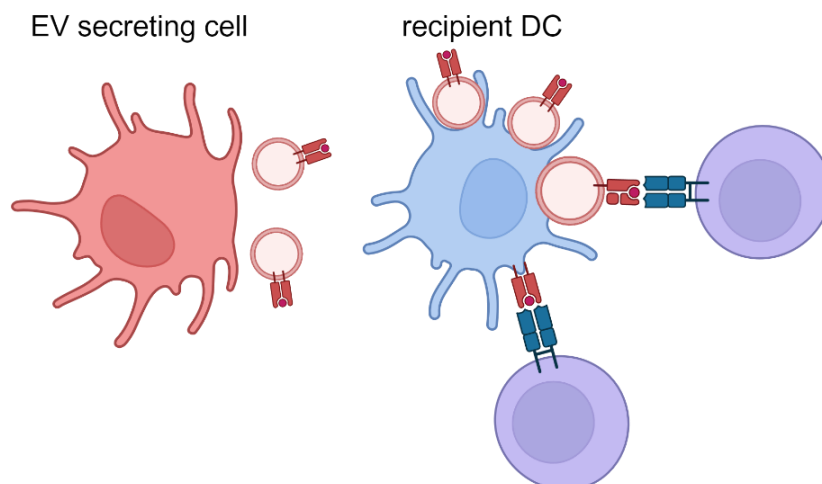


Figure 7 The role of EVs in antigen-presentation. EVs secreted from virus-infected cells can incorporate viral antigens and even pre-loaded MHC-antigen complexes. With that, EVs can contribute to T-cell activation (A) by direct antigen-presentation by free EVs, (B) by cross-presentation pathways by recipient DCs or (C) via cross-dressing of whole EVs or MHC-antigen complexes received from the EV secreting cell (red) on the recipient DC (blue) surface.¹³² Image created with BioRender.

1.7.2. Ovalbumin as a model antigen to study DC-T cell interactions

In order to facilitate investigations on antigen-specific DC-T cell interactions, immunological studies often utilize model antigens, such as chicken ovalbumin (OVA). OVA has been used widely in allergy, cancer immunology, and infection research. Many techniques have been developed to track OVA throughout the DC-T cell interaction from antigen-presentation to T-cell proliferation. Especially important was the development of the OT-1¹³⁵ and OT-2¹³⁶ mouse strain, which contain transgenic TCR that specifically recognize the OVA-peptide SIINFEKL presented in the context of MHC-I and MHC-II, respectively.

Recently, a recombinant EBOV expressing OVA as a non-structural protein (EBOV-OVA) has been developed by us and our collaboration partners at the Friedrich Löffler Institute, Greifswald, Germany. The OVA-gene is inserted between the NP and VP35 (Figure 8), ensuring high expression levels of OVA in infected cells. EBOV-OVA replicates in cell culture as efficiently as the wildtype (wt) EBOV.¹³⁷

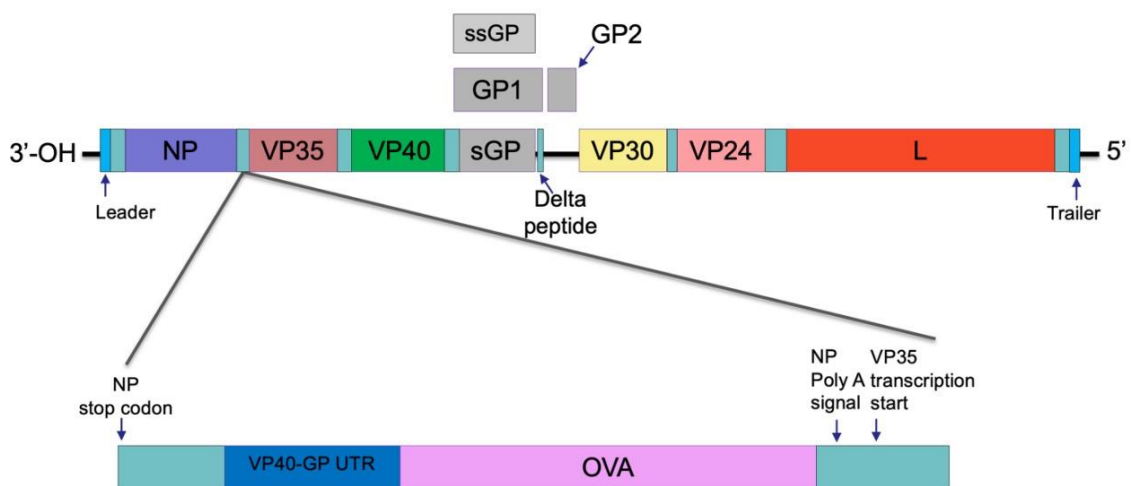


Figure 8 Schematic showing the genome organization of EBOV-OVA. OVA is inserted between NP and VP35 (from Olal, 2023).

1.8. Aim of the study

The severity of EVD has been linked to high inflammation, high levels of virus dissemination and excessive, dysregulated T-cell activation. In contrast to the immune activation observed in EVD patients, other studies have described that in cell culture, EBOV inhibits DC maturation and IFN-I signaling in infected cells. It was suggested that the lack of DC maturation due to EBOV infection leads to poor T-cell activation and immunosuppression. However, all of these *in vitro* studies have been performed exclusively on moDCs, which do not reflect the heterogeneity of the DC lineage.

The aim of this thesis was to investigate the tropism of EBOV for conventional, plasmacytoid and monocyte-derived DCs, the response of these DC subsets to infection and the consequences of infection for antigen presentation and T-cell activation. We hypothesized that not all DCs may be equally infected by EBOV and that cross-presentation of EBOV antigens by bystander uninfected DCs could play an important role in T-cell activation.

The main objectives of the study were:

1. To assess the cell tropism of EBOV for different murine DC subsets *in vitro*, and to investigate the effect of EBOV infection on DC activation.
2. To develop an *in vitro* DC-T cell co-culture model suitable to study the ability of EBOV-infected mixed DC cultures to activate cognate CD8 T cells.
3. To investigate whether DCs can utilize antigens, acquired from cellular debris or EVs from EBOV-infected cells, for cross-presentation and T-cell activation. Further, the effect of EBOV infection on DC cross-presentation capacity will be examined.
4. To determine the contribution of different DC subsets to CD8 T-cell activation in EBOV infections.

To fulfill these objectives, a mixed DC culture was derived from murine bone marrow, utilizing developmental pathways distinct from those of moDCs. Experimental infections of DCs with wildtype EBOV and the recombinant EBOV-OVA were performed in the BSL4-laboratory at the Bernhard Nocht Institute in Hamburg. The study mainly included *in vitro* co-culture experiments and multiparametric flow cytometry.

2. Materials

2.1. Cell lines

Vero E6 cells (Vero C1008, ATCC) were used for virus propagation, virus amplification, virus titration (immunofocus assay), and for the IFN-bioassay.

2.2. Viruses

The following virus strains were used in the present study:

- Ebola virus H.sapiens-tc/COD/1976/Yambuku-Mayinga (wt EBOV)
- Recombinant EBOV-OVA
- Recombinant Newcastle disease virus (NDV)-GFP

All experiments with recombinant viruses were approved by the Ministry of Environment, Climate, Energy and Agriculture under the approval number IB-17-42/13.

2.3. Mouse strains

Table 4 List of mouse strains

Mouse strain	Origin
C57Bl/6J	Jackson laboratories
Thy1.1 x OT-1 x C57Bl/6	Helmholtz Centre for Infection Research, Braunschweig

All mice were bred in the animal facility of the Bernhard Nocht Institute for Tropical Medicine. Mice were housed in individually ventilated cages and fed and watered ad-libitum.

Male and female mice between 9 and 15 weeks of age were used in this study. Sex and age were selected randomly upon availability. All mice were euthanized exclusively for organ collection. Organ collection for cell isolation was approved by the Committee on the Ethics of Animal Experiments of the federal state of Hamburg (Behörde für Gesundheit und Verbraucherschutz, Hamburg) under the approval 2021-T007. Mice were euthanized in accordance with the prescribed rules and regulations of the German Society for Laboratory Animal Science. A total of 60 C57Bl/6J and 31 Thy1.1xOT-1 mice were utilized in this study.

2.4. Reagents

Table 5 List of reagents

Reagent	Company
2% uranyl acetate solution	Science Services GmbH
Accutase cell detachment solution	BioLegend
Acrylamide/bis-acrylamide solution	Roth
Ammonium per-sulphate	Roth
BD Cytofix Fixation Buffer	BD Biosciences
Beta-mercapthoethanol (1000x) 55nM in DPBS	Gibco
Dulbecco's Modified Eagle Medium (DMEM) w: 4.5 g/L Glucose, L-Glutamine, w/o: Sodium pyruvate, w:3.7 g/L NaHCO ₃	Pan Biotech
Dulbecco's Phosphate Buffered Saline (DPBS) w/o: Ca and Mg	Pan Biotech
Ethylenediaminetetraacetic acid (EDTA)	Roth
Fetal Bovine Serum, qualified, heat inactivated, Brazil	Gibco
HyPure Cell Culture Grade Water (endotoxin-free)	Cytiva
Isoflurane	Piramal Critical Care
Lipopolysaccharide from E. coli O55:B	Sigma Aldrich
Methyl cellulose (viscosity 400 cP)	Sigma Aldrich
Ovalbumin Endofit	InvivoGen
Paraformaldehyde 37%	Biocyc GmbH CO &KG
Penicillin/Streptomycin (10,000 U/mL)	Gibco
Recombinant murine FMS-like Tyrosine kinase 3 ligand	Peprotech
Red blood cell (RBC) lysis buffer (10x)	BioLegend
Roswell Park Memorial Institute medium (RPMI) 1640 (+L-Glutamine)	Gibco
Sodium dodecyl sulfate (SDS)	Sigma Aldrich
TEMED	Roth
Tetramethylbenzidine (TMB)	Mikrogen Diagnostics
Tris	Appllichem
TruStain FcX Plus (anti-mouse CD16/CD32) antibody	BioLegend
Trypsin – EDTA solution	Sigma-Aldrich

2.5. Consumables

Table 6 List of consumables

Consumables	Company
Amicon Ultra-15 centrifugal filters (10K)	Merck Millipore
EASYstrainer Cell strainer 70 μ m, for 50 mL tubes, blue, sterile	Greiner bio-one
General plastic consumables	Sarstedt, Eppendorf
LS columns	Miltenyi Biotec
Luna Cell Counting Slides	Logos biosystems
Polystyrene round-bottom tube with cell-strainer cap (5 mL)	Falcon
qEV original/70nm Gen 2 column	IZON
Ready to use gauze compresses, sterile	MaiMed
Ultra-clear centrifuge tubes	Beckman Coulter

2.6. Buffers and Media

Table 7 Recipes for buffers and media

Buffer/Medium	Composition
MACS buffer	1x PBS
	2 % FBS
	2 mM EDTA
	100 U/mL Penicillin/Streptomycin
DC medium	RPMI 1640
	10 % FBS
	0.055 mM Mercaptoethanol
	100 U/mL Penicillin/Streptomycin
DC infection medium	RPMI 1640
	5 % FBS
	0.055 mM Mercaptoethanol
	100 U/mL Penicillin/Streptomycin
Vero medium	DMEM
	5 % FBS
Vero infection medium	DMEM
	2 % FBS

2.7. Antibodies

2.7.1. Antibodies for Flow Cytometry and FACS

Table 8 Dendritic cell antibody panel #1 (flow cytometry)

Marker	Fluorophore	Clone	Company
CD11c	BV421	N418	BioLegend
CD45R/B220	PE-Dazzle594	RA3-6B2	BioLegend
CD11b	PE	M1/70	BioLegend
CD24	BUV395	M1/69	BD Biosciences
CD80	BV711	16-10A1	BioLegend
CD86	BV650	GL-1	BioLegend

Table 9 Dendritic cell antibody panel #2 (extended) (flow cytometry)

Marker	Fluorophore	Clone	Company
Anti-EBOV GP	self-labeled AF555	5E6	Merck Millipore
Anti-EBOV GP	self-labeled AF555	5D2	Merck Millipore
H-2Kb-SIINFEKL	APC	25-D1.16	BioLegend
CD11c	BV786	N418	BioLegend
CD24	BV605	M1/69	BioLegend
XCR1	BV421	ZET	BioLegend
CD11b	BV510	M1/70	BioLegend
SIRPa	BUV661	P84	BD Biosciences
Siglec-H	Pacific Blue	551	BioLegend
Ly6C	BV570	HK1.4	BioLegend
CD14	FITC	Sa14-2	BioLegend
F4/80	PerCP-Cy5.5	BM8	BioLegend
CD64	BV711	X54-5/7.1	BioLegend
MHC-II	AF700	M5/114.15.2	BioLegend
CD86	BV650	GL-1	BioLegend
CD80	BV711	16-10A1	BioLegend
CD103	BUV395	M290	BD Biosciences

Table 10 T-cell antibody panel (flow cytometry)

Marker	Fluorophore	Clone	Company
CD25	BV711	PC61	BioLegend
CD3e	BUV395	145-2C11	BD Biosciences
CD4	BUV737	GK1.5	BD Biosciences
CD44	BV510	IM7	BioLegend
CD62L	BV785	MEL-14	BioLegend
CD69	BV605	H1.2F3	BioLegend
CD8a	Pe/Cyanine 7	53-6.7	BioLegend

2.7.2. Antibodies for Immunofocus assay

Table 11 Antibodies for immunofocus assay

Antibody	Company
Polyclonal mouse anti-EBOV primary antibody	in-house
Sheep anti-mouse (IgG H+L) HRP-conjugated	Jackson Immuno Research Laboratories, Inc.

2.7.3. Antibodies for Western Blot

Table 12 Antibodies for western blot

Antibody	Company
Rabbit anti-Ovalbumin (3G2E1D9)	Santa Cruz Biotechnology
Goat anti-rabbit-horseradish peroxidase	Thermo Fisher

2.8. Kits

Table 13 List of Kits

Kit	Company
Antibody labeling kit	InvitroGen
BD CompBeads Anti-mouse Ig, κ / negative control compensation particles set	BD Biosciences
BD CompBeads Anti-Rat and Anti-Hamster Ig κ / negative control compensation particles set	BD Biosciences
CD8 ⁺ T-cell isolation kit, mouse	Miltenyi Biotec

CellTrace Violet cell Proliferation kit	Thermo Fisher
Milliplex Mouse CD8 ⁺ T cell Magnetic Bead panel	Merck Millipore
Pierce BCA Protein assay kit	Thermo Scientific
Zombie NIR Fixable Viability kit	BioLegend

2.9. Machines and equipment

Table 14 List of machines and equipment

Machine/ Equipment	Company
5415C Microcentrifuge	Eppendorf
BD FACS Aria III	BD Biosciences
Centrifuge 5810 R	Eppendorf
Cytek Aurora 5-Laser Spectral Flow Cytometer	Cytek Biosciences
Eppendorf Thermomixer C	Eppendorf
Luminex 200	Merck Millipore
Luna II automated Cell counter	Logos biosystems
MACS separators	Miltenyi Biotec
Microcentrifuge, VWR Micro Star 17 R	VWR
Microscope Olympus CKX41	Olympus
NanoSight LM10 with LM14C viewing unit	Malvern Panalytical
Optima XE-90 Ultracentrifuge with SW32 Ti Swing-Bucket-Rotor	Beckman Coulter
Photospectrometer	Eppendorf
qEV original rack	IZON
SDS electrophoresis chamber	BioRad
Sunlab 3D shaker SU1030	Sunlab
Tecnai Spirit TEM	Thermo Fisher Scientific
Transilluminator	Vilber
UVP handheld UV lamp SW&LW 254/365nm	Fisher Scientific
Vortex mixer	Thermo Scientific

2.10. Software

Table 15 List of computer programs and softwares

Program/ Software	Company
Biorender.com	BioRender
FlowJo, V10.9	FlowJo LLC
GraphPad Prism 10	GraphPad Software, Inc
Mendeley	Elsevier
Microsoft Office	Microsoft Corporation
NTA 3.0	Malvern Panalytical
SpectroFlo version 3.1.0	Cytek Biosciences
ViralZone (viralzone.expasy.org)	Swiss Institute of Bioinformatics

3. Methods

3.1. Immune cell isolation and differentiation

Primary immune cells utilized in this study were isolated from organs of donor mice. DCs were differentiated from murine bone marrow and CD8 T cells were directly isolated from mouse spleen.

3.1.1. *In vitro* generation of Dendritic cells

Different DC subsets can be derived from progenitors by harnessing distinct developmental pathways. As the present study focused on the role of cDCs in EBOV infection, we derived cDCs from bone marrow progenitors by stimulation with Flt3L.

3.1.1.1. Isolation of bone marrow progenitor cells

To generate DCs, bone marrow progenitor cells were isolated from femur and tibia bones of C57Bl/6 mice. Mice were euthanized by cervical dislocation under isoflurane anesthesia as per our approved ethics protocol. The skin was removed from the hind limbs before they were cut off above the pelvic-hip joint. Muscles and residue tissue were removed from femur and tibiae with sterile forceps and scissors, and sterile gauze compresses. The clean bones were placed in PBS in a 50 mL tube on ice until all mice were processed and their bones were collected. The following procedure was continued under a laminar flow hood.

Femurs and tibiae were separated with sterile scissors at the knee joint without exposing the bone marrow. The bones were placed in 70 % ethanol for approximately 20 seconds and thereafter, washed twice in PBS for at least 20 seconds. The epiphyses on both ends of the bone were cut to expose the bone marrow. A syringe with a 30-gauge needle, filled with cold PBS, was used to flush out the bone marrow into a 50 mL tube. Bones were flushed with approximately 2 mL until they appeared white. The bone marrow from all bones was pooled unless experimental approach required separation of biological replicates (different mice). The isolated bone marrow in the 50 mL tube was kept on ice.

The bone marrow was gently resuspended by pipetting up and down and transferred to another 50 mL tube through a cell strainer to remove potential bone fragments. The bone marrow was centrifuged at 500xg for 3 min to pellet the cells, the supernatant was discarded and the cells were resuspended in 5-10 mL 1x red blood cell lysis buffer diluted in cell culture grade water. The cells were incubated in red blood cell lysis buffer at room temperature for 3 min before the lysis was stopped by adding 35-40 ml PBS. Bone marrow cells were pelleted by centrifugation

at 500xg for 3 min, supernatant was discarded and cells were resuspended in DC medium. The bone marrow progenitor cells were counted with a Luna automatic cell counter from 10 μ L cell suspension stained with Trypan Blue (1:1 dilution). The cell suspension was diluted in DC medium to a cell concentration of 2×10^6 cells/mL.

3.1.1.2. Differentiation of Dendritic cells from bone marrow progenitor cells

The suspension of bone marrow cells was supplemented with 100 ng/mL recombinant Flt3L. Cells (2×10^6 cells/mL) were seeded into 6-well suspension culture plates with 5 mL per well resulting in 1×10^7 cells/well and were incubated at 37 °C and 5 % CO₂. After 3 days, the cells in suspension were carefully harvested from the 6-well plates and transferred into a 50 mL tube. The wells were carefully flushed with PBS to collect the remaining suspension cells but without detaching the adherent cells. The cells in PBS were collected in a separate tube, pelleted by centrifugation at 300xg for 5 min, the cell supernatant was discarded and the cells were added to the suspension cells harvested before. Half of the medium was replaced with fresh DC medium containing fresh Flt3L. Cells were seeded under the same conditions as described above in new 6-well plates and incubated for another 5 to 6 days depending on the experimental setup. After differentiation, again, only the suspension cells were harvested, discarding the adherent cells. All manipulation of differentiated DCs was done with minimal disturbance to avoid cell activation. Differentiation of bone marrow progenitor cells yielded approximately 1.0 - 1.5×10^7 differentiated DCs per mouse.

3.1.2. CD8 T cells

3.1.2.1. CD8 T-cell isolation from mouse spleen

CD8 T cells were isolated from spleens of Thy1.1xOT-1xC57Bl/6 mice for DC-T cell co-culture experiments. The spleen was taken out with sterile forceps and scissors and placed into a 1,5 mL tube containing 700 μ L cold PBS. Herein, the spleen was cut into pieces with sterile scissors. The spleen pieces were then transferred to a 50 mL tube through a cell strainer. The cell strainer was rinsed with 20 mL PBS, the cells were pelleted by centrifugation at 500xg for 5 min at 4°C and the supernatant was discarded. The cells were resuspended in 5-10 mL 1x red blood cell lysis buffer diluted in cell culture grade water and incubated for 3 min at room temperature before the lysis was stopped by adding 40 mL PBS. The cells were pelleted by centrifugation at 500xg for 5 min at 4°C, supernatant was discarded and the cells were resuspended in 20 mL PBS. Splenocytes were counted with a Luna automatic cell counter from 10 μ L cell suspension stained with Trypan Blue (1:1 dilution). On average, a yield of 1×10^8 splenocytes per mouse spleen was obtained.

From the splenocyte suspension, CD8 T cells were isolated using the CD8 T-cell isolation kit (mouse) from Miltenyi Biotec, following the manufacturer's protocol. Briefly, cells were pelleted by centrifugation at 500xg for 3 min at 4°C and resuspended in 40 µL MACS buffer per 10⁷ cells. Ten microliters of Biotin-antibody cocktail per 10⁷ cells was added to the cell suspension and incubated at 4°C for 5 min. Then, 30 µL MACS buffer per 10⁷ cells and 20 µL anti-biotin microbeads per 10⁷ cells were added to the cell suspension and were incubated for 10 min at 4°C. In the meantime, an appropriate number of LS columns were placed into the magnetic field of a MACS separator and rinsed with 3 mL of MACS buffer. One LS column could be used for a maximum of 2x10⁹ total cells with maximum 10⁸ labeled cells. After incubation with the Microbeads, the cell suspension was added to the column. All flow through, containing the unlabeled enriched CD8 T cells was collected in a 15 mL tube. LS columns were washed with 3 mL MACS buffer and flow through was again collected in the same 15 mL tube. The remaining, labeled cells in the column were not needed and were discarded with the column. CD8 T cells in the flow through were counted with a Luna automatic cell counter as described above. On average, a yield of 4-6 x10⁶ CD8 T cells per mouse was obtained. The cells were pelleted by centrifugation at 500xg for 3 min, the supernatant was discarded and the cells were resuspended in the desired media or buffer.

3.1.2.2. CellTrace Violet staining of CD8 T cells

Isolated CD8 T cells were stained with CellTrace Violet following the manufacturer's protocol. In short, CD8 T cells were resuspended in a 50 mL tube in 1 mL per 10⁶ cells PBS, containing 1 µL/mL CellTrace Violet stock solution. The cell suspension was incubated for 25 min at 37 °C (in incubator). After incubation, the 50 mL tube containing the cell suspension was filled up with RPMI 5% FBS and incubated for another 5 min at 37 °C. Thereafter, cells were pelleted by centrifugation at 500xg for 5 min, the supernatant was discarded and cells were resuspended at 5x10⁶ cells per mL in DC medium. The CD8 T cells were then directly added to the DC cultures for DC-T cell co-culture assays.

3.2. Dendritic cell-T cell co-cultures

Differentiated non-adherent DCs were harvested from the differentiation culture plate (6-well plate) after 8 days of differentiation by carefully collecting the cell culture supernatant including the suspension cells, leaving the adherent cells behind. Each well was carefully flushed with DC medium to collect the remaining suspension cells and loosely adherent DCs. The number of cells at the end of the differentiation was estimated to be 5x10⁶ cells per well. Only as many DCs as needed for a specific experiment or part of experiment were collected from the differentiation plates to avoid unnecessary disturbance of the cells. The cells were collected in

Methods

a 50 mL tube and pelleted by centrifugation at 300xg for 5 min, the supernatant was discarded and the cells were resuspended in 1 mL DC medium per harvested well. The cells were counted with a Luna automatic cell counter and brought to a cell density of 3×10^6 cells/mL. For each DC-T cell co-culture, 100 μ L of this cell suspension was seeded into a 96 U-bottom plate per well (300.000 cells/well).

DCs were stimulated with 50 μ L UV-inactivated cell debris or extracellular vesicles, soluble ovalbumin (final concentration 100 μ g/mL) and 100 ng/mL LPS, or 50 μ L DC medium (mock stimulated). The DCs were incubated with the stimulant for 4-5 hours. In the meantime, the CD8 T cells were isolated from OT-1 mice and stained with CellTrace Violet as described above. Five hundred thousand OT-1 CD8 T cells in 100 μ L DC medium were added to each well of the 96-well plate containing the stimulated DCs.

For the DC-T cell co-cultures with infected DCs, DCs were harvested after 8 days of differentiation, infected or mock infected as described below, and then seeded into the 96-U-bottom well plate. In that case, the DC stimulation and addition of T cells was done 24 hours post-infection.

DC-T cell co-cultures were incubated for 4 days before T-cell activation and proliferation were analyzed.

3.3. Infections

All experimental infections with EBOV described in this study were performed within the BSL4 facility at the Bernhard Nocht Institute for Tropical Medicine in Hamburg in accordance with the institutional safety guidelines. Infection with NDV-GFP was performed in the BSL2 or BSL4 laboratory, depending on the biosafety requirements of any additional experimental procedures.

3.3.1. Infection of Dendritic cells (suspension cells)

Appropriate numbers of non-adherent DCs, according to the experimental setup, were harvested from the differentiation culture, washed with PBS and placed into a 1.5 mL or 2 mL tube, depending on the volume of virus inoculum required later. The cells were transferred into the BSL4 laboratory for infection. Here, the DCs were pelleted by centrifugation at 300xg for 3 min and supernatant was discarded. DCs were resuspended in virus inoculum (MOI 3), which was diluted beforehand in RPMI without FBS. The DCs in virus inoculum were plated into one well of a cell culture plate depending on total volume (<100 μ L: 96-well, <200 μ L: 48-well, <500 μ L: 24-well, <1000 μ L: 12-well, >1000 μ L: 6-well). Cells were incubated with the virus for 1 hour at 37 °C and 5 % CO₂. After incubation, the cells were transferred back into the

original tube. The cells that adhered during infection were detached with accutase, collected in a separate tube, washed with PBS and added to the remaining cell suspension. This step was only required if the cells were not to be transferred back into the same well for subsequent culture, but seeded into other cell culture formats. The cells were pelleted by centrifugation at 300xg for 3 min, the supernatant was discarded and the cells were resuspended in DC infection medium to a cell density of 2×10^6 cells/mL, unless experimental setup required differently (e.g. for DC-T cell co-culture). The DCs were cultured in an appropriate cell culture format according to the total volume.

3.3.2. Infection of Vero E6 (adherent cells)

Vero E6 cells were infected with recombinant EBOV-OVA for collection of cell debris or EVs for the cross-presentation experiments. Vero E6 were seeded in a 6-well plate or T75 flask in Vero medium 24 hours before infection. Prior to infection, the supernatant was discarded and the cells were washed with PBS. The EBOV-OVA stock was diluted in DMEM without FBS for an MOI of 0.1 in a total volume of 750 μ L for 6-well plates or 5 mL for T75 flasks. The cells were incubated with virus inoculum at 37 °C and 5 % CO₂ for 1 hour. After incubation, the virus inoculum was discarded and 3 ml (6-well plate) or 15 mL (T75 flask) Vero infection medium was added to the cells. The cells were incubated for 7 days.

Vero E6 cells were infected with EBOV-OVA or wt EBOV in 24-well plates in the context of focus forming assay as described below.

Vero E6 cells were infected with recombinant NDV-GFP in the context of the interferon bioassay as described below.

3.3.3. Virus inactivation methods

3.3.3.1. Inactivation with Paraformaldehyde or Formaldehyde

Virus-infected cells were inactivated with paraformaldehyde (PFA) for flow cytometry analyses. For that, the cells were harvested from the cell culture plates and pelleted by centrifugation at 300xg for 5 min. The cells were resuspended in 1 mL Cytotfix/Cytoperm containing 4% PFA and transferred to a fresh 1.5 mL tube. The cells were incubated in PFA for 1 hour at room temperature. Afterwards, the cells were pelleted by centrifugation at 500xg for 5 min, supernatant was discarded and the cells were resuspended in PBS for further analysis.

Adherent cells in the cell culture plates were inactivated with 4.5 % formaldehyde (stabilized with methanol and buffered PBS) for focus forming assay. For that, the cell culture supernatant was discarded and the plates were put into a plastic box filled with 4.5 % formaldehyde

(stabilized with methanol and buffered PBS). The plates were incubated for 1 hour, then carefully taken out of the box and washed with tap water.

3.3.3.2. Inactivation by UV-irradiation

Cell culture plates containing cells, cell culture supernatants, virus stocks or EV samples were placed without a lid under the UV-lamp at a distance of 15 cm. Samples or cells were irradiated with UV light of short wavelength (254 nm) for 10 min. Afterwards, the cell culture supernatants or samples were carefully flushed with a 1000 μ L pipette three times per well. The cell culture plate was turned (180°) and was placed back under the UV lamp for a second UV-irradiation for 10 min at a distance of 15 cm. During irradiation, UV light is contained by placing a non-transparent plastic box over the UV-lamp. Successful UV-inactivation was confirmed by immunofocus assay (no infectious virus detectable).

3.4. Isolation of cell debris

For the isolation of cell debris for the cross-presentation experiments, Vero E6 cells were infected with EBOV-OVA (MOI 0.1) in 6-well plates as described above, or left uninfected (mock infected). For each single DC-T cell co-culture cell debris from one well of a 6-well plate was used. All procedures were performed identically for infected and uninfected cells. First, infectious EBOV-OVA in the Vero E6 cultures (6-well plate) were inactivated by UV-irradiation as described above. After inactivation, the cell culture supernatant was transferred into a 50 mL tube. In this step, the supernatant from all the wells of the 6-well plate were pooled to homogenize the cell debris harvest. The cell debris was pelleted by centrifugation at 2000xg for 10 min and the supernatant was carefully but thoroughly removed, leaving only the cell debris pellet with no remaining liquid. 1 mL of the supernatant was stored at -80 °C for the confirmation of absence of infectious viral particles by immunofocus assay at a later timepoint. The cell debris was resuspended in DC medium (50 μ L per well of 6-well plate) for the stimulation experiments. Cell debris was always freshly isolated just before the stimulation.

3.5. Isolation of extracellular vesicles (EVs)

All experiments with EVs were designed according to the guidelines of the International Society for Extracellular Vesicles published as Minimal information for studies of extracellular vesicles (MISEV) 2014 and updated 2018.

Vero E6 cells were infected with EBOV-OVA (MOI 0.1) in T75 flasks as described above, or left uninfected. From these cells, EVs were isolated for cross-presentation experiments. For each cross-presentation reaction EVs from one T75 flask (12-15 million cells) were used. Vero

E6 cells were infected for 5 days, then medium was exchanged for EV-depleted Vero E6 infection medium. Medium was depleted of EVs by ultracentrifugation for 18 hours at 4 °C and subsequently sterile filtered. The cells were kept in culture with EV depleted medium for another 2 days.

Then, the cell culture supernatant was harvested from uninfected and EBOV-OVA-infected flasks in 50 mL tubes for each condition. The supernatant was depleted of dead cells and larger cell debris by differential centrifugation at first 500xg for 5 min and then 2000xg for 10 min. The supernatant was then concentrated with Amicon filter units (cutoff 10 kDa) to a final volume of 0.5 mL by centrifugation at 4000xg for approximately 25 min. From the retained sample EVs were separated from proteins by size-exclusion chromatography with Izon qEV Gen 2 columns.

To determine the elution volume of the EV fraction, 21 fractions of 0.5 mL each from uninfected cells were collected in 1.5 mL tubes. Each fraction was analyzed by nanoparticle tracking analysis for nanoparticle concentration (see below) and by BCA protein assay (see below) for total protein concentration.

As a result, for EV harvest for cross-presentation experiments the first 2.5 mL of eluent were discarded as void volume, then 2 mL were collected as EV fraction, 2 mL as intermediate fraction and finally 2 mL as protein fraction. These results from the uninfected cells were presumed to apply for the infected cells as well. Nanoparticle tracking analysis with the infected cells could not be performed due to biosafety reasons.

The fractions (EV, intermediate, protein) were transferred into one well of a 12-well plate each for UV-irradiation as described above. After UV-inactivating co-isolated virus particles, EV samples were reduced to a volume of 100 μ L/original T75 flask with an Amicon filter unit (cutoff 10 kDa). Isolated EVs were stored at 4 °C overnight for functional experiments the next day. EVs were always freshly isolated for each experiment. To validate the absence of infectious viral particles after UV-inactivation, samples were stored at -80 °C for longer storage for focus forming assay at a later timepoint.

3.6. Analytical methods

3.6.1. Flow cytometry

The suspension cells (DCs or T cells), which were to be analyzed by flow cytometry, were transferred into an appropriately sized tube, depending on the culture format. For EBOV-OVA infected DC cultures, the remaining adherent cells were washed with PBS. Then, accutase was

added to thinly cover the adherent cells for 5 min at 37°C for cell detachment. Detached cells were resuspended in DC medium and transferred to a separate tube, pelleted by centrifugation at 500xg for 3 min and added to the respective suspension cells. For T cells, only the suspension cells were collected.

All cells were pelleted by centrifugation at 500xg for 3 min. An aliquot of the cell culture supernatant was transferred to a 1.5- or 2 mL tube for storage at -80 °C for further analyses. The cells were washed by adding 500 µL PBS, were pelleted by centrifugation at 500xg for 3 min and the supernatant was discarded. The cells were then resuspended in 100 µL Fc-block (1:100 diluted in PBS) and incubated for 10 min at room temperature. The cells were washed as described above and resuspended in 50 µL Zombie NIR (1:500 diluted in PBS) and were incubated protected from light at room temperature for 15 min. Then, without washing, 50 µL of the respective antibody cocktail diluted in PBS was added to the cell suspension and the cells were incubated for 30 min protected from light at room temperature. (Cells were stained with the DC panel #1 or #2, or the T-cell panel as listed in the materials section.) The cells were washed as described above and resuspended in 1 mL of Cytofix/Cytoperm containing 4% PFA for fixation and inactivation. The cells were incubated for 1 hour at room temperature protected from light and then washed as described above. The cells were resuspended in 100-200 µL PBS, depending on estimated cell number, and transferred into FACS tubes through a cell strainer cap. The samples were stored at 4°C protected from light until analysis. The analysis was performed within 3 hours after fixation for all experiments. Measurement was performed with the Cytex Aurora flow cytometer. All available cells in each sample were measured. Single-stained beads or cells were utilized as controls for live unmixing. Data were analyzed using the FlowJo software. Population gates were determined with fluorescence-minus-one (FMO) controls for each marker.

3.6.2. Antibody labeling

Anti-EBOV-GP antibodies clone 5E6 and 5D2 were labeled with Alexa Fluor555 using the antibody labeling kit from Invitrogen following the manufacturer's protocol. First, 1 M solution of sodium bicarbonate was prepared by adding 1 mL of deionized water to the provided vial of sodium bicarbonate (component B). The vial was vortexed until sodium bicarbonate was fully dissolved. Antibodies (25 µg per antibody) were mixed in a 1:1 ratio and diluted to 75 µL total volume with PBS. Then 1/10 of the antibody volume, meaning 7.5 µL, of 1M sodium bicarbonate was added to the antibody solution to raise the pH. The antibody solution was transferred to the vial with the reactive dye and gently inverted a few times to mix. The mixture was incubated for 1 hour at room temperature protected from light and gently inverted every 10 to 15 min.

Meanwhile, the purification column was prepared. For that, purification resin (component C) was stirred and 1 mL of that suspension was added into the column. Resin was allowed to settle down by gravity. Then settling was supported by placing the column in a 15 mL tube and centrifuging at 1100xg for 3 min. More suspension was added until the resin reached 1 mL.

After the incubation, the labeled antibody was purified by transferring the antibody solution dropwise onto the center of the purification column. The solution was allowed to absorb into the resin before the column was placed into a 15 mL tube and centrifuged at 1100xg for 5 min. After centrifugation, the collection tube contained the labeled antibody in approximately 125 μ L PBS, pH 7.2 with 2 mM sodium azide. Free dye remained in the column bed. The labeled antibody was aliquoted and stored at -20°C.

3.6.3. Fluorescence-activated cell sorting (FACS)

Uninfected non-adherent DCs were harvested from differentiation culture after 8 days of differentiation. DCs were stained as described above for flow cytometry analysis with the DC antibody panel #2. DCs remained unfixed and were live sorted using the FACS AriaIII. Conventional DC1 and cDC2 were sorted into separate tubes containing 1 mL DC media. After sorting, the medium was exchanged for fresh DC medium and the separate DC subsets were seeded into one well of 12-well plate each. The cells rested in the incubator overnight and were used for infection, stimulation and DC-T cell co-culture the next day.

3.6.4. Nanoparticle tracking analysis (NTA)

Nanoparticle concentration in a solution was determined by nanoparticle tracking analysis (NTA) using the Malvern Panalytical NanoSight LM14C equipped with a CCD camera. NTA was exclusively performed for EV isolated from uninfected cells. 100 μ L of an EV sample was diluted 1:10 in 0.22 μ m filtered PBS. Approximately 500 μ L of the diluted sample were injected into the capillary of the NanoSight with a 1 mL syringe. The focus of the camera was adjusted. A camera level of 16 and screen gain of 2 were applied as capture settings. A temperature of 25 °C in the capillary was ensured by a thermostat. First capture was taken, then about 50 μ L of sample are advanced into the capillary for the next measurement. The measurement was performed as a “standard measurement” with five captures per sample of 30 sec each. From 5 captures, the mean nanoparticle concentration per mL was calculated by the NTA 3.0 software with a detection threshold of 6 and screen gain of 10. Only measurements with at least 6 particles per frame were defined as valid measurements. After each sample the capillary was rinsed with 5 mL PBS.

3.6.5. Transmission electron microscopy (TEM)

Extracellular vesicles were isolated from uninfected Vero E6 cells as described above. The EV fraction was concentrated by reducing the total sample volume to 1/3 by centrifugation in amicon filter units (10 kDa cutoff). The concentrated EV fraction, intermediate fraction and protein fraction were visualized by TEM. Negative staining of samples and imaging were performed by Dr. Katharina Höhn at the BNITM electron microscopy facility.

Glow-discharged copper grids were placed into the sample solution in 1.5 mL tubes. Samples were loaded onto the grids by centrifugation at full speed in a table-top centrifuge for 15 min. Grids were washed twice with PBS for 3 min, followed by blotting with Whatman paper. The samples were fixed onto the copper grids using 2 % aqueous uranyl acetate for 15 seconds, followed by washing with H₂O for 3 min. The grids were dried at room temperature. Imaging was performed using a Tecnai Spirit electron microscope at 80 kV. Images were recorded with a digital CCD camera.

3.6.6. Immunofocus assay (virus titration)

Immunofocus assays were performed to determine infectious viral (EBOV) particle concentration in a liquid sample, such as cell culture supernatant. The day before the experiment, Vero E6 cells were seeded in 24-well plates with 150.000 cells/well in Vero medium. Test samples were serial diluted (half-logarithmic) in DMEM without FBS in a 96-well plate. The supernatant from Vero E6 cells was discarded, the cells were washed with PBS and 200 µL diluted sample were added to one well each. Cells were incubated with the inoculum for 1 hour. Thereafter, the inoculum was discarded and 1 mL overlay medium, consisting of 2/3 DMEM 5 % FBS and 1/3 methylcellulose, was added to each well. Cells were incubated for 7 days and then inactivated with 4.5 % formaldehyde (stabilized with methanol and buffered PBS). The cells were then permeabilized for 25 min on a shaker with 100 µL/well 0.5 % Triton diluted in PBS. Thereafter, the cells were washed with tap water and blocked with 200 µL/well blocking solution (5% FBS in PBS) for at least 1 hour on a shaker. Blocking solution was discarded without washing and EBOV-infected cells were labeled with an anti-EBOV-NP antibody (mouse, 100 µL/well) 1:2000 diluted in blocking solution. Cells were incubated with the primary antibody over night at 4 °C. The next day, the antibody solution was discarded and cells were washed with tap water. 100 µL secondary antibody (anti-mouse-POD) diluted 1:5000 in blocking solution was added to each well and incubated for 30 min to 1 hour protected from light on a shaker. Thereafter, the cells were again washed with tap water. Then, 100 µL TMB substrate, diluted 1:3 in deionized water were added to each well and incubated for 15-30 min on a shaker protected from light. TMB substrate was discarded and the cells were

washed with tap water. The foci were counted in each well with clear countable foci, and infectious viral particle concentration in focus forming units (FFU)/mL was calculated as (foci number)×5×(dilution factor).

3.6.7. Bead-based cytokine assay (Luminex)

Concentration of cytokines associated with T-cell activation were determined in supernatants of DC-T cell co-cultures with the Milliplex mouse CD8⁺ T cell magnetic bead panel. Beads, antibodies, buffers, quality controls and standards were prepared according to the manufacturer's protocol. DC-T cell co-culture supernatants were thawed and depleted of cell debris by centrifugation at 15.000xg for 10 min. The assay was performed in a black 96-flat-bottom plate following the manufacturer's guidelines. In brief, 25 µL of standard, quality controls, assay buffer as background control and supernatant samples were added in duplicates to the 96-well plate. The wells containing standard, quality controls or assay buffer received 25 µL of RPMI without FBS, whereas wells containing supernatant samples received 25 µL of assay buffer. Then, the beads were vortexed and 25 µL of mixed beads were added to each well. The plate was sealed and incubated with agitation (500 rpm) on a plate shaker overnight at 4°C. The next day, the plate was washed using a handheld magnet. For that, the plate was placed on the magnet and rested for 60 sec to allow the magnetic beads to settle. Then, all supernatant was gently but thoroughly decanted. The plate was taken off the magnet and 200 µL of wash buffer was added to each well. The plate was gently shaken for 30 sec and reattached to the magnet. Beads were again allowed to settle for 60 s before decanting the supernatant. Washing was repeated for a total of 2 washing steps. After washing, the plate was removed from the magnet and 25 µL of detection antibody was added to each well. The plate was sealed and incubated at room temperature with agitation on a plate shaker for 1 hour. Then, without washing, 25 µL of streptavidin-Phycoerytherin were added to each well and incubated for 30 min. Thereafter, the plate was washed twice as described above. The beads were resuspended in 150 µL sheath fluid per well on a plate shaker for at least 5 min. Data were acquired using the Luminex 200 (Merck Millipore). The mean of duplicate fluorescence intensities was used to interpolate cytokine concentrations in supernatants from the standard curve.

3.6.8. Newcastle disease virus (NDV)-based interferon bioassay

Vero E6 cells were seeded in 12-well plates with 2x10⁵ cells in 1 mL Vero medium per well and incubated overnight. DC culture supernatants to be tested were thawed and 750 µL of each sample were transferred into an empty 12-well plate. The samples were inactivated by UV-irradiation as described above. Inactivated DC supernatants were then transferred into 1,5 mL tubes and diluted 1:2, 1:5, and 1:12.5 in DMEM 2 % FBS. Supernatants from Vero E6

cell cultures were discarded and 800 μL diluted and UV-irradiated DC supernatants were added to one well each. Vero E6 cells were incubated with the DC supernatant for 24 hours. The next day, supernatants from Vero E6 cultures were discarded, the cells were washed with PBS and infected with NDV-GFP at MOI =1. NDV-GFP stock was diluted in DMEM without FBS to a final volume of 300 μL per well. The cells were incubated with virus inoculum for 1 hour. The virus inoculum was discarded and 1 mL DMEM with 2 % FBS was added to each well. The cells were incubated for 24 hours. The next day, the cells were harvested by discarding the supernatant, washing with PBS and detaching with 200 μL Trypsin per well. Cells were stained with Zombie NIR and fixed with Cytotfix/ Cytoperm including 4% PFA for flow cytometry analysis as described above. The infection rate was determined as mean fluorescence intensity of GFP of all live cells.

3.6.9. BCA protein assay

The Pierce bicinchoninic (BCA) protein assay was applied to measure total protein concentration of a solution. For that, the manufacturer's protocol was followed. The standard BCA test procedure was applied for samples with high total protein concentration (25-2000 $\mu\text{g}/\text{mL}$). If the upper limit of detection was exceeded, samples were diluted in PBS. If the lower limit of detection was not reached, the measurement was repeated with enhanced BCA test procedure for samples with lower protein concentration (5-250 $\mu\text{g}/\text{mL}$).

Briefly, an albumin standard was diluted in PBS, and the BCA working reagent was prepared by mixing 50 parts reagent A with 1 part reagent B. 0.1 mL of standard or sample was mixed with 2 mL of working reagent. The mixtures were incubated in a water bath for 30 min at 37 °C for the standard procedure, or for 30 min at 60 °C for the enhanced test procedure. After incubating, all tubes were cooled to room temperature. Samples were transferred into cuvettes and the absorption at 562 nm was measured with a spectrophotometer. The absorption of PBS was measured as blank. PBS mixed with working reagent was measured as background. For each sample the measurement was performed in triplicates and mean optical density was used after background subtraction to calculate the protein concentration.

3.6.10. SDS-PAGE and Western Blot

Vero E6 cells were infected with EBOV-OVA or left uninfected. The cells were harvested with trypsin, lysed in 3x SDS lysis buffer and heated for 20 min to 95 °C. Ovalbumin as a positive control was mixed with 2x Laemmli buffer and heated for 5 min to 95°C. A 12% SDS gel was prepared and placed into a SDS chamber, filled with 1x running buffer. The gel was loaded with 10 μL biotinylated protein marker and 15 μL of the samples. Electrophoresis was performed at

Methods

80 V for 15 min and 120 V for 2 hours. Afterwards, the gel was taken out of the chamber, washed with distilled water, stacked onto nitrocellulose membrane between wet Whatman paper and loaded into a blotting chamber. The blotting chamber was filled with 1x transfer buffer, freshly prepared with methanol. Blotting was performed at 60 V for 60 min. Thereafter, the membrane was washed with PBS 0.1% Tween 20 (PBS-T) and blocked with 5 % skimmed milk in PBS-T for 1 hour at room temperature with agitation. The membrane was washed once with PBS-T and incubated with polyclonal anti-ovalbumin antibody diluted 1:1000 in 3 % skimmed milk in PBS-T. The membrane was incubated with primary antibody overnight at 4 °C with agitation. The next day, the membrane was washed 3 times for 10 min with PBS-T and then incubated with secondary antibodies – anti-rabbit-HRP and anti-biotin HRP – for 1 hour at room temperature with agitation. Secondary antibodies were diluted 1:2500 in PBS-T. The membrane was again washed 3 times for 10 min with PBS-T. The membrane was placed inside a foil and 1mL HRP substrate was added onto the membrane. The substrate was incubated on the membrane at room temperature protected from light for 1 min. The substrate solution was then pressed out of the foil and the membrane was imaged with a transilluminator.

3.7. Statistics

Statistical analyses were performed using GraphPad Prism 10 software. Mock-infected and EBOV-infected groups were compared by non-parametrical t-test for unpaired samples (Mann-Whitney test).

4. Results

4.1. Deriving murine conventional dendritic cells *in vitro*

DCs have been identified as early infection targets of EBOV in mouse and NHP models, a finding that initiated studies on DC functionality during EBOV infections.^{47,51} To date, *in vitro* studies on DCs in the context of EBOV infections were based exclusively on DCs derived from monocytes isolated from human peripheral blood or murine bone marrow. However, DCs are a highly heterogeneous class of immune cells with diverse DC subsets with distinct functionality. The present study aimed to expand the knowledge on DC functionality in EBOV infections to other DC subsets, essentially cDCs. For that, cDCs were derived from murine bone marrow progenitor cells *in vitro*.

4.1.1. Differentiation of murine conventional dendritic cells from bone marrow progenitor cells

Murine DCs can be derived *in vitro* from progenitor cells in different ways by harnessing distinct developmental pathways. Classically, DCs are mostly derived *in vitro* from monocytes by stimulation with GM-CSF and IL-4. This method, however, is limited to the generation of mDCs, which are distinct from cDCs. Advances in DC research in recent decades led to the development of novel methods for the generation of DC subsets derived from pre-DCs *in vitro*. Hereby, cDCs and pDCs can be derived from bone marrow progenitor cells by stimulation with Flt3L, mirroring the development of steady state DC subsets *in vivo*. This method was utilized in the present study by adapting procedures of DC differentiation from Naik et al., 2005 and Sadiq et al., 2020. Briefly, bone marrow was isolated from the hind limbs of C57Bl/6J mice and depleted of red blood cells. Bone marrow cells were cultured in DC medium in the presence of recombinant murine Flt3L for up to 9 days with media change after 3 days.

The differentiation procedure was optimized by monitoring the CD11c DC marker expression by flow cytometry in living cells after differentiation for 5 to 9 days, with different concentrations of Flt3L (Figure 9A). The culture of bone marrow progenitor cells without Flt3L stimulation resulted in low cell viability and very low background expression of CD11c (Figure 9B,C). Stimulation with 50-, 100-, 200- and 300 ng/mL Flt3L gave rise to a growing population of CD11c⁺ cells, reaching a maximum population size of around 80 % after 8 to 9 days. There was no difference between the tested Flt3L concentrations, except for the lowest concentration of 50 ng/mL Flt3L at which differentiation initiated slightly slower at early time points (Figure 9B).

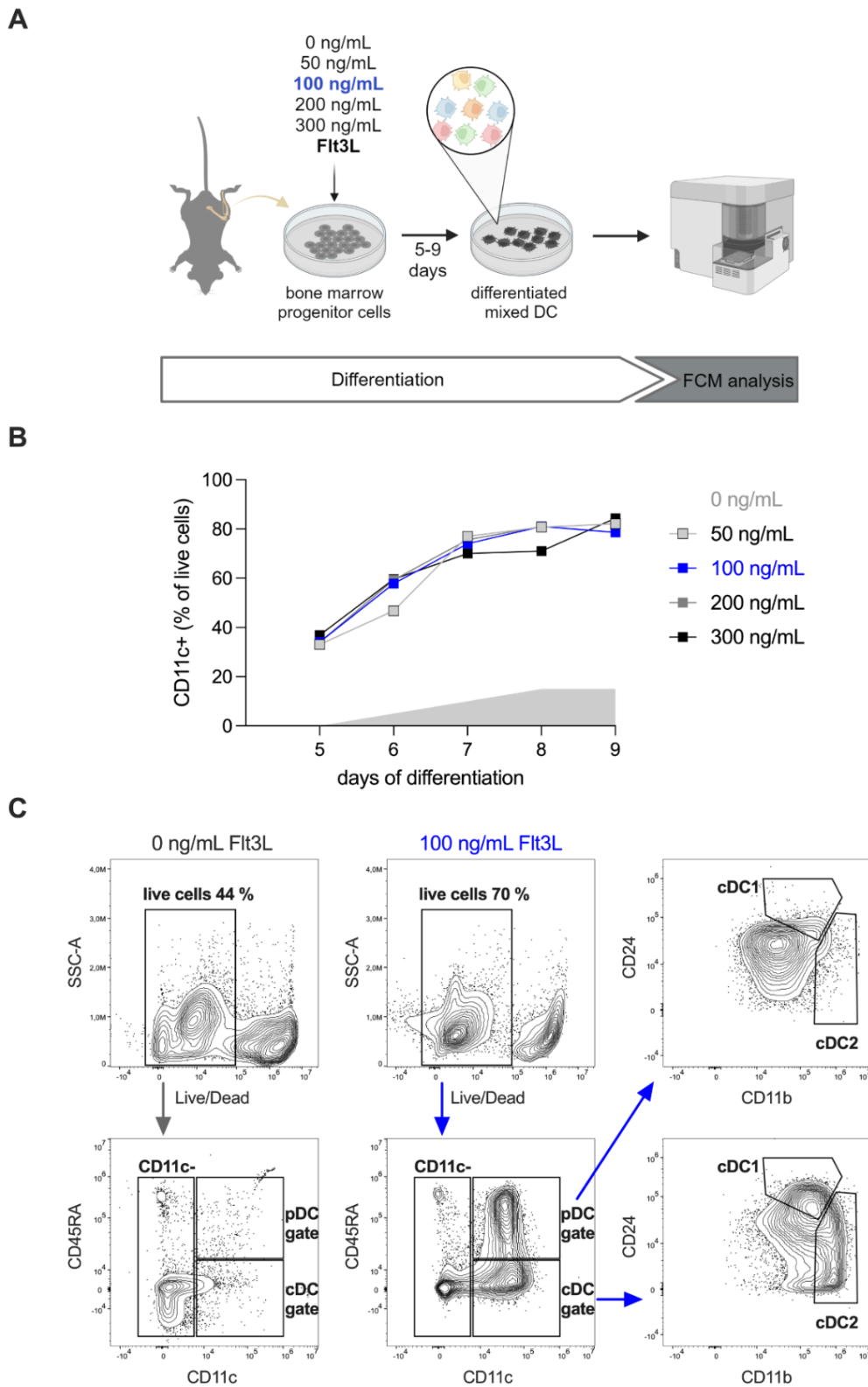


Figure 9 Differentiation of murine DCs from bone marrow progenitors. (A) Experimental procedure: Bone marrow progenitor cells were isolated from hind limbs of C57Bl/6J mice and cultured for 5-9 days with different concentrations of Flt3L. Differentiated DCs were characterized by flow cytometry. (B) Percent of CD11c⁺ cells in live cell population after 5-9 days of differentiation with 0- (grey area), 50-, 100-, 200-, or 300 ng/mL Flt3L. (C) Characterization of DC culture differentiated with 0- (grey) or 100 ng/mL (blue) Flt3L for 8 days. Cells were stained with dendritic cell panel #1. Shown is the gating of live cells, CD11c⁻, pDC, cDC1 and cDC2.

Therefore, 100 ng/mL was the minimum Flt3L concentration chosen for maximum DC yield. These results suggested that a concentration of 300 ng/mL Flt3L as used in the reference studies^{90,91} could be reduced to 100 ng/mL Flt3L without loss of DC differentiation efficiency. In conclusion, for further experiments in this study, DCs were derived from bone marrow progenitor cells by stimulation with 100 ng/mL Flt3L for 8 days.

Differentiation of progenitor cells to different DC subsets was validated by flow cytometry. For that, an antibody panel was adapted from Naik et al., 2005, investigating the expression of CD11c as a general DC marker, CD45RA as a pDC marker, and CD24 and CD11b to distinguish between cDC1 and cDC2, respectively. The selection of markers allowed identification of pDCs, cDC1 and cDC2 like in the reference study (Figure 9C). However, distinction between the different populations was not always clear, especially between cDC1 and cDC2. Also, the pDC gate included some events in downstream cDC1 and cDC2 gating, indicating insufficient separation between pDCs and cDCs. Additionally, recent studies have shown that the applied markers are not exclusively expressed by one DC subset and, therefore, lack specificity.

In conclusion, the data suggested that stimulation of bone marrow progenitor cells with 100 ng/mL Flt3L for 8 days resulted in differentiation into various DC subsets, but an extension of the antibody panel was required for robust characterization of the DC culture.

4.1.2. Extended characterization of the mixed dendritic cell culture

Characterizing a mixed DC culture with respect to current knowledge on DC heterogeneity, requires examination of diverse protein markers. While few protein markers are specific for a certain DC subset, usually a combination of different markers with different expression levels defines a cell type. Here, an extended antibody panel allowed in depth characterization of the mixed DC culture by flow cytometry.

DCs were derived from bone marrow progenitor cells with Flt3L as described above. Differentiation of progenitor cells resulted in a mixed cell culture in which 91 % of live cells expressed the general DC marker CD11c. Of these CD11c⁺ cells, a small population of under 1 % was identified as moDCs (CD11c⁺/CD14⁺/F4/80⁺/CD64⁺/SIRPα⁺/CD11b⁺/XCR1⁻), which also had a higher SSC than the other populations. 18 % of CD11c⁺ cells were cDC1 (CD24⁺/XCR1⁺/CD11b⁻/SIRPα⁻), 10 % were cDC2 (CD24⁻/XCR1⁻/CD11b⁺/SIRPα⁺), and 19 % were pDCs (CD24⁻/XCR1⁻/CD11b⁻/SIRPα⁻/SiglecH⁺/Ly6C⁺) (Figure 10A, C), according to the chosen gating strategy. DC subset population sizes were determined as average percentage of CD11c⁺ cells of five replicates (Figure 10B).

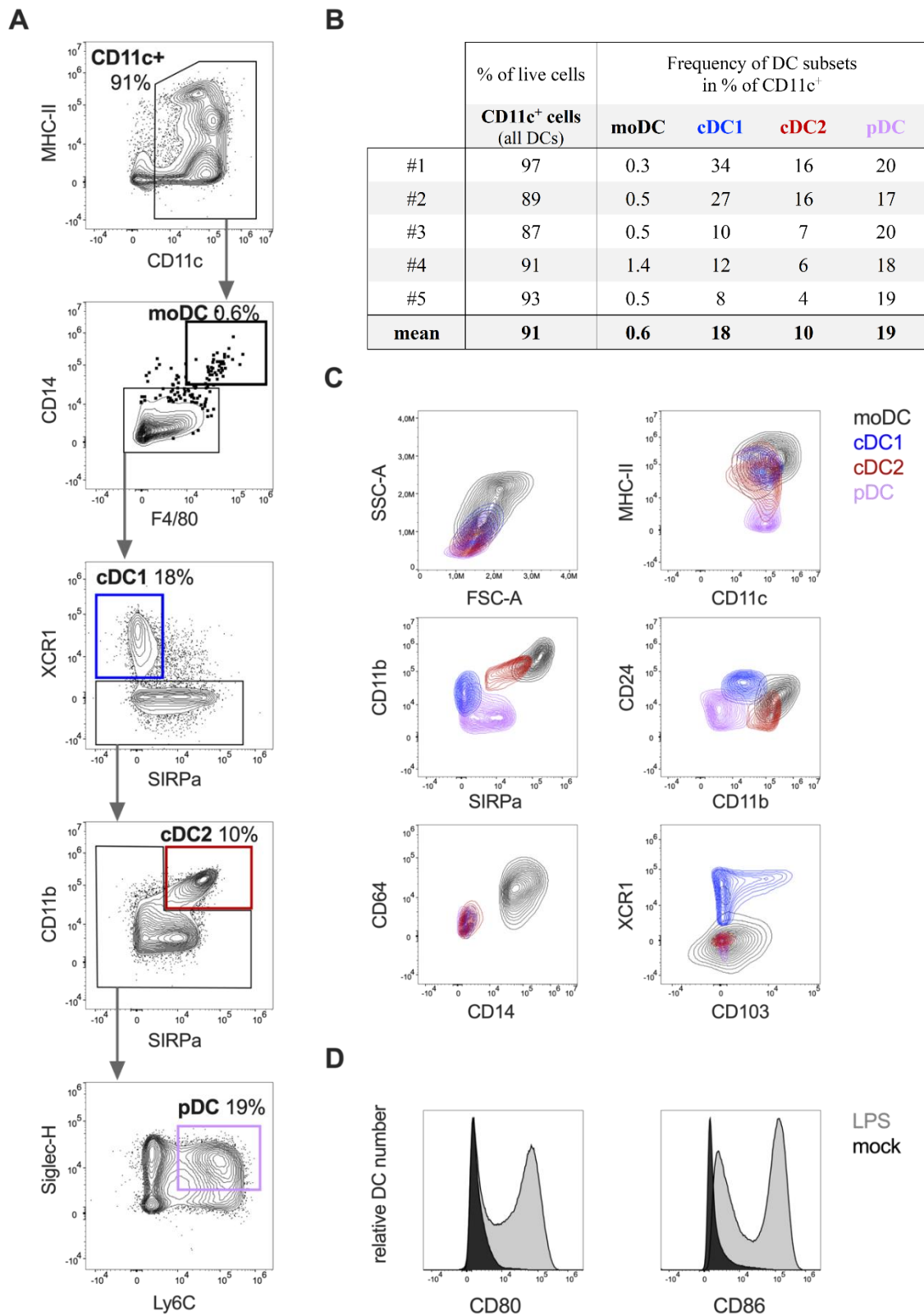


Figure 10 Extended characterization of the mixed DC culture. (A) Gating of CD11c⁺ cells, moDC, cDC1, cDC2 and pDC stained with dendritic cell panel #2. Population of subsets are given in percent of live cells (for CD11c⁺ cells) or in percent of CD11c⁺ cells as mean of 5 replicates. (B) Table of DC subset population sizes in the five replicates and mean values. (C) Further characterization of moDCs (black), cDC1 (blue), cDC2 (red) and pDCs (purple) with selected protein markers. (D) Expression of CD80 and CD86 of CD11c⁺ cells in mock stimulated (black) or LPS-stimulated (grey) cultures.

Some cDC1 also expressed CD103 on the cell surface, a marker commonly expressed on cells with a migratory phenotype (Figure 10C). The remaining CD11c⁺ cells could not be assigned to a fully differentiated DC subset but represent DC progenitors. This is supported by the fact that Siglec-H expression is high in many of these progenitors (Figure 10A).

Generally, all CD11c⁺ cells showed low expression of the maturation markers CD80 and CD86 indicating an immature phenotype. To test whether the DCs could be activated, LPS was added to the cell culture supernatant during the final 24 hours of differentiation. Stimulated DCs showed increased expression of CD80 and CD86 compared to unstimulated DCs (Figure 10D).

In summary, these data indicated that the differentiated DC culture included defined populations of fully differentiated cDC1, cDC2, pDCs, and some moDCs, but also consisted of not fully differentiated DC progenitors. The DC culture presented with an immature phenotype but DCs matured upon LPS stimulation.

4.2. Infection of dendritic cells with EBOV-OVA

Previous EBOV studies in mice suggested that DC subsets are not equally infectable by EBOV.⁵¹ Here we wanted to examine which DC subsets are infectable with EBOV *in vitro*. Viral tropism, meaning the ability of a virus to infect and replicate in a certain cell type, depends on several factors. Whether a virus is able to infect a cell depends initially on the presence of matching cell surface receptors or attachment factors to facilitate virus uptake. Through its glycoprotein, EBOV can bind to many different surface receptors, making many cell types susceptible for EBOV attachment³⁰. However, viral attachment is only the initial step of viral entry. Moreover, a virus has to be able to evade the lysis in the endosome inside the cell. Here, studies have shown that EBOV utilizes the endosomal receptor Niemann-Pick C1 (NPC1)¹³⁸, which is also abundantly expressed in various cell types, including DCs, making them potentially permissive for EBOV. Beyond virus entry, cell tropism is also determined by the ability of the virus to replicate within the cell, which is often suppressed by cell intrinsic innate immune mechanisms.

4.2.1. EBOV cell tropism for different dendritic cell subsets *in vitro*

To determine which DC subsets allowed EBOV entry and replication *in vitro*, we infected the mixed DC culture with recombinant EBOV-OVA (Figure 11A). We aimed to identify the infected cells by taking advantage of molecular processes within infected cells. Firstly, viral replication in the cell leads to location of viral surface proteins, namely EBOV-GP, on the cell surface for viral budding. Therefore, we reasoned that infected DCs could be identified by surface expression of EBOV-GP. Secondly, viral antigens expressed within an infected cell are

Results

cleaved into peptides and loaded onto MHC-I molecules for antigen presentation on the cell surface. Thus, we made use of the model antigen ovalbumin (OVA) expressed upon replication of EBOV-OVA. Expression of OVA upon EBOV-OVA replication was validated by western blot (Supplementary Figure 1). In the infected cell, OVA is cleaved into the H-2Kb-restricted immunodominant CD8 T-cell peptide SIINFEKL, which is subsequently loaded onto MHC-I. These MHC-I-SIINFEKL complexes on the cell surface can be detected using the specific monoclonal antibody 25-D1.16.¹³⁹ Detection of EBOV-GP and MHC-I-SIINFEKL on the cell surface allowed us to identify EBOV-infected cells within an infected mixed DC culture.

We infected the mixed DC culture with EBOV-OVA at an MOI of 1 and 3, or mock infected them with RPMI without FBS. Twenty-four hours post infection we harvested the cells and stained them for flow cytometry analysis with antibodies of the extended DC characterization panel #2, as well as anti-EBOV-GP and anti-MHC-I-SIINFEKL (25-D1.16) antibodies. The infection experiment with EBOV-OVA at an MOI of 3 was repeated 5 times. The experiment revealed that less than 1 % of all CD11c⁺ cells were infected with EBOV-OVA, independent of the MOI. These results indicated that the overall infection rate of a mixed DC culture is generally low and was presumably saturated at the MOI of 3 (Table 16).

Examining the DC subsets in detail, we found that the small population of moDCs showed the highest infection rate of 44-83 %. Besides moDCs, EBOV-OVA positive cells could be detected within the cDC2 population, even though at a much lower infection rate of 1-5 %. cDC1 and pDC on the other hand, were refractory to the infection, like all remaining CD11c⁺ DC progenitor cells in the culture. In the mock infected cultures, no EBOV-OVA-infected cells were detectable, highlighting the specificity of the double staining procedure (Figure 11B, Table 16).

To confirm that the detection of EBOV-GP and MHC-I-SIINFEKL on the cell surface was a result of viral replication, we inactivated EBOV-OVA by UV-irradiation prior to infection. As UV-irradiation damages the genomic RNA of the virus, but leaves the proteins functional, the virus still enters the cell, but viral replication is obviated. We did not detect any cells expressing EBOV-GP and MHC-I-SIINFEKL upon infection with UV-inactivated EBOV-OVA (Table 16). These results emphasized that our procedure specifically detected cells that supported viral replication.

Previous studies suggested, that EBOV infection rates are increased in mature moDCs compared to immature moDCs.³⁵ Therefore, we also wanted to test, whether a previous activation of the mixed DC culture increased EBOV infection rates. For this, we stimulated the DCs with LPS during the final 24 hours of differentiation and infected them with EBOV-OVA

at an MOI of 3 for 24 hours. However, infection rates were not augmented by prior activation (Table 16).

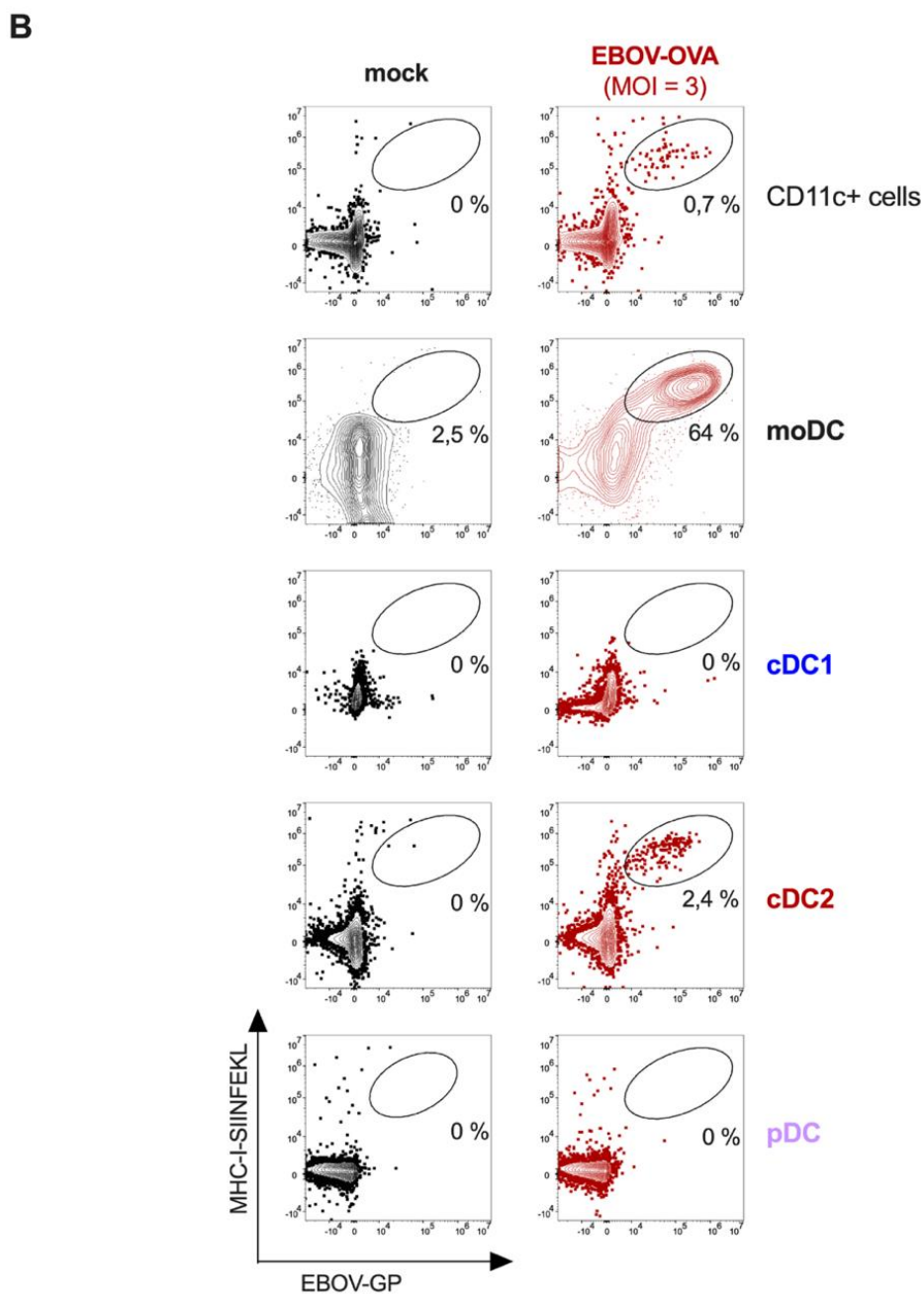
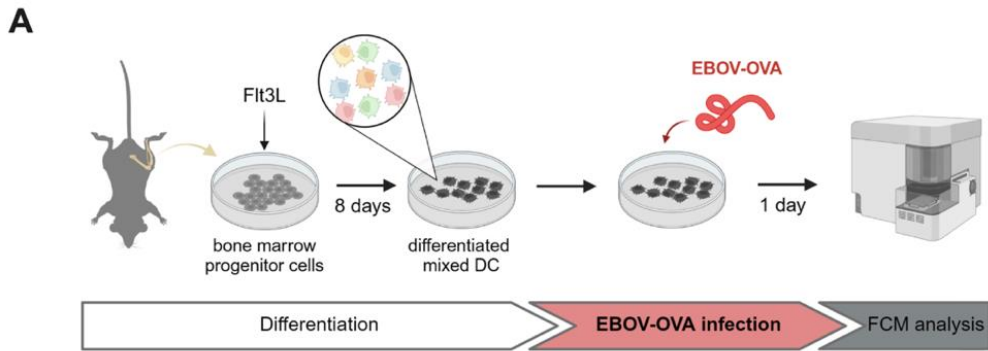


Figure 11 EBOV-OVA infection of the mixed DC culture. (A) Experimental setup: A mixed DC culture was derived from mouse bone marrow progenitor cells by stimulation with Flt3L for 8 days. DC were mock infected or infected with EBOV-OVA. Infected DCs were characterized by flow cytometry one day post-infection. (B) Surface expression of EBOV-GP and MHC-I-SIINFEKL in CD11c⁺ cells, moDC, cDC1, cDC2, and pDC in mock infected (black) and EBOV-OVA infected (red) cultures. Gate on double positive cells represents EBOV-OVA infected cells. Infection rate in percent is the mean of 5 replicates. Shown is one representative experiment. Values from individual experiments are presented in Table 16.

Table 16 EBOV-OVA infection rate in different DC subsets under various conditions.

		Frequency of EBOV-OVA positive cells in % of DC subset					
condition		CD11c ⁺ cells	moDC	cDC1	cDC2	pDC	all other cells
MOI 3	#1	0.54	71.9	0.01	0.73	0.01	0.09
	#2	0.74	67.2	0.01	1.72	0.00	0.04
	#3	0.94	81.9	0.01	4.96	0.02	0.03
	#4	0.83	43.7	0.00	3.16	0.02	0.01
	#5	0.42	55.2	0.01	1.61	0.04	0.02
	mean	0.70	64.0	0.01	2.44	0.02	0.04
MOI 3	LPS	0.93	35.1	0.00	1.01	0.01	0.00
	UV	0.02	0.26	0.00	0.03	0.01	0.00
MOI 1		0.82	83.3	0.00	1.07	0.01	0.01

= replicate number, LPS = stimulation of DCs with LPS 24 hours prior to infection, UV = UV-inactivation of EBOV-OVA prior to infection

EBOV has a slow replication cycle. It is estimated that it takes about 30 hours before an infected cell releases infectious virions.¹⁴⁰ To test whether the infection rate in EBOV infected DC cultures increased over time, we examined the infection rate at day 1, 2 and 3 post infection. The infection rate did not increase over a period of 3 days, but rather reduced mildly. Simultaneously, cell viability decreased stronger in EBOV infected cultures from 81 % to 62 %, compared to mock infected cultures from 84 % to 78 % from day 1 to day 3 post-infection (Table 17). These data suggested that the mixed DC culture did not support productive viral replication over time.

In summary, we inferred from our data that moDCs and cDC2 were preferred initial infection targets of EBOV, while cDC1 and pDCs were spared from infection.

Table 17 Cell viability and infection rate in mock infected and EBOV-OVA infected DC cultures (MOI 3) and EBOV-OVA infection rate in different DC subsets 1-3 days post infection (dpi).

time	mock	EBOV-OVA infected (MOI 3)			
	cell viability in %	cell viability in %	Frequency of EBOV-OVA positive cells in % of DC subset		
			CD11c ⁺ cells	moDC	cDC2
1 dpi	84	81	0.74	67	1.72
2 dpi	84	74	0.60	63	0.88
3 dpi	78	62	0.52	35	0.85

4.2.2. Activation of dendritic cells upon EBOV infection

The functionality of DCs is based on their ability to be activated after encountering stimulating factors. Upon activation, also called maturation, DCs undergo morphological, phenotypical and functional changes. DC activation can be induced by detection of PAMPs or DAMPs by pattern recognition receptors (PRRs). EBOV-GP and EBOV-RNA are such PAMPs that can potentially be detected by PRRs on the DC surface or in the DC cytosol. Previous studies, however, suggested that EBOV inhibits maturation of infected moDCs through the capacity of two viral proteins, VP35 and VP24, to antagonize the IFN-I response^{57,58}, which is required for DC activation.^{141,142} Here, we investigated whether a mixed DC culture showed signs of maturation upon EBOV-OVA infection.

For that, DCs were infected with EBOV-OVA at an MOI of 3 for 24 hours and stained for flow cytometry analysis. The surface expression of the DC activation markers CD80 and CD86, which are involved in co-stimulation for T-cell activation, were examined to validate maturation.

CD11c⁺ cells in uninfected cultures showed an immature phenotype characterized by low surface expression of CD86 and CD80, but were activated upon stimulation with LPS. In comparison to LPS-stimulated cultures, CD11c⁺ cells in an EBOV-OVA infected culture showed mild activation as CD86, but not CD80, was upregulated in some cells. Of note, specifically the EBOV-OVA infected cells within an EBOV-OVA infected culture were highly activated (Figure 12A). Looking at the separate DC subsets, we found that cDC1, despite being spared from infection showed a mild upregulation of CD86, but not CD80, suggesting at least a partial activation. In the cDC2 population, EBOV-infected as well as some uninfected cells showed upregulation of CD86. CD80 only increased in infected cDC2. pDCs remained

immature upon EBOV-OVA infection or LPS-stimulation. Conversely, moDCs presented with a high basal expression of CD80 and CD86 already in uninfected cultures, which increased only mildly upon EBOV-OVA infection (Figure 12A,B). The DC activation seemed to be replication dependent as cultures infected with UV-inactivated EBOV-OVA did not show the same upregulation of CD86 (Supplementary Figure 2).

Both, pDCs as well as cDCs have been shown to secrete IFN-I upon infection with different viruses.¹⁴³ To test whether the mixed DC culture releases IFN-I upon EBOV-OVA infection, we performed a Newcastle disease virus (NDV)-GFP-based IFN bioassay. The assay is based on the fact that NDV is highly IFN sensitive, meaning that cells that have been stimulated with IFN were protected from NDV infection. Vero E6 cells are utilized for this assay. These cells are deficient in IFN production, but can react to external IFN and induce an antiviral state. The NDV-infection rate of Vero E6 cells is initially very high but will be reduced if the cells were previously stimulated with IFN. We collected cell culture supernatants from uninfected, EBOV-OVA or NDV-GFP-infected DCs and inactivated the samples by UV-irradiation to prevent replication of viruses from the DC supernatant. Vero E6 cells were stimulated with a serial dilution of DC culture supernatants for 24 hours. Then, Vero E6 cells were infected with NDV-GFP for 24 hours. The NDV-GFP infection rate was determined by flow cytometry and analyzed as mean fluorescence intensity (MFI) of GFP. We found that Vero E6 cells stimulated with supernatants from NDV-infected DCs showed a lower infection rate of NDV-GFP than Vero E6 cells stimulated with supernatants from uninfected DCs, or unstimulated Vero E6 cells. The complete inactivation of NDV-GFP in supernatants from NDV-GFP infected DCs was validated by the absence of GFP signal in stimulated Vero E6 cells. These controls validated the experimental procedure.

Supernatants from EBOV-OVA infected DCs did not reduce the NDV-GFP infection rate in Vero E6 cells compared to the controls, suggesting that the DCs did not release IFN-I in amounts detectable by this assay (Figure 12C).

In summary, the mixed culture showed little increase of overall activation upon EBOV-OVA infection. Looking at infected as well as some uninfected, bystander cDC2 in more detail we found individual cells that were highly activated. Also uninfected cDC1 showed signs of maturation. moDCs had a comparably high basal expression of CD80 and CD86, which increased only mildly in spite of high EBOV infection rates.

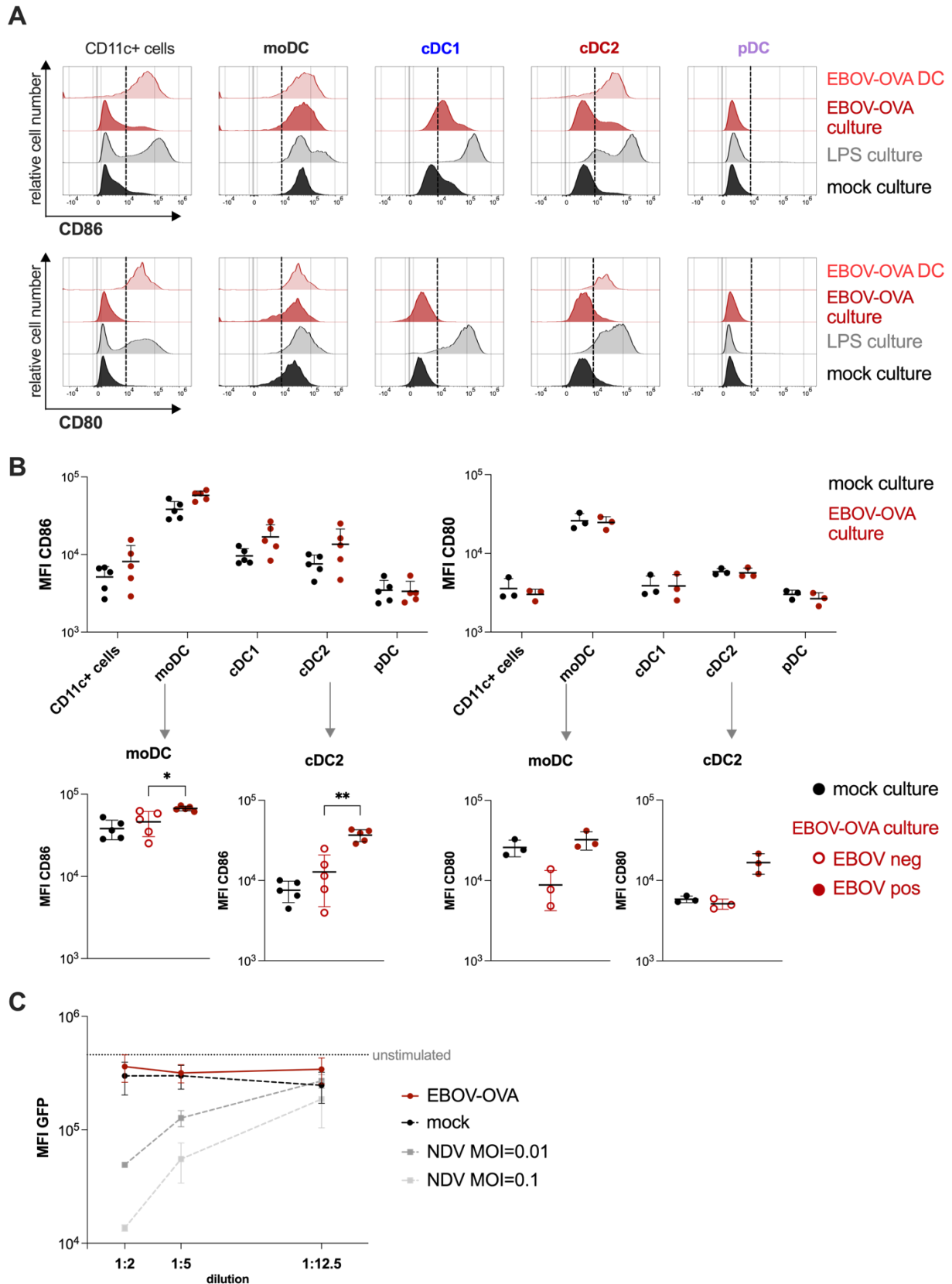


Figure 12 DC activation upon EBOV-OVA infection. A mixed DC culture was infected with EBOV-OVA (MOI 3) or mock infected for 24 hours and then analyzed by flow cytometry. (A) Expression of CD86 and CD80 in CD11c⁺ cells, moDCs, cDC1, cDC2 and pDCs in mock infected- (black), LPS stimulated – (grey), EBOV-OVA infected cultures (dark red) and EBOV-OVA infected cells (DCs)

within an infected culture (light red) is shown as histograms. **(B)** Mean fluorescence intensities (MFI) of CD86 (n=5) and CD80 (n=3) in CD11c⁺ cells, moDCs, cDC1, cDC2 and pDCs in EBOV-OVA infected- (red) compared to mock infected cultures (black) are shown for the different experiments on the upper panel. MFI of CD86 and CD80 in moDC and cDC2 in mock infected culture (black), and EBOV-OVA negative cells (red, empty) or EBOV-OVA positive cells (red, filled) within an infected DC culture are shown in the lower panel. Unpaired non-parametric t-test (Mann-Whitney test) was performed to analyze differences between the MFI, *p<0,05, ** p<0,01 **(C)** NDV-based IFN bioassay. MFI of GFP in Vero E6 cells infected with NDV-GFP (MOI 1) after stimulation with DC culture supernatant from EBOV-OVA infected (red, n=4), mock infected (black, n=4), or NDV-GFP infected (grey, MOI 0.1 and 0.01, n=2) cells. Each point presents mean with standard deviation.

4.3. An *in vitro* DC-T cell co-culture model to study T-cell activation

In order to examine the ability of DCs to activate T cells *in vitro*, we adapted a DC-T cell co-culture model by Sadiq et al., 2020. The setup utilizes OVA as a model antigen, which is widely used in immunological studies, especially in allergy- or cancer studies investigating DC-T cell interactions. OVA, taken up by murine DCs, is cleaved into the H-2Kb-restricted CD8 T-cell peptide SIINFEKL, which is subsequently loaded onto MHC-I for antigen presentation on the cell surface. The MHC-I-SIINFEKL-complex can be recognized by the transgenic T-cell receptor (TCR) of CD8 T cells from transgenic OT-1 mice.¹³⁵ These OVA-specific CD8 T cells were utilized in the DC-T cell co-culture setup in this study.

DCs can only provide sufficient co-stimulation for T-cell activation if they are activated themselves. Therefore, we first wanted to test, if DCs were activated upon stimulation with soluble OVA (sOVA). For that, we generated DCs from mouse bone marrow progenitor cells by stimulation with Flt3L for 8 days. The mixed DC culture was pulsed with different concentrations of sOVA or 100 ng/mL LPS for 5 hours. Expression of CD80 and CD86 was examined by flow cytometry to examine DC activation (Figure 13A). Stimulation with 0.1-, 1-, 50-, 100- and 250 µg/mL sOVA resulted in the same expression levels of CD80 or CD86 as mock stimulation. Stimulation with LPS, on the other hand, increased expression of CD80 and CD86 (Figure 13B). These data, showing that sOVA alone did not activate DCs, strongly suggested that addition of LPS to DCs stimulated with OVA will be required for efficient T-cell activation.

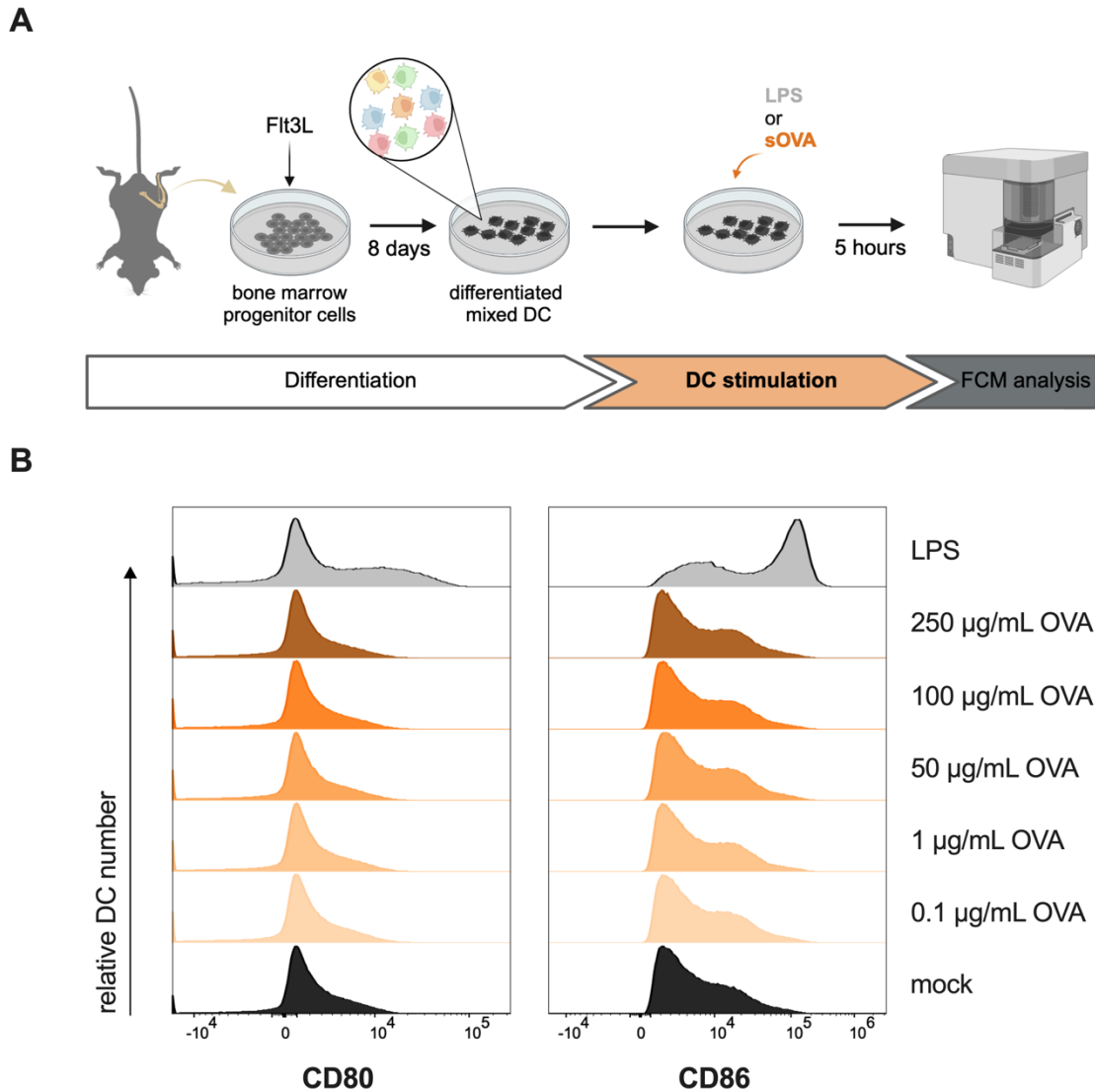


Figure 13 DC activation upon sOVA and LPS stimulation. (A) Experimental setup: A mixed DC culture was derived from mouse bone marrow progenitor cells by stimulation with Flt3L for 8 days. DC were stimulated with sOVA or LPS for 5 hours. DC activation was analyzed by flow cytometry. (B) Expression of CD80 and CD86 of CD11c⁺ cells after stimulation with 0- (black), 0.1-, 1-, 50-, 100 or 250 µg/mL sOVA (orange) or 100 ng/mL LPS (grey).

Next, we wanted to test, whether the sOVA-pulsed DCs can activate OT-1 CD8 T cells, and wanted to optimize the DC-T cell co-culture model. DC-T cell ratio and co-culture time were optimized to the conditions described in the following passage (Supplementary Figure 3).

We pulsed 300,000 DCs with 100 µg/mL sOVA and 100 ng/mL LPS, only sOVA, only LPS, or left them unstimulated. After 4 hours of stimulation 500,000 CellTrace Violet-stained OT-1 CD8 T cells were added to each condition. The DC-T cell co-culture was incubated for 4 days. After that time, cells were harvested from the co-culture and T cells were analyzed by flow cytometry (Figure 14A). T cells were identified by expression of CD8 (Figure 14B). T-cell

Results

proliferation was assessed as signal reduction of the proliferation dye CellTrace Violet. Generally, T cells that were originally added to the co-culture and did not proliferate show a high signal intensity for CellTrace Violet. However, upon proliferation, CellTrace Violet becomes more and more diluted with each cell division, which can be seen in the proliferation plot. Furthermore, T-cell activation was assessed by expression levels of the surface activation markers CD69, CD25, CD44 and CD62L.

DCs stimulated with sOVA and LPS induced strong T-cell proliferation, while unstimulated DCs and control cells stimulated only with sOVA or LPS, failed to induce robust T-cell proliferation (Figure 14C). We tested the T-cell activation capacity of DCs stimulated with different concentrations of sOVA and LPS. The strongest T-cell proliferation was measured for co-cultures with DCs stimulated with 100-, and 50-, and 10 $\mu\text{g}/\text{mL}$ sOVA and LPS, suggesting that the T-cell activation capacity was maximized at these concentrations. While T-cell proliferation was still induced by DCs stimulated with 10 $\mu\text{g}/\text{mL}$ sOVA and LPS, lower concentrations failed to do so. DCs stimulated with 100 $\mu\text{g}/\text{mL}$ sOVA induced T-cell proliferation for 7 generations, which is indicated by the number of peaks in the proliferation plot. Stimulation of DCs with 50-, and 10 $\mu\text{g}/\text{mL}$ sOVA even reached a total of 8 and 9 generations respectively. Moreover, the generation “0” peak is higher in cultures stimulated with 10 $\mu\text{g}/\text{mL}$ sOVA than in cultures stimulated with higher sOVA concentrations, which suggests that initially less T cells have been driven into proliferation upon stimulation with lower sOVA concentrations (Figure 14D). In conclusion, DCs pulsed with 100 $\mu\text{g}/\text{mL}$ sOVA and LPS induced a stronger T-cell proliferation than lower sOVA concentrations. Additionally, proliferating T cells showed high expression of the T-cell activation markers CD44, CD69 and CD25 and low expression of CD62L (Figure 14E).

Taken together, these results established the optimal conditions for the DC-T cell co-culture model. T-cell proliferation and activation by DCs pulsed with 100 $\mu\text{g}/\text{mL}$ sOVA and 100 ng/mL LPS was included as positive control for all following experiments. This study is based exclusively on data from DC-T cell co-culture experiments with a positive control, even if data of the positive control are not depicted. Data from experiments in which the positive control failed were excluded (n=2).

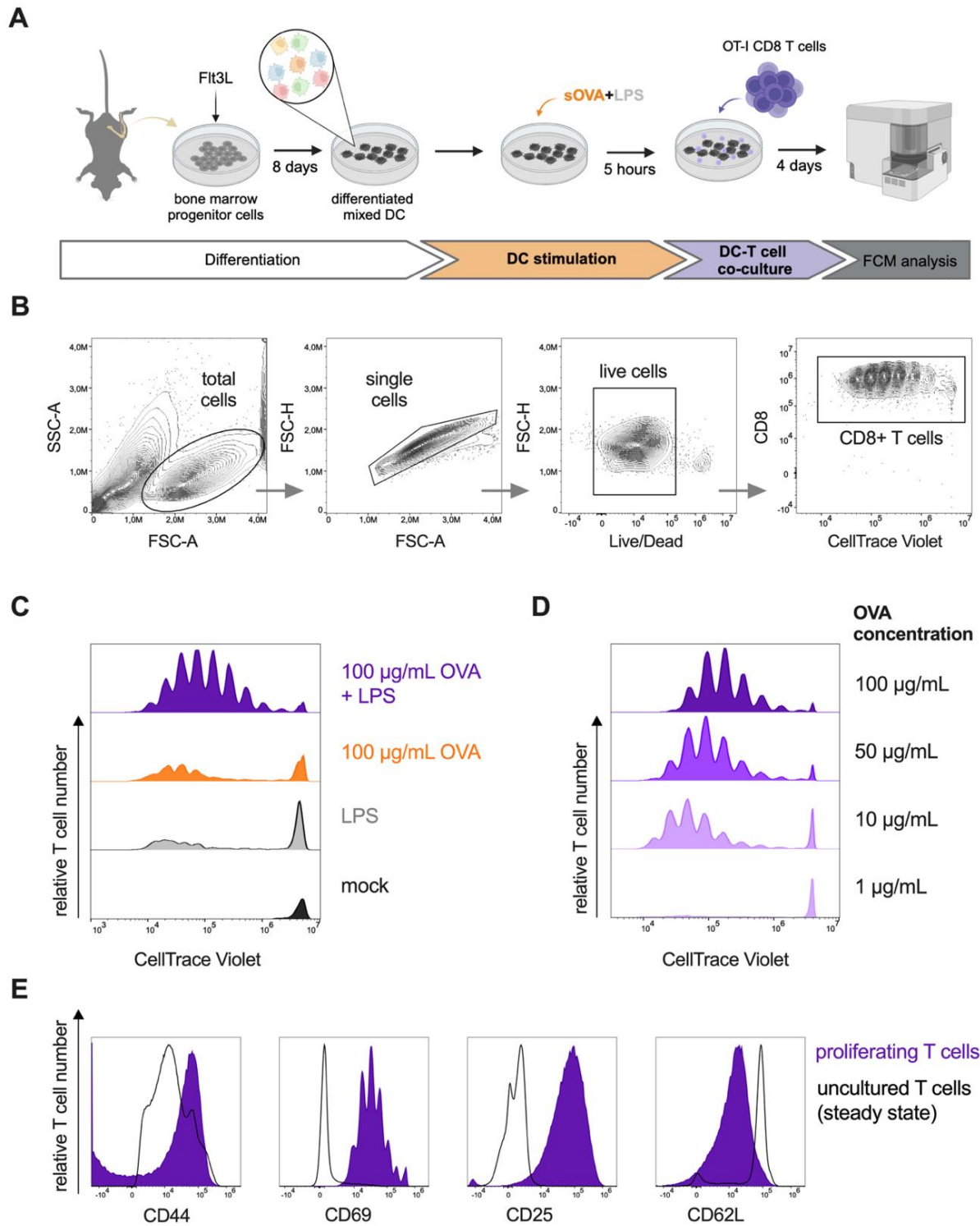


Figure 14 T-cell proliferation and activation induced by sOVA pulsed DCs. (A) Experimental setup: A mixed DC culture was stimulated with sOVA and LPS for 5 hours and subsequently co-cultured with CellTrace Violet stained OT-1 CD8 T cells. T-cell proliferation and activation was assessed by flow cytometry. (B) Examples for gating of CD8⁺ cells in live cell population. (C) T-cell proliferation as signal reduction of CellTrace Violet induced by DCs stimulated with 100 $\mu\text{g/mL}$ sOVA and 100 ng/mL LPS (purple), only 100 $\mu\text{g/mL}$ sOVA (orange), only LPS (grey), or mock stimulation (black) or (D) 0.1-, 1-, 10-, 50-, 100 $\mu\text{g/mL}$ sOVA and 100 ng/mL LPS. T-cell proliferation is shown as histogram plots for the CellTrace Violet signal. (E) Expression of CD44, CD69, CD25, and CD62L in proliferating T cells (purple) compared to uncultured steady state T cells (black line).

4.4. T-cell activation by EBOV-OVA-infected dendritic cell cultures

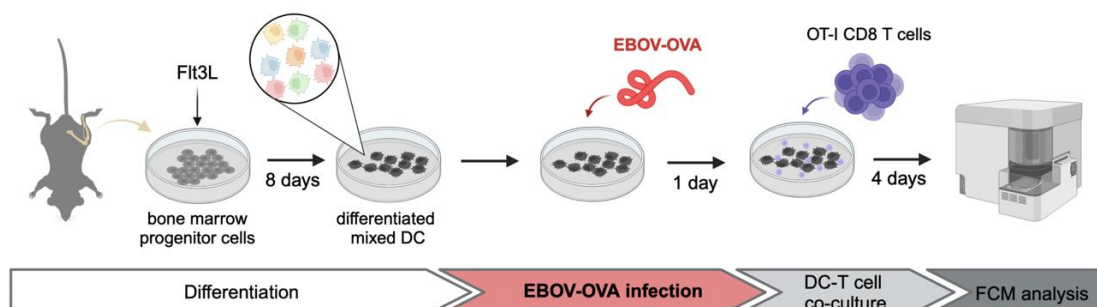
With the established OVA-based DC-T cell co-culture model, we were able to study the DC-T cell interaction in the context of EBOV-OVA infection *in vitro*. First, we investigated whether an EBOV-OVA infected mixed DC culture was able to activate OVA-specific CD8 T cells. For that, we infected the mixed DC culture with EBOV-OVA at different MOIs. Twenty-four hours post-infection, OT-1 CD8 T cells were added to the infected DC culture according to the established co-culture model described above. After 4 days, T-cell proliferation and activation was examined by flow cytometry (Figure 15A). All DC cultures infected with EBOV-OVA successfully induced T-cell proliferation, while wt EBOV infected, and mock infected DCs failed to do so. All EBOV-OVA infected DC cultures induced 5 generations of T-cell division (5 peaks). However, CD8 T cells activated by DCs infected with EBOV-OVA at an MOI of 3 reached the highest absolute T-cell number at time of analysis. Infections at lower or higher MOI than 3 resulted in lower absolute T-cell numbers (Figure 15B).

To confirm that T-cell proliferation was due to EBOV-OVA infection and replication, DCs were infected with UV-inactivated EBOV-OVA at an MOI of 3. These DCs induced only weak T-cell proliferation with low absolute T-cell numbers at end point (Figure 15B). These data suggested that some background T-cell proliferation was attributed to infection-independent T-cell activation, possibly due to cross-presentation of sOVA from the EBOV-OVA virus stock. However, this background proliferation was considerably lower than the T-cell proliferation observed in EBOV-OVA infected DC-T cell co-cultures.

All proliferating T cells showed high expression of the T-cell activation markers CD44, CD69 and CD25, and low expression of CD62L compared to uncultured steady-state T cells (Figure 15C). This data indicated that proliferating T cells were highly activated.

In summary, our data suggests that an EBOV-OVA infected mixed DC culture was able to activate cognate CD8 T cells and induced robust T-cell proliferation.

A



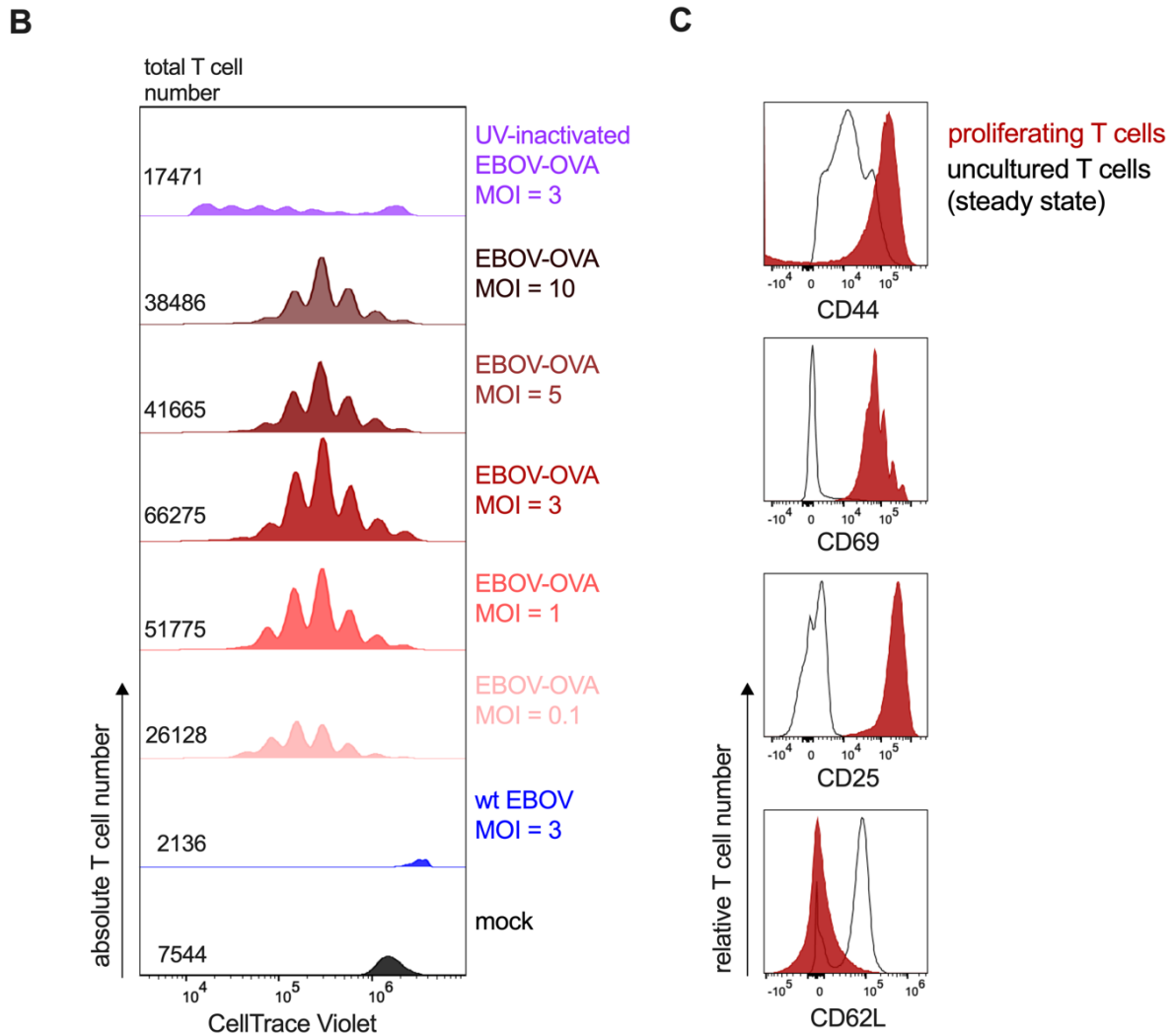


Figure 15 T-cell proliferation and activation by EBOV-OVA infected DCs. (A) Experimental setup: A mixed DC culture was infected with EBOV-OVA. 24 hours post infection DCs were co-cultured with CellTrace Violet stained OT-1 CD8 T cells. T-cell proliferation and activation was assessed by flow cytometry. (B) T-cell proliferation induced by DCs infected with EBOV-OVA at MOI of 0.1, 1, 3, 5, and 10 (red from light to dark), UV-inactivated EBOV-OVA (purple), wtEBOV (blue), and mock-infected DCs (black) is shown as histogram plots of CellTrace Violet. (C) Expression of CD44, CD69, CD25, and CD62L in proliferating T cells co-cultured with EBOV-OVA infected DCs (MOI=3, red) compared to uncultured steady state T cells (black line). Depicted are the results from one representative experiment.

4.5. The role of cross-presentation in T-cell activation during EBOV infection

Generally, direct infection of DCs is not required for antigen presentation on MHC-I, because DCs bear the capacity to direct exogenously acquired antigens to MHC-I in a process called cross-presentation. In consequence, not only EBOV-OVA infected DCs may be able to activate OT-1 CD8 T cells, but also uninfected DCs that acquired antigens from infected cells. Due to

the fact that less than 1 % of the mixed DC culture were infected, we next wanted to investigate whether uninfected, bystander DCs were able to activate EBOV-specific T cells via cross-presentation.

Uninfected DCs may acquire viral antigens for cross-presentation from infected cells via different routes. Live cells constantly release high numbers of extracellular vesicles (EVs), small nanoparticles generally known to contribute to cell-cell communication. Interestingly, previous studies have shown that EVs from EBOV infected cells contain viral proteins.^{133,134} Furthermore, infected cells may also transfer viral antigens to uninfected DCs via cell debris (e.g. necrotic and apoptotic bodies) that is produced upon cell death. Therefore, we wanted to test whether EVs or cell debris from EBOV-OVA infected epithelial cells could serve as antigen sources for cross-presentation.

4.5.1. Isolation of cell debris and extracellular vesicles (EVs) from EBOV-OVA-infected epithelial cells

As epithelial cells, Vero E6 cells were utilized as donor cells of cell debris and EVs, because they are highly infectable with EBOV and support viral replication to high titers. This ensured that high levels of OVA were expressed upon EBOV-OVA infection. Additionally, Vero E6 cells were originally isolated from the kidney of an African green monkey and therefore, harbor monkey MHC molecules that cannot present antigens to mouse OT-1 CD8 T cells. That means that cell debris or EVs from Vero E6 cells alone are not able to activate OT-1 CD8 T cells directly, but depend on uptake and antigen presentation by mouse DCs.

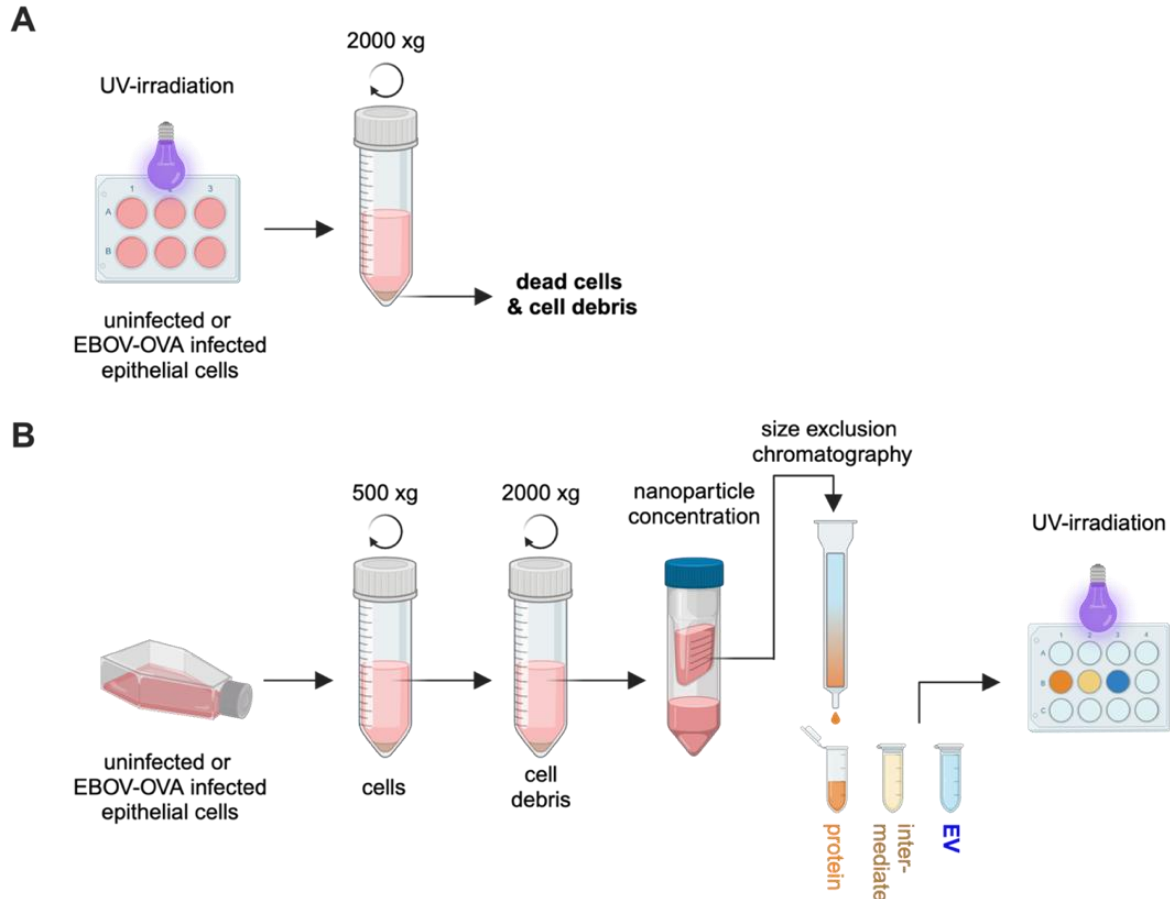
For the isolation of cell debris, Vero E6 cells were cultured in 6-well plates and infected with EBOV-OVA at an MOI of 0.1 for 7 days. At the day of cell debris harvest, Vero E6 cultures were first inactivated by UV-irradiation. Then, supernatants containing cell debris and detached dead cells were collected and pooled into 50 mL tubes. Cell debris and dead cells were pelleted by centrifugation at 2000xg. Supernatant was discarded, leaving only the cell debris, which was resuspended in fresh DC medium (Figure 16A).

EVs were isolated from Vero E6 cells cultured in T75 flasks and infected with EBOV-OVA at an MOI of 0.1 for 7 days. For the isolation of EVs, supernatants were collected and depleted of cells and cell debris by differential centrifugation at first 500xg and then 2000xg. The supernatant was then concentrated with Amicon filter units to 0.5 mL. The concentrated sample contained EVs and soluble proteins above 10 kDA. Finally, the EVs were separated from smaller proteins by size exclusion chromatography (Figure 16B).

Results

The isolation procedure was optimized and validated with uninfected Vero E6 cells. For that, 21 elution fractions of 0.5 mL each were collected from the size-exclusion chromatography column directly after loading the sample. For each fraction the nanoparticle concentration and total protein concentration was determined by NTA and BCA protein assay. A confident NTA detection limit was defined at time of analysis for a measurement of at least 6 particles per frame. Even though it was possible to measure particle concentrations with lower particle numbers per frame, these measurements resulted in high standard deviations between single captures, which is why they were considered less reliable.

The highest nanoparticle concentration at simultaneously low protein concentrations were measured for the elution fractions 6-8. From fraction 10 onwards, protein concentrations increased substantially while nanoparticle concentrations dropped below the assay detection limit (Figure 16C). We reasoned that after elution of the initial loading volume (0.5 mL) and flushing with additional 2 mL PBS, EVs can be collected in an elution volume of 2 mL (fraction 6-9, EV fraction). The following 2 mL elution volume were collected as intermediate fraction with potentially some EVs and rising protein concentrations. Finally, 2 mL were collected as protein fraction with high protein concentrations and small EV numbers.



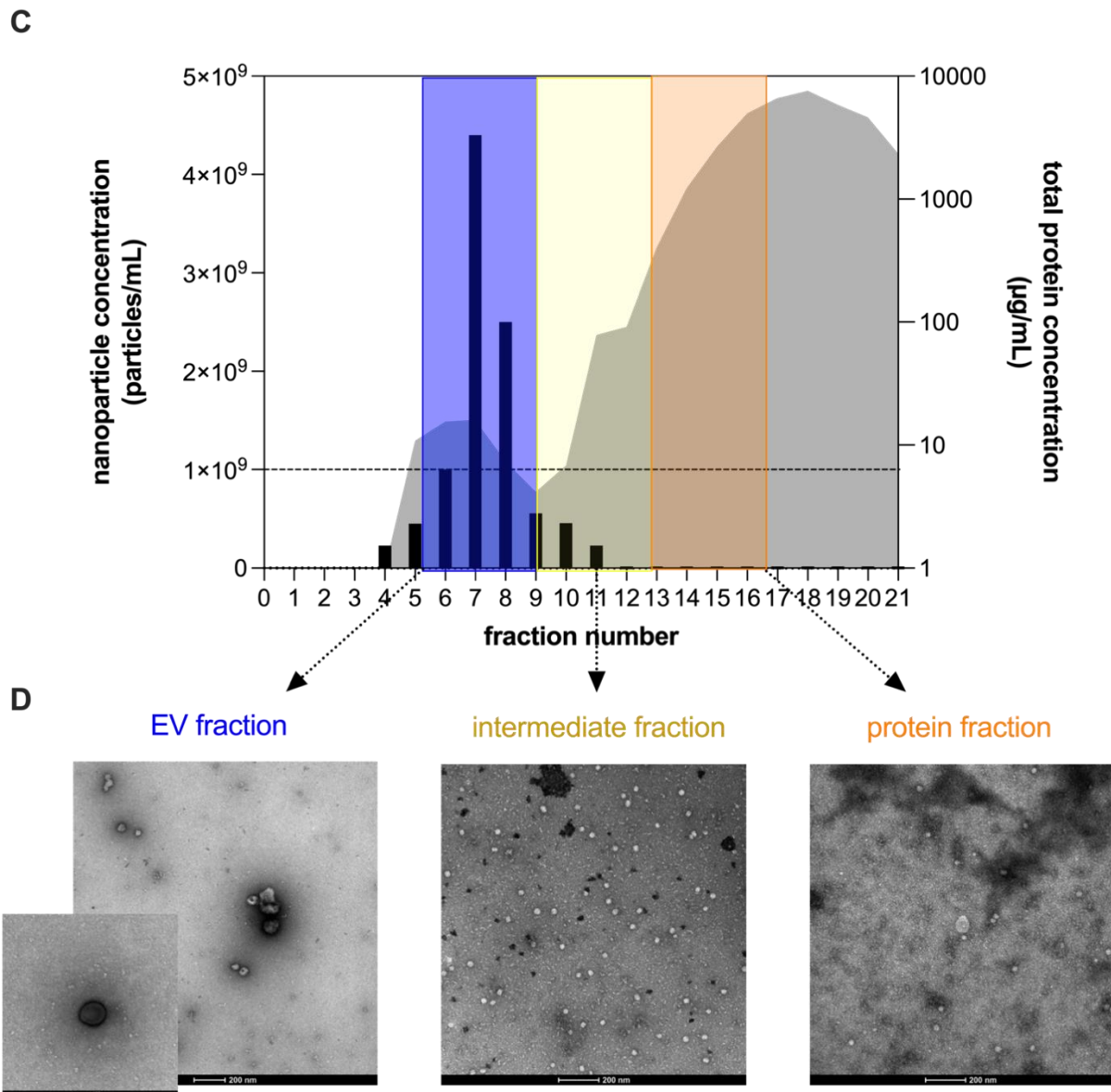


Figure 16 Isolation of cell debris and extracellular vesicles (EVs) from Vero E6 cells. (A) Isolation procedure for cell debris: Vero E6 cells were infected with EBOV-OVA (MOI 0.1) in 6-well plates. Cells and supernatants were inactivated by UV-irradiation. Cell debris was harvested from cell culture supernatants by centrifugation at 2000xg. (B) EV-isolation procedure: Vero E6 cells were infected with EBOV-OVA (MOI 0.1) in T75 flasks. EVs were isolated by differential centrifugation, concentration with Amicon filter units and size-exclusion chromatography. (C) EV isolation from uninfected cells. Nanoparticle concentration (black bars) and total protein concentration (grey area) in 21 elution fractions of 0.5 mL each were measured, to identify the EV fraction (blue), the intermediate fraction (yellow), and the protein fraction (orange). The dotted line presents the detection limit for nanoparticle tracking analysis based on a minimum of 6 particles per frame. (D) Transmission electron microscopy images of EV-, intermediate-, and protein fraction. The scale bar represents 200 nm.

EV fraction, intermediate fraction and protein fraction were further characterized by transmission electron microscopy (TEM) to validate the presence of intact EVs. Indeed, the EV fraction comprised intact EVs of 100-200 nm in size, while being mostly free from protein

Results

contamination as seen by low background on the images. Contrary, images of the intermediate fraction were much darker implying higher protein contamination. However, the intermediate fraction also included a large number of very small EVs of approximately 50 nm or smaller. The number of small EVs was reduced in the protein fraction, but they were still present. Protein contamination was clearly increased in the protein fraction compared to the intermediate fraction (Figure 16D).

Taken together the data showed that EVs can be isolated from Vero E6 cultures by differential centrifugation, followed by concentration with Amicon filter units and subsequent size exclusion chromatography. The isolated EVs had a size of 100-200 nm and were successfully separated from free protein. However, a large number of very small EVs were lost during the isolation procedure and could not be successfully separated from free protein.

The EV isolation procedure from EBOV-OVA infected cell cultures was performed in analogy to uninfected cell cultures, assuming that EVs will be eluted in the same elution fractions. EBOV-OVA titers were determined by immunofocus assay for different samples during the EV isolation procedure. High viral titers in all samples indicated that EBOV-OVA was co-isolated and concentrated with the EVs (Table 18). These high viral titers, especially in the EV fraction, showing 10^9 FFU/mL, exceeded the titers for which EBOV-inactivation methods were validated. Therefore, EVs from EBOV-OVA infected cells could not be analyzed by NTA, BCA protein assay or TEM outside the BSL4. Of note, EV fractions collected from EBOV-OVA infected cells were much denser than EV fractions from uninfected cells, suggesting high nanoparticle concentrations.

Table 18 EBOV-OVA titer in samples throughout the EV isolation procedure.

Sample	Absolute volume	Virus titer in FFU/mL	Absolute virus amount in FFU
Cell culture supernatant	34 mL (2x T75 flask)	6.90×10^7	2.35×10^9
Concentrated cell culture supernatant (Concentration with Amicon filter)	0.55 mL	3.30×10^9	1.82×10^9
Size exclusion chromatography	EV fraction	2 mL	2.88×10^8
	Protein fraction	2 mL	1.48×10^6

FFU = focus forming units

4.5.2. Dendritic cell maturation by stimulation with cell debris or EVs

As described under 4.3, DCs can only efficiently activate T cells if they develop a mature phenotype, thus, providing sufficient co-stimulation. Therefore, we next aimed to investigate whether DCs are activated upon stimulation with cell debris or EVs. For that, we stimulated DCs with cell debris or EVs from uninfected -, EBOV-OVA infected -, or wt EBOV infected cells for 24 hours and then examined the expression of CD80 and CD86 by flow cytometry (Figure 17A). DCs stimulated with LPS or medium (mock) served as controls.

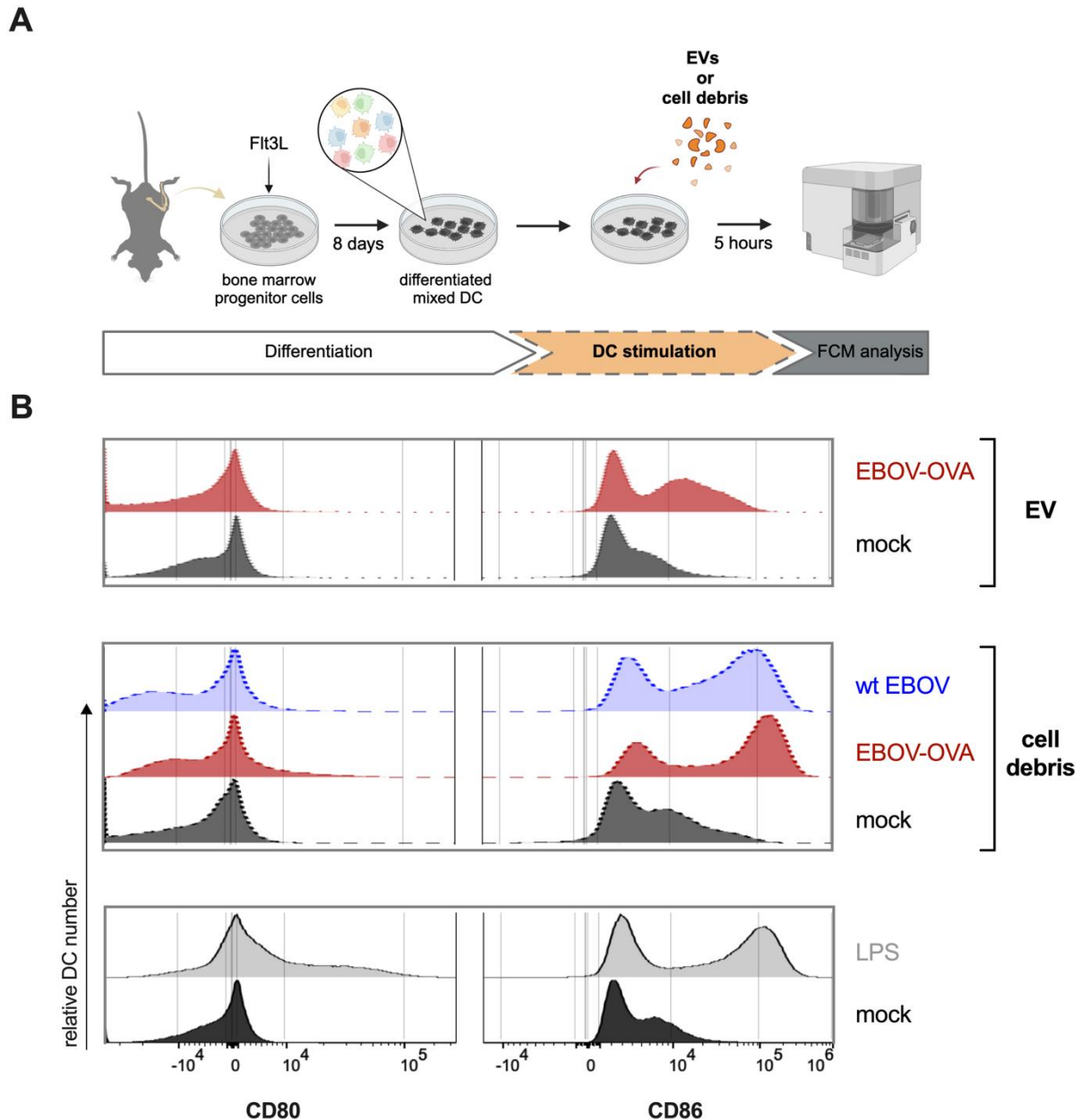


Figure 17 Activation of DC after stimulation with cell debris or EVs. (A) Experimental setup: DCs were stimulated with cell debris or EVs for 24 hours and analyzed by flow cytometry. (B) Expression of CD80 and CD86 in CD11c⁺ cells within a mixed DC culture stimulated with medium (mock, black), LPS (grey), or cell debris (dashed lines) or EVs (dotted lines) from uninfected - (black), wt EBOV infected - (blue) or EBOV-OVA infected cells (red) is shown as histogram plots.

CD11c⁺ cells within the mock stimulated mixed DC culture showed low expression of CD80. Expression of CD80 increased upon stimulation with LPS but remained low upon stimulation with cell debris or EVs. Contrary, mock-stimulated DCs already showed a low background activation by low expression of CD86. This expression of CD86 increased to a great extent upon stimulation with LPS and cell debris, especially with cell debris from wt EBOV or EBOV-OVA infected cells. Similarly, stimulation with EVs from EBOV-OVA infected cells, but not from uninfected cells, induced upregulation of CD86 (Figure 17B). Of note, the EV isolation procedure led to co-isolation of high concentrations of EBOV particles. Therefore, it was not clear whether DC activation upon stimulation with EVs from EBOV infected cells was induced by EVs or free EBOV particles. In summary, cell debris as well as EVs, especially from infected cells, induced at least partial activation of CD11c⁺ cells.

4.5.3. Cross-presentation of antigens from cell debris or EVs

Cell debris and EVs from EBOV-OVA infected cells can potentially contain viral antigens, including the model antigen OVA. Taken up and processed by DCs these antigens could then be presented to T cells leading to antigen-specific T-cell activation. Here, we wanted to test whether DCs can utilize antigens from cell debris or EVs from EBOV-OVA infected cells for cross-presentation to activate OT-1 CD8 T cells.

First, the mixed DC culture was stimulated with UV-inactivated EVs or cell debris from uninfected, EBOV-OVA or wt EBOV infected cells or left unstimulated (mock). Each stimulation was performed with and without addition of LPS. 5 hours post stimulation, DCs were co-cultured with CellTrace Violet-stained OT-1 CD8 T cells. T-cell proliferation and activation was assessed by flow cytometry analysis after 4 days of co-culture (Figure 18A).

Unstimulated DCs and DCs stimulated with cell debris from uninfected or wt EBOV infected cells failed to induce T-cell proliferation independent of additional LPS stimulation. Conversely, DCs stimulated with cell debris from EBOV-OVA infected cells induced strong T-cell proliferation. As cell debris from EBOV-OVA infected cells induced strong DC activation by itself, LPS stimulation was not required for efficient T-cell activation. However, additional stimulation with LPS increased the T-cell activation, driving more CD8 T cells into proliferation. This effect was especially noticeable when DCs were stimulated with increasingly diluted cell debris (Figure 18B). This finding suggested that activated DCs activate T cells more efficiently, which becomes especially important when less antigen is available. Cell debris from EBOV-OVA infected cells alone failed to activate the T cells, suggesting that T-cell proliferation was a result of efficient DC-T cell interaction (Supplementary Figure 4).

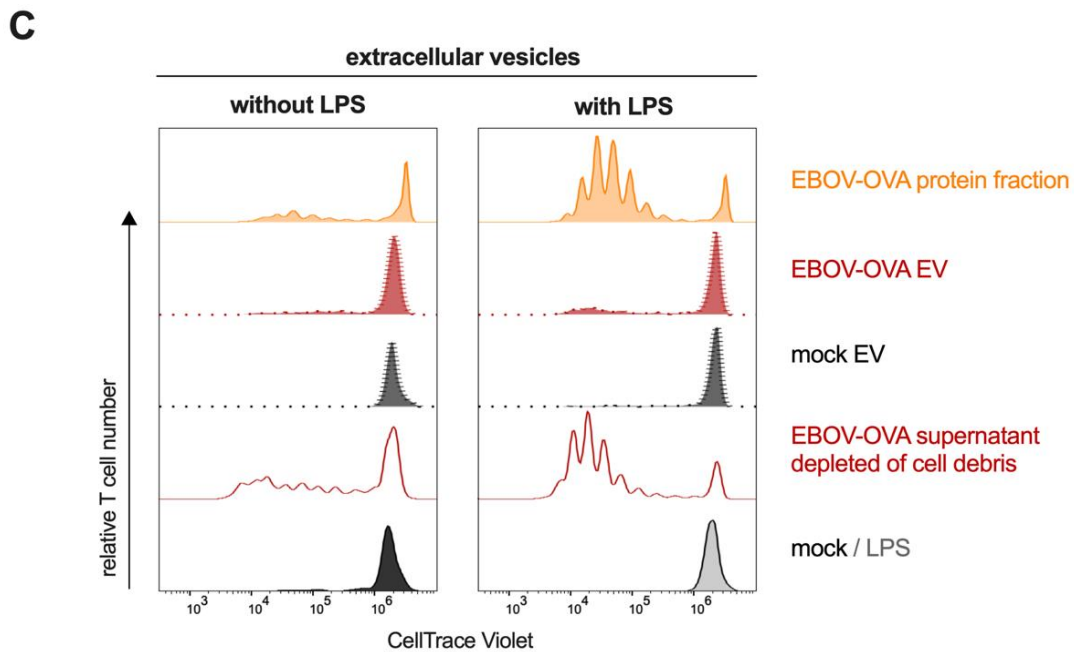
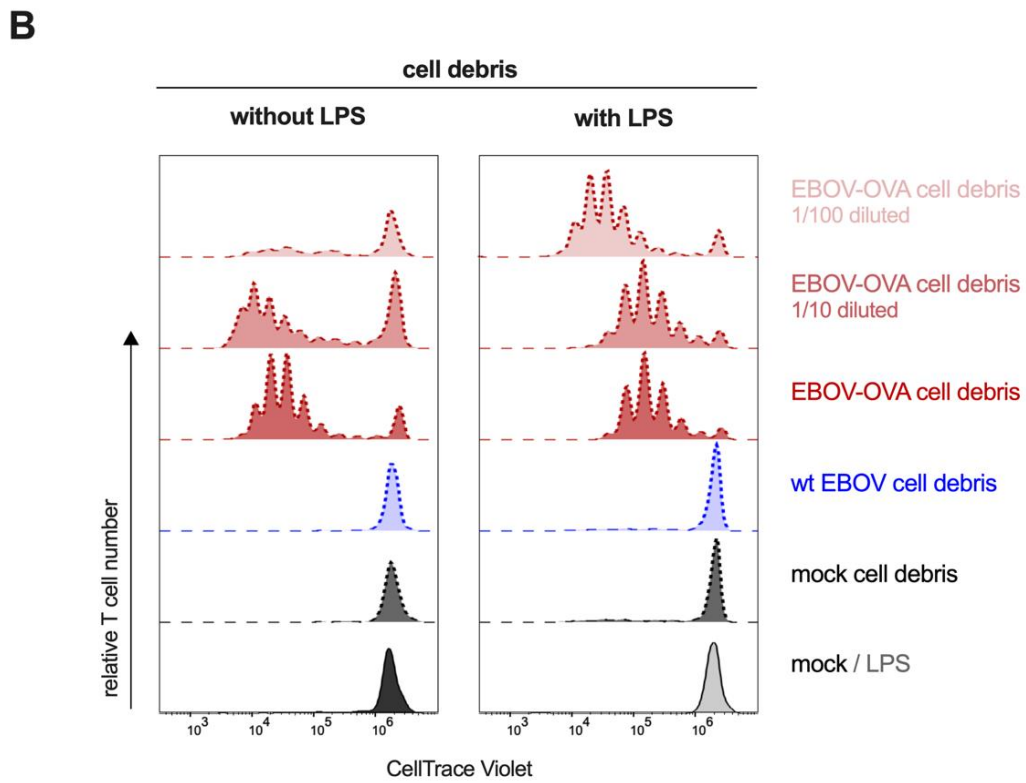
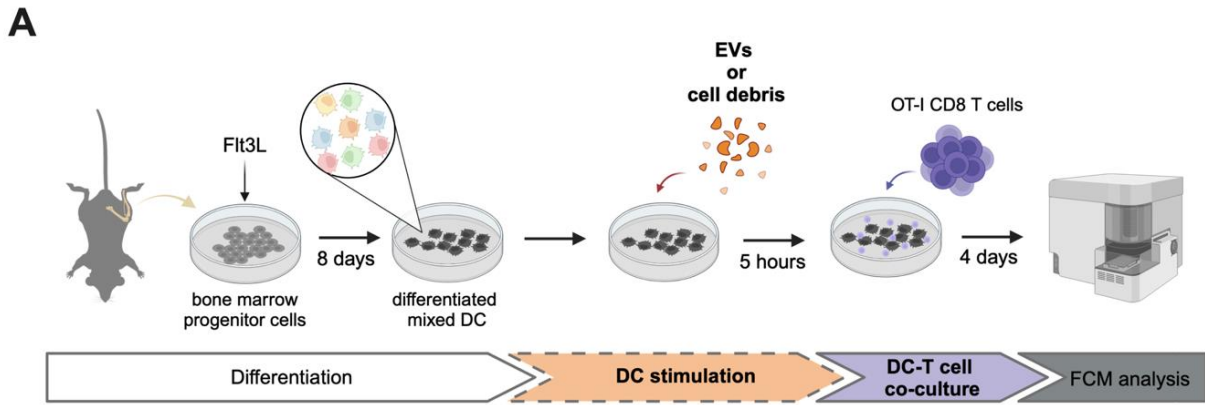


Figure 18 T-cell proliferation after cross-presentation of antigens from cell debris or EVs. (A) Experimental setup: DCs were stimulated with UV-inactivated cell debris or EVs for 4 hours. Then, OT-1 CD8 T cells were added to the culture. DC-T cell co-culture was incubated for 4 days before T-cell proliferation was analyzed by flow cytometry. (B) T-cell proliferation induced by unstimulated DCs or DCs stimulated with cell debris (dashed line) from uninfected (black), wt EBOV infected (blue), or EBOV-OVA infected cells (red, undiluted, 1:10 or 1:100 diluted) with or without additional LPS stimulation is depicted as histogram plots for CellTrace Violet. (C) T-cell proliferation induced by unstimulated DCs or DCs stimulated with cell debris depleted cell culture supernatant (EBOV-OVA-infected, red line), EVs (dotted line) from uninfected (black) or EBOV-OVA infected cells (red), or free protein from EBOV-OVA infected cell cultures (orange) with or without additional stimulation with LPS is depicted as histogram plots for CellTrace Violet. Shown is one representative experiment.

DCs stimulated with UV-inactivated cell culture supernatant that was depleted of cell debris, but still contained EVs and free proteins, induced 8 generations of T-cell division, suggesting that besides cell debris there are additional antigen sources for cross-presentation (Figure 18C). Therefore, we next examined whether DCs stimulated with EVs separated from free protein can induce T-cell proliferation. However, DCs stimulated with UV-inactivated EVs from uninfected or EBOV-OVA infected cells failed to induce T-cell proliferation. This effect remained unaltered upon LPS stimulation. On the other hand, DCs stimulated with the protein fraction induced T-cell proliferation with up to 8 generations, but only with simultaneous stimulation with LPS (Figure 18C). The requirement of LPS stimulation in the context of protein stimulation was in line with findings described in chapter 4.3, indicating that DCs were not activated upon sOVA stimulation. Taken together these findings suggested that cell debris, but not EVs from EBOV-OVA infected cells served as antigen source for cross-presentation.

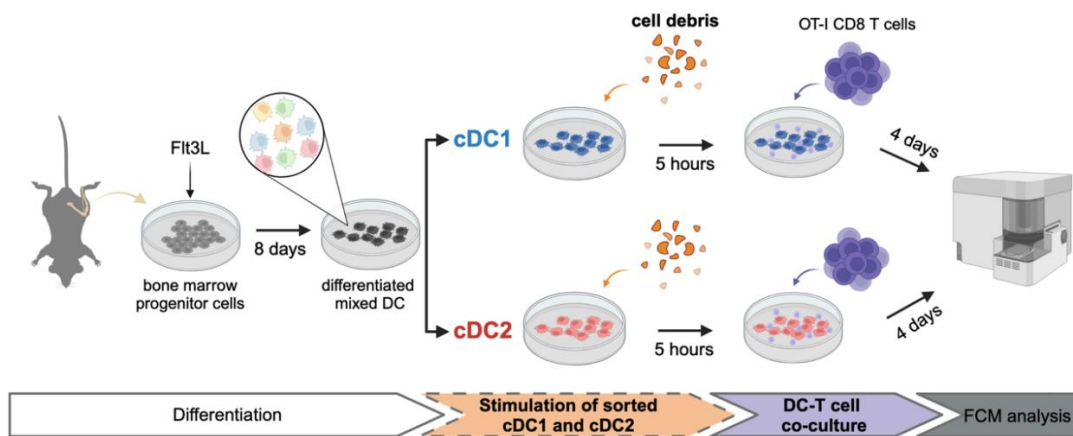
4.5.4. Cross-presentation of cell debris by cDC1 and cDC2

Generally, all DC subsets are able to activate CD8 T cells via cross-presentation. However, cDC1 are suggested to cross-present exogenous antigens more efficiently than other subsets and therefore, form the major subset responsible for CD8 T-cell activation.¹²⁰

To test whether this functional distinction applies also to the cDC1 and cDC2 populations present in the mixed DC culture utilized in this study, we generated cDC1 and cDC2 mono-cultures by fluorescence-activated cell sorting (FACS). The mono-cultures were stimulated with cell debris from EBOV-OVA infected epithelial cells as described above, and were subsequently co-cultured with CellTrace Violet stained OT-1 CD8 T cells for 4 days (Figure 19A).

As shown by others before, both – cDC1 and cDC2 – were able to induce strong CD8 T-cell proliferation. However, T-cell co-culture with stimulated cDC1 resulted in marginally higher viable absolute T-cell numbers and higher percentage of proliferating T cells (76 %) compared to co-cultures with cDC2 (58 % proliferating T cells), suggesting that indeed, cDC1 cross-presented antigens more efficiently than cDC2 (Figure 19B). These data indicated that the functional distinction between cDC1 and cDC2 also applies to our setup. Yet, the difference in cross-presentation capacity was rather low.

A



B

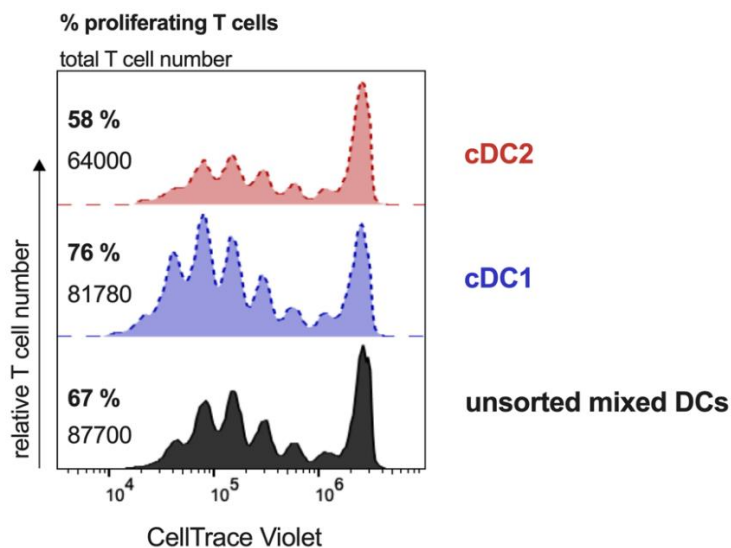


Figure 19 Cross-presentation and activation of T-cell proliferation by cDC1 and cDC2. (A) Experimental setup: cDC1 and cDC2 were sorted from a mixed DC culture and stimulated with cell debris from EBOV-OVA infected epithelial cells for 5 hours. Then, OT-1 CD8 T cells were added to the mono-cultures. DC-T cell co-culture was incubated for 4 days before T-cell proliferation was analyzed by flow cytometry. (B) T-cell proliferation upon co-culture with unsorted DCs (black), cDC1 (blue) or cDC2 (red) stimulated with cell debris. Numbers represent total T-cell number and percent of proliferated T cells. T-cell proliferation is shown as histogram plots for CellTrace Violet. Data were acquired in a single experiment.

4.5.5. Effect of EBOV-infection on cross-presentation capacity of dendritic cells

In order to fine-tune the T-cell response, avoid over reaction or autoreactive activation, cross-presentation is a highly regulated process. Various circumstances, like an infection, can disturb cross-presentation pathways. We showed above that in an EBOV-OVA infected mixed DC culture, infected as well as some uninfected DCs are activated. Therefore, we next aimed to investigate whether EBOV infection of a DC culture influenced its cross-presentation capacity.

For that, we utilized the same cross-presentation model as described in 4.5.3., but this time infected the mixed DC culture with wt EBOV 24 hours prior to stimulation with cell debris from EBOV-OVA infected cells (Figure 20A). As shown in Figure 15B, wt EBOV-infected DC cultures alone were not able to activate OT-1 CD8 T cells. Therefore, we could apply this setup to investigate the effect of EBOV infection on the cross-presentation capacity of DCs.

We compared the T-cell proliferation induced by uninfected or wt EBOV infected DCs after stimulation with cell debris from EBOV-OVA infected cells. In FlowJo, the software used to analyze flow cytometry data, we utilized the proliferation modeling tool to quantify the proliferation in each co-culture. Herein, we first defined the population of undivided T cells as generation “0” in one sample. The automatic proliferation model was then applied to all samples. The peak numbers considered by the model were manually adjusted for each sample. FlowJo automatically calculates from the model how many T cells originally added to the co-culture went into cell division. For that, the absolute cell number of each peak/generation was considered. Cells from peak “1” underwent one cell division and therefore originate from half the number. Cells from peak “2” underwent 2 cell divisions and therefore originate from a fourth of the cell number and so on. Adding up these original cell numbers from each generation and putting them into relation of how many cells did not divide the program calculates the percentage of cells that went into cell division.

Applying these calculations for the cross-presentation setup, we found that wt EBOV infected DCs drove more CD8 T cells into proliferation than uninfected DCs, suggesting that the cross-presentation capacity of DCs was enhanced by EBOV infection (Figure 20B). In the experiments with uninfected DCs between 7 and 55 % of T cells proliferated and this number was increased to 43 and 72 % if the DCs were infected with wt EBOV. In half of the replicates the absolute T-cell number was increased in co-cultures with wt EBOV infected DCs compared to co-cultures with uninfected DCs, in the other half the absolute T-cell numbers were the same (Supplementary Table 1). To examine whether these proliferating T cells differed in their activation status we compared the expression of T-cell activation markers CD44, CD69, CD25

and CD62L in both groups. However, T cells driven into proliferation by uninfected or wt EBOV infected DCs did not differ in the expression of activation markers, suggesting robust activation under both conditions (Figure 20C). Additionally, DC-T cell co-cultures contained similar amounts of cytokines associated with T-cell proliferation (Supplementary Figure 5).

Taken together, these data suggest that the cross-presentation capacity of DCs was increased upon EBOV infection, but infection does not change the activation status of the proliferating T cells.

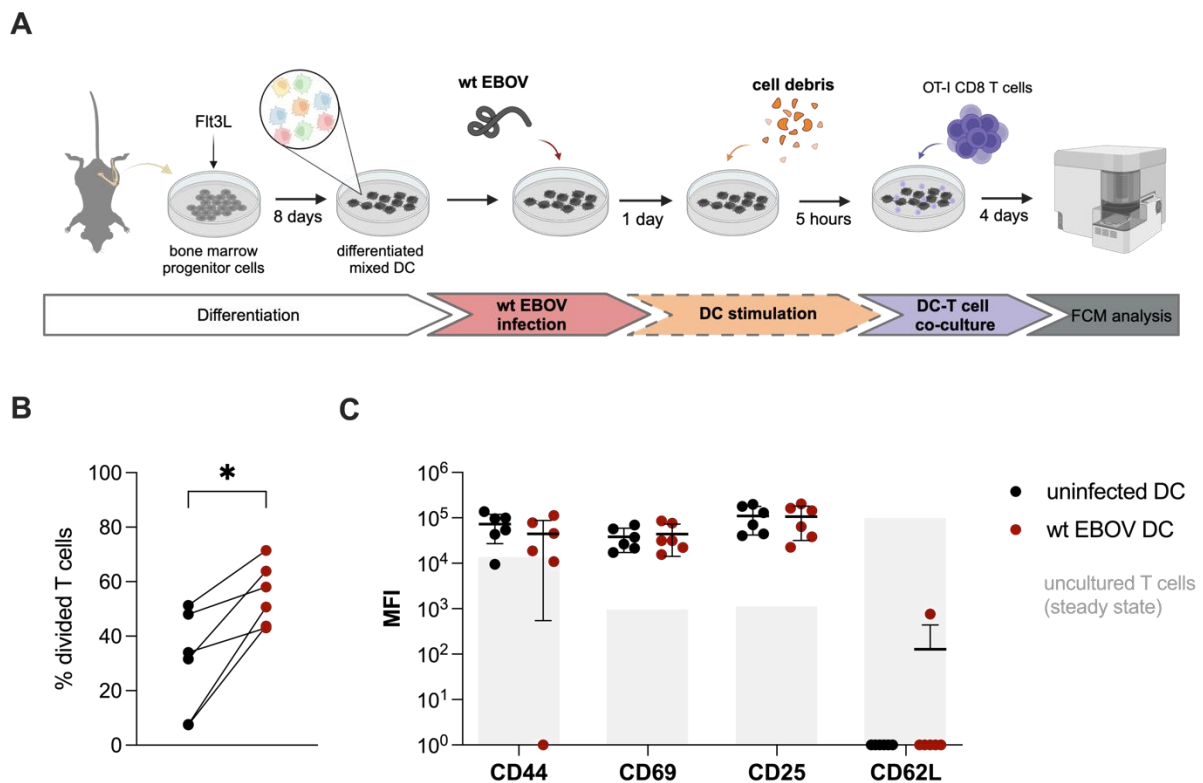


Figure 20 Effect of EBOV infection on T-cell proliferation and activation via cross-presentation of cell debris. (A) Experimental setup: DCs were infected with wt EBOV 24 hours prior to stimulation with UV-inactivated cell debris. Then, OT-1 CD8 T cells were added to the culture. DC-T cell co-culture was incubated for 4 days before T-cell proliferation was analyzed by flow cytometry. (B) Percent of dividing T cells (T cells driven into proliferation) induced by uninfected (black) or wt EBOV infected (red) DCs stimulated with cell debris from EBOV-OVA infected cells. Shown are the results of individual experiments (n=6, non-parametric t-test (Mann-Whitney), * p<0.05, lines connect groups of same experiment). (C) MFI of CD44, CD69, CD25 and CD62L in proliferating T cells in both groups (uninfected, black; and wt EBOV infected DCs, red) compared to uncultured steady state DCs (grey bars).

4.6. Contribution of cDC1 and cDC2 to T-cell activation

In co-culture with DCs, T cells can potentially be activated in two ways. On one hand, EBOV-OVA-infected cells – namely moDCs or cDC2 – could activate OT-1 CD8 T cells via

direct presentation of endogenous viral antigens. On the other hand, we showed that uninfected DCs could activate OT-1 CD8 T cells via cross-presentation of OVA from exogenous sources (e.g. cell debris). Which role these two pathways played in the T-cell activation by an EBOV-OVA infected mixed DC culture (Figure 15B) was yet to be elucidated.

To dissect the roles of cDC1 and cDC2 in T-cell activation in an EBOV-infected mixed DC culture, we adapted the DC-T cell co-culture model. First, we FACS-sorted cDC1 and cDC2 from the mixed DC culture. Next, we infected only the cDC2 culture with EBOV-OVA and co-cultured infected cDC2 and uninfected cDC1 at different ratios. Twenty-four hours post infection, we added OT-1 CD8 T cells to the co-culture and analyzed T-cell proliferation and activation after 4 days (Figure 21A).

This approach was based on the following assumptions. By preventing direct contact of cDC1 with the virus stock, we ruled out any antigen uptake (e.g. soluble OVA) by cDC1 from the virus stock. Thus, all antigen-presentation performed by cDC1 must result from antigen transfer from infected cDC2. Even though EBOV can potentially be transmitted from cDC2 to cDC1 in our setup, we argue that direct presentation due to infection of cDC1 is unlikely, because cDC1 are largely refractory to infection (Figure 11). Therefore, the number of EBOV-positive cells performing direct antigen-presentation correlates with the number of cDC2 in the culture. Thus, the numbers of cDC1 and cDC2 in the different co-cultures reflect the contribution of cross-presentation and direct presentation respectively, even though cross-presentation by infected cDC2 cannot be excluded.

Similar to the data shown before, the EBOV-OVA infected cDC2 culture alone, without any cDC1, induced T-cell proliferation and activation. However, T-cell proliferation was progressively augmented by increasing numbers of cDC1 in the co-culture, as reflected by growing numbers of generations (peak number) and proliferating T-cell numbers (peak height). cDC2 alone were able to induce 51 % of T cells to proliferate. In a 1:1 mixture of cDC2 and cDC1 this number increased to 77 % and in a 1:5 mixture 88 % of T cells were proliferating. This result suggested an important contribution of cDC1 to the observed T-cell activation (Figure 21B). Proliferating T cells showed similar expression of the T-cell activation markers CD44 and CD62L for all cDC2:cDC1 ratios. Conversely, CD69 and CD25 surface expression in proliferating T cells decreased with increasing numbers of cDC1 in the co-culture due to enhanced T-cell proliferation (Figure 21C). Additionally, DC-T cell co-cultures contained similar amounts of cytokines associated with T-cell proliferation. However, similar to the downregulation of CD25 (the IL-2 receptor), the concentration of IL-2 decreased with enhanced T-cell proliferation (Supplementary Figure 6).

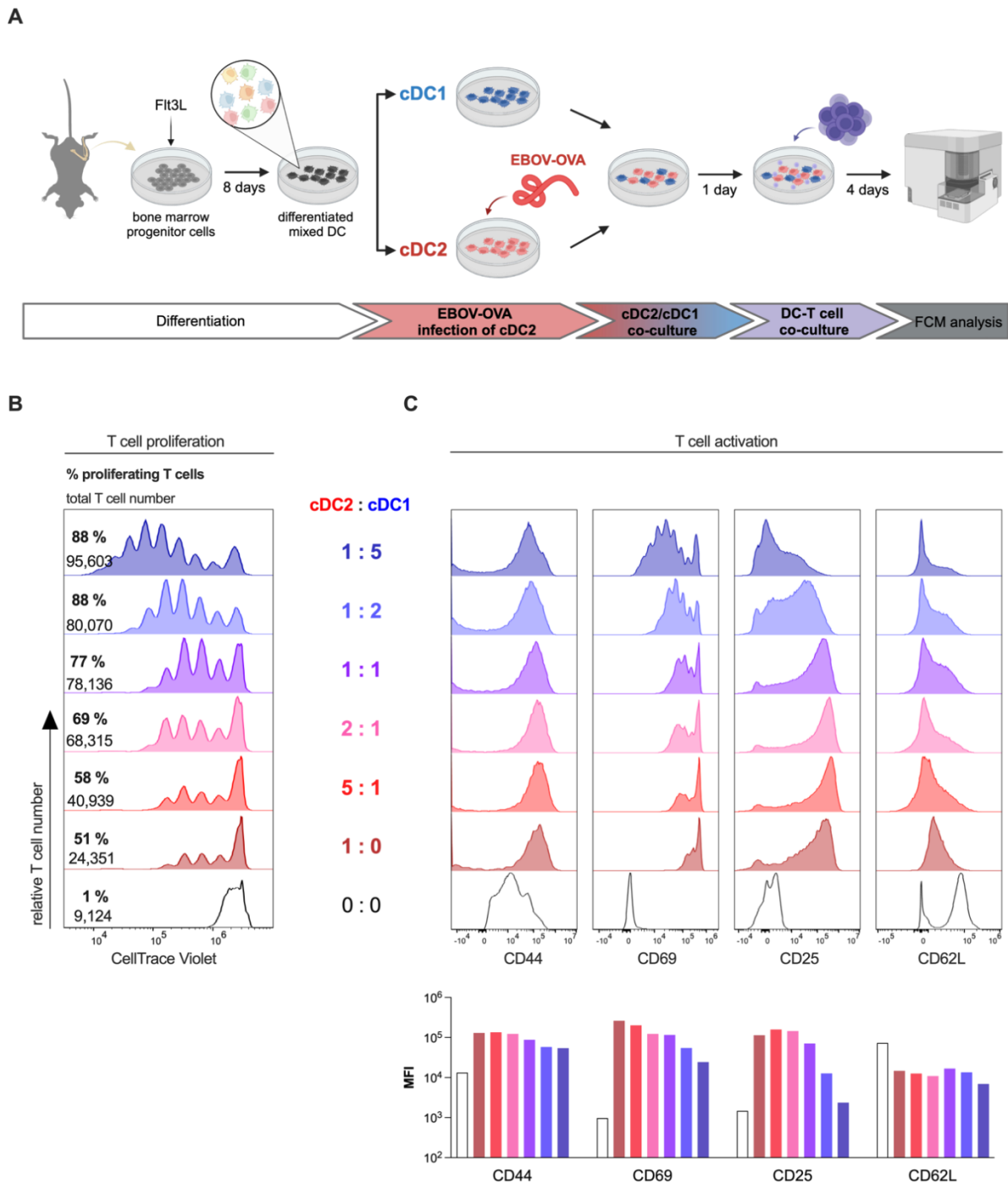


Figure 21 T-cell proliferation and activation by cDC2:cDC1 co-cultures of different ratio. (A) Experimental setup: cDC1 and cDC2 were FACS-sorted from mixed DC cultures. cDC2 were infected with EBOV-OVA (MOI 3) and co-cultured with uninfected cDC1 in different ratios. OT-1 CD8 T cells were added to the co-culture 24 hours post infection and analyzed after 4 days. (B) T-cell proliferation plots for different cDC2:cDC1 ratios. Numbers of cDC1 are increasing and numbers of cDC2 are decreasing from bottom to top. Shown are the histograms for CellTrace Violet of the CD8 population, indicating T-cell proliferation. The numbers on the left side represent percent of proliferating T cells for each condition (bold, top) and the total T-cell number (regular, bottom). (C) (top) Histograms of T-cell activation marker CD44, CD69, CD25 and CD62L expression in proliferating T cells compared to steady state, un-cultured T cells (black line). (bottom) Median fluorescence intensity (MFI) of T-cell activation markers in different conditions. Data were acquired in a single experiment.

Results

In conclusion, these data suggested that uninfected cDC1 were important contributors to T-cell activation upon EBOV infection in a mixed DC culture, while cDC2, on the other hand, contributed to a lesser extent. This finding suggested that T-cell proliferation was primarily induced by cross-presentation rather than direct antigen presentation.

5. Discussion

5.1. A summary of the findings

The goal of this study was to investigate EBOV tropism for different DC subsets, the subset-specific responses to EBOV infection, and the mechanisms by which DCs activate CD8 T cells in the context of EBOV infection. These questions were raised due to apparent contradictory data between clinical data and laboratory experiments performed with moDCs. While clinical immunology studies showed strong T-cell responses and high levels of inflammation in EVD patients⁶⁵⁻⁶⁷, *in vitro* studies in moDCs demonstrated immune inhibition resulting in poor T-cell activation^{53,54,56-58}. We hypothesized that some DC subsets could escape immunosuppression, remain functional and be responsible for the high levels of T-cell activation observed in EVD patients.

We found that in a mixed DC culture, moDCs were the preferred infection target of EBOV and cDC2 showed low infection rates, while cDC1 and pDCs were refractory to infection. Infected cells presented viral antigens in the context of MHC-I and in contrast to moDCs, cDCs showed an activated phenotype in both infected cells as well as in uninfected bystander cells. Infected mixed DC cultures were able to activate cognate CD8 T cells and induced strong T-cell proliferation. By establishing an *in vitro* cross-presentation setup, we showed that uninfected DCs were able to activate T cells via cross-presentation of antigens obtained from cell debris. Moreover, the cross-presentation capacity of the DCs was enhanced upon EBOV infection. In contrast, EVs did not induce T-cell activation via cross-presentation, suggesting poor antigenic content. Finally, we showed evidence that cDC1 highly contributed to T-cell activation despite being spared from infection, suggesting a substantial role of cross-presentation in T-cell activation observed in EBOV infections.

With these findings, we provide further insight into the key role of DCs bridging innate and adaptive immunity in EBOV infection and suggest a division of labor in which some subsets respond to infection with activation rather than inhibition. With that, we propose a mechanistic explanation for the excess T-cell activation observed in severe EVD. The present study developed and utilized techniques that are novel to EBOV research but also comprises several limitations, which will be discussed in the next chapters.

5.2. The mixed dendritic cell culture – a good representation of *in vivo* dendritic cell subsets?

Studies on DCs most often utilize DCs which are derived from monocytes by stimulation with GM-CSF and IL-4.⁸⁸ The biggest advantage is the accessibility of large numbers of monocytes

from human peripheral blood, enabling studies directly with human DCs. However, these GM-CSF-derived DC cultures have been seen more critically in recent years as it was shown that they contain not only moDCs but also macrophages and monocytes in various transitional stages, which makes it difficult to dissect the distinct roles of these populations in the experimental setup.¹⁴⁴ Additionally, GM-CSF-derived DC cultures mainly represent inflammatory DCs, which are scarce in peripheral tissues in the steady state. Thus, newer methods have been developed to *in vitro* derive steady-state DCs – namely cDC1, cDC2, and pDCs – from DC progenitors *in vitro* by stimulation with Flt3L.⁹⁰ While this is feasible for murine DCs, it becomes much more complicated for human DCs because it requires the access to DC progenitors that mainly reside in the bone marrow. However, equivalents of the major human DC subsets have been identified in mice, which is why murine DCs can be utilized as a model for human DCs. Nevertheless, it has to be considered that not all protein markers are conserved between human and mice and the functionality of the DC subsets may differ.

The Flt3L-derived DCs are considered to better represent peripheral, steady-state DC subsets than GM-CSF-derived DCs^{90,145,146}, but they still do not represent the complete heterogeneity of DC subsets seen *in vivo*. This is due to the fact, that the final steps of DC development occur in the periphery and are shaped by the microenvironment of different organs. This is corroborated by the fact that cDC1 in the Flt3L-derived DC culture lacked expression of CD8, a distinct marker for murine lymphoid tissue-resident cDC1 *in vivo*. This expression of CD8 can be rescued by adoptive transfer of *in vitro*-differentiated cDC1 into mice⁹⁰, which shows that more stimuli than Flt3L contribute to cDC differentiation, especially in late developmental stages. Later it was shown that NOTCH signaling plays a substantial role in the final development of cDCs. Addition of NOTCH stimulation to the *in vitro* Flt3L DC differentiation through co-culture with stromal cells expressing NOTCH-ligands, results in fully differentiated cDC1¹⁴⁷ and increases the expression of the endothelial cell adhesion molecule (ESAM) on cDC2.¹⁴⁸ However, the CD8 and CD4 T-cell priming capacity *in vitro* of these fully differentiated cDC1 and cDC2 is only mildly increased compared to the Flt3L-derived cDCs¹⁴⁷, which is why the latter were a sufficient model for the present study.

Even though the presence of moDCs in Flt3L-derived DC cultures has not been reported previously, the mixed DC culture described in this study contained a small cell population that showed characteristics of moDCs and macrophages due to the distinct surface expression of CD14, F4/80 and CD64. These markers, as well as CD11c, SIRP α and CD11b, can be found in moDCs, macrophages and various subclassifications of cDC2, making it difficult to distinguish between these cell types.⁷⁸ While CD11c is mostly considered a distinct marker of the DC lineage, some studies describe the presence of CD11c on CD64⁺ macrophages.^{94,149} These

studies, however, excluded the possibility of CD64 on DCs. In contrast, other studies suggested that CD64 can be expressed on DCs but excluded the possibility of CD11c on macrophages.^{78,150} Thus, whether the small population in the mixed DC culture represents an inflammatory cDC2 subclass, macrophages or moDCs cannot be definitely determined based on the immunophenotyping strategy. However, the presence of CD14 and the cell morphology (high SSC in FCM analysis) suggests a monocytic origin. Considering that CD11c is widely used as a DC lineage marker, and CD11b and SIRP α were highly expressed in these cells, we suspected that cells of this small population resemble moDCs. In agreement with this hypothesis, previous studies have shown that unstimulated bone marrow cultures contained low numbers of moDCs¹⁵¹, suggesting low levels of spontaneous differentiation. The development of moDCs could have been prevented by sorting the common DC progenitors from the bone marrow prior to differentiation, excluding all monocytes and monocyte progenitors. However, we decided to take advantage of the presence of moDCs in the mixed DC culture to be able to directly compare the tropism of the virus in a mixed culture containing all subsets.

Besides moDCs, the Flt3L-derived DC culture contained cDC1, cDC2 and pDCs as described previously.^{90,145} cDC1 and cDC2 could be distinguished by the selective expression of XCR1/CD24 and SIRP α /CD11b, respectively. Even though cDC1 are not as heterogenous as cDC2, *in vivo* cDC1 can be further subclassified by the expression level of CD103.⁹⁹ The *in vitro*-derived cDC1 reflected this subclassification as some cDC1 expressed CD103, suggesting a migratory phenotype. Expression of CD103 on cDC1 has been shown to be increased upon NOTCH signaling, similar to CD8 expression.¹⁴⁷ Subclassifications of cDC2 are more difficult to determine and would require investigation of additional markers such as ESAM or CCR2. Whether these markers would be expressed in an *in vitro* setting is however questionable due to the requirement of additional stimuli during the final steps of DC development as explained above, and the detailed characterization of cDC2 subclasses was not necessary to reach the goals of this study.

Important to note is, however, that the mixed DC culture did not only include (almost-)fully differentiated cDCs and pDCs, but also direct progenitors of these subsets. This became clear with the identification of a big cell population expressing Siglec-H in the absence of Ly6C, which can give rise to cDCs and pDCs, even though Siglec-H is considered a selective pDC marker in fully differentiated DCs.¹⁵²

Taken together, the Flt3L-derived DC culture comprised a heterogenous mix of DC subsets, representing the main *in vivo* APCs present in skin and mucosa. Thus, the mixed DC culture is an appropriate model to study the effect of EBOV infection on DC subsets early after infection at the sites of EBOV entry.

5.3. The recombinant EBOV-OVA – a key to a bigger toolbox

Cell culture studies examining DC functionality are often limited to DC-activation marker expression profiles, cytokine release and allogeneic T-cell reactions. However, the use of model antigens such as OVA, enable the investigation of antigen-specific immune responses. To date, many tools have been developed around OVA as a model antigen, as it has been widely used in allergy and vaccination research. Many different viruses such as MVA¹⁵³, Herpes viruses¹⁵⁴, and Influenza virus¹⁵⁵ have been genetically engineered to express OVA. With the recombinant EBOV expressing OVA as a non-structural viral protein, we gained access to this toolbox.

Firstly, a specific antibody detecting MHC-I-SIINFEKL complexes enables the simple identification of cells, which present the OVA-peptide SIINFEKL as a model of viral antigens to CD8 T cells. This would otherwise require complicated peptide screening and mass spectrometry techniques. Furthermore, a mouse strain with a transgenic TCR designed to recognize MHC-I-SIINFEKL complexes – so-called OT-1 mice – enable studies on antigen-specific T-cell activation by DCs, which otherwise depended on unspecific allogeneic T-cell reactions, or complex immunization experiments and development of functional pentamers.

While these OT-1 CD8 T cells have the advantage of antigen-specificity, they are still a model and have certain limitations when it comes to the validation of the T-cell activation, which will be further explained in the following chapter.

5.4. The difficulty of validating and comparing T-cell proliferation

T-cell activation can be easily investigated through the expression levels of T-cell activation markers such as CD69, CD44, CD25, and CD62L, and the concentration of secreted cytokines. Additionally, the T-cell proliferation can be traced with proliferation dyes, allowing conclusions on how many T cells are driven into proliferation and how many cell divisions they undergo. While high numbers of T-cell progeny and cell divisions are generally considered beneficial for viral clearance several parameters have to be considered when analyzing T-cell proliferation. In fact, T-cell proliferation profiles can be highly heterogenous. For example, the T-cell proliferation in two different setups may result in the same total T-cell number, but in the first setup more T cells initially started dividing but stopped proliferating after only a few cell divisions, while in the second setup less T cells were activated but underwent more rounds of cell division. These proliferation profiles are determined by several factors, including the strength of the MHC-I-TCR interaction, the efficiency of co-stimulation, and the cytokine environment.¹⁵⁶

Furthermore, it is important to consider the phenotype of the naïve T cells. Transgenic OT-1 CD8 T cells comprise the same OVA-specific TCR, which makes them not directly comparable with a population having a polyclonal TCR-repertoire. Thus, a high number of initially activated OT-1 CD8 T cells suggests a strong T-cell activation capacity of the DCs. In contrast, a similar initial T-cell activation of a polyclonal T-cell population may additionally imply unspecific bystander activation. Furthermore, SIINFEKL is an immunodominant peptide that may not always reflect the real immunogenicity of viral antigens.

It also has to be considered that in an *in vitro* setup, T-cell cultures, which do not receive sufficient stimulation by DCs or cytokines, experience high levels of T-cell death, which may alter the ratio of proliferating T cells to non-responsive T cells. This becomes important when analyzing parameters like the percentage of dividing T cells, which depend on the number of non-responsive T cells. However, in all cultures in which T cells proliferated, we detected high levels of IL-2, which promotes T-cell survival.¹⁵⁷ Therefore, in the present study, the percentage of dividing T cells could be used as a parameter to compare T-cell proliferation profiles in different conditions when a quantitative comparison was required. Additionally, we always considered this parameter in relation to the total T-cell number. In non-responsive T-cell cultures (e.g. negative controls), only a low number of live T cells could be recovered after the co-culture time, suggesting high levels of cell death. In line with this we did not detect IL-2 in these non-responsive cultures.

Despite the fact that the upregulation of T-cell-activation markers, T-cell proliferation and cytokine release suggests an efficient T-cell response, final conclusions about the cytotoxic capacity of activated T cells can only be drawn with functional assays.

5.5. Dendritic cell functionality in EBOV infections – not so impaired after all

A previous study in our lab suggested that not all DC subsets in mice were equally infected by EBOV.⁵¹ Therefore, we hypothesized that not all DC subsets are functionally impaired upon EBOV infection – as shown for moDCs.^{54,57,58} Furthermore, we aimed to find a mechanistic explanation for the excess T-cell activation observed in severe human EVD. We recognize that the mouse model has limitations in this approach as laboratory mice are resistant to EBOV disease.⁵⁰ However, despite being resistant to disease, mice experimentally infected with EBOV support virus replication and show evidence of virus dissemination.⁵¹ Moreover, we have previously shown that EBOV infects mouse DCs *in vivo* and *in vitro* regardless of their IFN-I competency and with virus titers similar to those observed in human DCs.^{51,52} Perhaps more importantly, the OT-1 mouse model allowed us to track T-cell responses to a model antigen

(OVA) expressed as viral protein and, therefore, to characterize DC function beyond the expression of surface activation markers and allogeneic T-cell activation.

5.5.1. EBOV-infection of dendritic cells – not every subset is susceptible

To test our hypothesis, we generated a mixed DC culture, reflecting the main APCs present at EBOV entry sites and wanted to see if EBOV shows the same cell tropism for different DC subsets *in vitro* as seen *in vivo*. The double staining of EBOV-GP in combination with MHC-I-SIINFEKL provided high specificity to identify infected cells.

Generally, the mixed DC culture displayed a low early EBOV infection rate of under 1 %. Interestingly, moDCs were the main target of EBOV, despite their low abundance in the mixed DC culture. This further supports the notion that this cell type may play a chief role in supporting high levels of virus replication. These results are also in agreement with the finding that high expression of Siglec-1 in activated moDCs may be a key attachment factor favoring entry of EBOV in these cells.³⁵

Besides moDCs, cDC2 were also susceptible to EBOV infection. A reason for that could be the phenotypical similarity between moDCs and cDC2. Yet, infection rates in cDC2 were much lower than in moDCs. In contrast, cDC1 and pDCs were protected from EBOV infection. This distinct infectability of cDC1 and cDC2 has been shown previously for other enveloped viruses, including HIV and Influenza. Here, cDC1 resistance to virus infections has been linked to the distinct expression of the vesicle trafficking protein RAB15 as well as to langerin-TRIM5 α -dependent virus recirculation to autophagosomes.^{158,159} Whether the same or similar molecular mechanisms protect cDC1 also from EBOV and other viral infections remains an open question. Like cDC1, pDC were not infected by EBOV, which supports data from previous studies utilizing EBOV-like particles that showed that pDCs do not support viral entry.¹⁶⁰ Plasmacytoid DCs have been shown to be susceptible to some viruses, such as human respiratory syncytial virus (RSV), VSV or Sendai virus (SV),^{161,162} but are refractory to most other viruses.

All in all, the cell tropism of EBOV for different DC subsets *in vitro* was in line with what was previously seen in mice.

5.5.2. Conventional dendritic cells are activated upon EBOV infection and activate CD8 T cells

Previous studies on GM-CSF moDCs showed that EBOV inhibits the maturation of DCs by the action of VP35 and VP24.^{53,54,56-58} In line with this, uninfected moDCs in the mixed DC culture displayed a high basal expression of CD86 and CD80, which increased only moderately upon

EBOV infection, despite high infection rates. In contrast, infected cDC2 were highly activated compared to uninfected cDC2. In fact, also uninfected bystander cDC2 and cDC1 within the infected mixed DC culture showed a certain degree of upregulation of the maturation marker CD86. Considering that we observed maturation as early as 24 hours post-infection, an explanation for the fact that CD80 is not as strongly upregulated might be the distinct kinetics of these maturation markers. Studies have shown, that CD86 is upregulated earlier than CD80 during maturation.¹⁶³ We therefore argue that DC maturation is not completely inhibited upon EBOV infection and encourage further research on a single cell level. Considering that EBOV-GP, in opposition to VP35, induces strong DC activation⁵⁸, we propose that timing and levels of viral protein production may determine the degree of maturation in infected moDCs and cDCs. Besides that, investigating signaling pathways of pattern recognition receptors leading to DC maturation may allow further understanding of molecular mechanisms leading to the activation of uninfected cDCs. Meanwhile, pDCs showed no activation upon EBOV infection of the mixed DC culture, which is in line with previous studies utilizing EBOV-like particles.¹⁶⁰ pDC activation is generally initiated in different ways upon virus infection. On one hand, pDC activation can be induced by virus replication in the cytoplasm and recognition via autophagy, as shown for SV and VSV.¹⁶¹ On the other hand, pDCs can recognize viruses independent of intracellular replication by direct interaction with virus-infected cells or endocytosis of free virus particles or RNA-containing EVs.^{101,164-166} Understanding why pDCs were not activated upon EBOV infection of the mixed DC culture requires further investigations of these activation pathways. Furthermore, we have not investigated the phenotype of DCs after co-culture with T cells, which may be especially interesting in co-cultures with proliferating T cells, as the altered cytokine environment may promote DC activation.

An advantage of the present study, is the use of recombinant EBOV-OVA, expressing the model antigen OVA as a non-structural protein. Firstly, we showed that EBOV-antigens are successfully loaded onto MHC-I and are presented on the cell surface of infected DCs. In combination with the observed DC activation, we speculated that infected DC cultures could be able to activate cognate CD8 T cells. Indeed, OVA-specific OT-1 CD8 T cells were activated and proliferated upon co-culture with EBOV-OVA-infected mixed DC cultures. This finding was contrary to previous *in vitro* findings that EBOV infection of DC results in reduced T-cell activation^{57,167}, but was in line with clinical studies reporting excess T-cell activation in EVD patients.⁶⁵⁻⁶⁷ This is further supported by the fact that the phenotype of activated CD8 T cells in EVD patients suggested engagement of the TCR, rather than unspecific bystander activation.⁶⁷

5.6. The role of cross-presentation in EBOV infections

Initially, our data indicated presentation of OVA on MHC-I only by EBOV-OVA infected DCs, but not uninfected DCs. However, this does not exclude OVA presentation on MHC-I by uninfected DCs below the limit of detection and, thus, does not exclude a contribution of uninfected DCs to T-cell activation. Indeed, we showed that uninfected DCs are able to activate OT-1 CD8 T cells via cross-presentation of antigens obtained from cell debris from EBOV-OVA-infected epithelial cells. UV-inactivation of cell debris before DC stimulation excluded infection of DCs and possible direct antigen-presentation. Furthermore, the cell debris was collected purposely from epithelial cells that do not HLA-match the OT-1 TCR, and therefore eliminates direct T-cell activation by cell debris independent of DCs.

It becomes even more important considering our next finding that wt EBOV infection of a DC culture further increases its cross-presentation capacity. This might be associated with the observed DC activation of uninfected DCs in an EBOV-infected culture, because DCs increase their antigen uptake and presentation within the first hours of maturation.¹⁶⁸ As we stimulated DCs with cell debris within 24 hours post-infection, we possibly hit the time window of increased antigen uptake and subsequent presentation. However, further experiments investigating different time points for stimulation and other maturation stimuli than EBOV infection are necessary to validate this hypothesis. One might argue that the moderate DC maturation upon EBOV infection is insufficient for such an effect. However, recent studies on Newcastle disease virus (NDV) demonstrate that excessive DC activation upon NDV infection inhibits T-cell activation by DCs.¹⁶⁹ In conclusion, a moderate rather than excessive DC activation is required for efficient T-cell activation via cross-presentation. These findings further contradict the assumption that DC function is impaired upon EBOV infection.

5.6.1. Extracellular vesicles in cross-presentation – high potential with limitations

Cell debris may not be the only antigen source for cross-presentation. Unlike cell debris, EVs are constantly secreted by all living cells. EV content includes proteins, lipids or RNAs of the host cell and the content changes depending on the current cell state. As EVs can be taken up by all cells, their contribution to cell-cell communication has caught the interest of many research fields.^{170,171} In recent years, EVs have been shown to be involved in the transfer of antigens to DCs for T-cell activation or even activate T cells directly.^{132,172} Interestingly, EVs secreted from cells infected with EBOV or EBOV-like particles were shown to contain EBOV proteins.^{133,134} Due to this, we hypothesized that EVs from EBOV-infected cells may function

as antigen source for cross-presentation. However, in our setup, DCs stimulated with EVs from EBOV-OVA-infected epithelial cells did not activate OT-1 CD8 T cells.

This was even though we stimulated DCs with EVs isolated from cell numbers comparable or higher to those applied in other studies.¹⁷³ However, infected cells may release higher or lower numbers of EVs, which unfortunately we were not able to test due to the co-isolation of infectious EBOV particles in concentrations that exceeded the validated range of the virus inactivation methods. Besides, even if inactivation had been possible, co-isolated EBOV particles would have been difficult to distinguish from EVs in the nanoparticle tracking analysis due to their similar sizes. Furthermore, electron microscopy analysis of the EV samples showed that we lost large numbers of small EVs during the isolation process. For these small EVs we could not test a contribution to T-cell activation as the separation from soluble protein, possibly including soluble OVA, was insufficient. Experiments applying novel, more specific EV isolation protocols, such as immunoaffinity- or charge-based techniques¹⁷⁴, are required to further elucidate a possible contribution of small EVs in T-cell activation in EBOV infections.

As with the cell debris, we purposely collected EVs from cells that do not HLA-match the OT-1 TCR to avoid direct T-cell activation. Hereby, however, we also excluded the possibility of T-cell activation via recycling of the whole MHC-I-antigen-complexes rather than directing acquired antigens to the cells own antigen presentation machinery.¹³² Further, experiments using EVs from HLA-matched DCs are required to examine whether EVs incorporating MHC-I-antigen complexes can be recycled for T-cell activation or activate T cells directly in EBOV infections. These experiments become especially important considering that EVs have been shown to contribute to T-cell activation in lymphocytic choriomeningitis virus (LCMV) and VSV infections mainly via cross-dressing, rather than cross-presentation.¹⁷⁵

5.7. Direct presentation vs. cross-presentation – who is doing the job?

After demonstrating that uninfected DCs can contribute to T-cell activation via cross-presentation, we wanted to investigate whether EBOV-positive DCs are able to directly activate CD8 T cells. However, this would require live cell sorting after EBOV infection, but unfortunately, cell sorting under BSL-4 containment is not possible in our facilities. Furthermore, blockage of different cross-presentation pathways with specific inhibitors would not rule out cross-presentation altogether. Alternatively, we aimed to dissect the T-cell activation capacity of uninfected and infected DCs with a new co-culture setup. Herein, we co-cultured EBOV-OVA-infected cDC2 with uninfected cDC1 in different ratios and co-cultured those with OT-1 CD8 T cells to examine T-cell activation. By avoiding contact of cDC1 with the virus stock, we ruled out any antigen uptake (e.g. soluble OVA) by cDC1 from the virus

stock. Thus, all antigen presentation performed by cDC1 must result from antigen transfer from infected cDC2. Even though EBOV can potentially be transmitted from cDC2 to cDC1 in our setup, we argue that direct presentation due to infection of cDC1 is unlikely, because cDC1 are largely refractory to infection, meaning that cDC1 only performed cross-presentation in this setup. cDC2 on the other hand were potentially able to do both, direct- and cross-presentation.

Of note, cDC2/cDC1 cultures showed distinct T-cell activation capacities depending on the cDC2/cDC1 ratios. Cultures containing more cDC1 and less cDC2 – and therefore less EBOV-positive DCs – induced the strongest T-cell proliferation. Paradoxically, stronger T-cell proliferation was connected to reduced expression of the T-cell-activation marker CD69 and CD25 on the cell surface. This is because CD69 is a very early T-cell-activation marker that is increased upon initial T-cell activation but is rapidly downregulated afterwards.¹²² Expression of CD25 (IL-2R α) is tightly connected to secretion and autocrine signaling of IL-2. As proliferating T cells reach the terminal effector phenotype, IL-2 secretion is reduced and with it the positive feedback loop that leads to upregulation of CD25.^{176,177} Therefore, CD25 as well as IL-2 are reduced in highly proliferated T cells as seen in co-cultures with high numbers of cDC1.

From these data, we concluded that in a mixed DC culture uninfected cDC1 are predominantly important for T-cell activation. We propose that cDC1 are activating T cells via cross-presentation of antigens that they receive from infected cDC2. In fact, the same mechanism has been suggested by another study showing that cDC1 are protected from infection by HIV and Influenza, while cDC2 are susceptible to infection.¹⁵⁸ This is further supported by data from us and others, showing that cDC1 are stronger inducers of CD8 T-cell proliferation via cross-presentation of antigens from cell debris than cDC2.¹⁷⁸ Although, this functional distinction of different cDC subsets has been highly debated in recent years.^{120,179,180} Whether EBOV-antigens are transferred from infected DCs to uninfected DCs via cell debris, EV or direct cell-cell contact is yet to be elucidated.

Nevertheless, we cannot exclude a contribution of direct T-cell activation by infected cDC2. On that note, we also cannot rule out the possibility that cDC1 indirectly induce T-cell activation by stimulating cDC2, rather than being directly involved in T-cell activation. Other experiments, for example with HLA-mismatched and/or sorted DC subsets, are required to further dissect the role of uninfected and infected cDC1 and cDC2 in T-cell activation. Blocking of specific cellular pathways of antigen processing, MHC-loading and antigen presentation would also allow deeper insights into the molecular mechanisms involved.

5.8. Conclusions about the role of conventional dendritic cells in EBOV infections

After it became clear that the DC lineage is heterogenous and comprises several distinct DC subsets, first each subset was assigned a specific function. For example, cDC1 and cDC2 were suggested to specifically activate CD8 and CD4 T cells respectively. However, in recent years it became apparent that this functional specialization is not as strict as it was first believed. Instead, DCs show high functional plasticity, which is shaped by the local microenvironment, formed by cytokines, chemokines and other stimuli from other cells or pathogens. Moreover, DCs do not act independently, but communicate with each other and perform functions that depend on each other. For example, cDC1 have been shown to be the most efficient cross-presenting subset and play a major role in activating CD8 T cells. However, they mainly reside in lymphoid tissue, which brought up the question of how they receive antigens from the periphery for CD8 T-cell activation. A possibility is that other migratory cells transport antigens from the site of infection to the lymph nodes, where antigens are transferred between cells.¹⁸¹

Our data support the concept of a division of labor among different DC subsets also in the context of EBOV infection, as we showed that some DC subsets, namely moDCs and cDC2, are infectable, while others like cDC1 and pDCs are refractory to infection. We speculate that infected DC subsets may provide the antigen source to cDC1 for cross-presentation, which we identified as the major driver of CD8 T-cell proliferation. Our data showed that this antigen transfer may occur after the cell death of the infected cell and the subsequent uptake of cell debris. Furthermore, we do not exclude a possible contribution of EVs to cross-presentation, even though we were not able to show evidence for that in our setup (Figure 22).

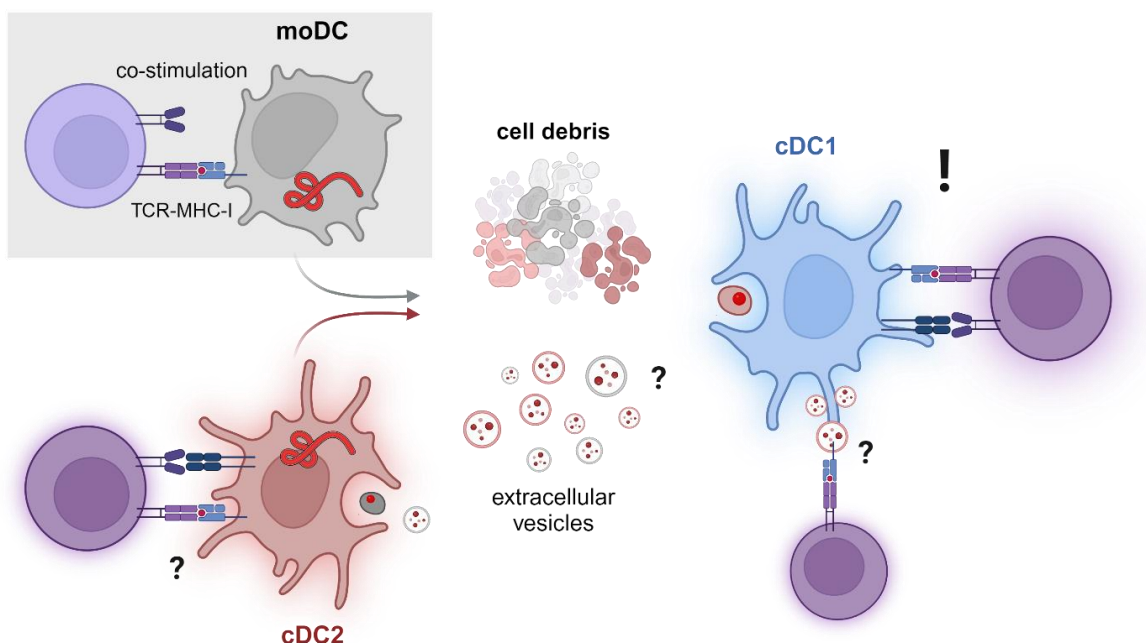


Figure 22 The role of cDCs in T-cell activation in EBOV infections. Previous studies showed that EBOV infection of moDCs (grey) inhibits DC maturation, resulting in insufficient T-cell activation (grey box). Here we showed that besides moDCs, also cDC2 (red) are infectable, are activated upon infection, and present viral antigens on MHC-I, whereas cDC1 (blue) are refractory to infection. Whether infected cDC2 can activate T cells (purple) via direct presentation is unsure (?). DCs can utilize antigens from cell debris for cross-presentation, whether extracellular vesicles play a similar role is still uncertain (?). cDC1 are the main cross-presenting subset and thereby highly contribute to T-cell activation (!).

Previous studies suggested that EBOV infection inhibits moDC maturation, which results in reduced T-cell activation. However, this is in conflict with the strong T-cell activation observed in EVD patients. In the present study, we demonstrated the significance of cDCs in T-cell activation in the context of EBOV infections and highlighted that the heterogeneity of DC subsets has to be considered when investigating DC-T cell interactions. All in all, we provide a mechanistic explanation for the excess T-cell activation observed in EVD patients and encourage further studies on the division of labor between different DC subsets in EBOV infections.

5.9. Outlook

Whether our findings are specific to pathogenic EBOV or also apply to other Orthoebolaviruses, filoviruses, or hemorrhagic fever viruses in general, is a question that should be addressed in the future to test possible implications in the pathogenesis of viral hemorrhagic fevers or even other highly inflammatory infections. The contribution of cross-presentation and direct antigen presentation to EVD pathogenesis or survival, can only be investigated in animal models that develop disease upon EBOV infection. In that respect, recent investigations from our group utilizing an avatar mouse model already suggested a link of DC-T cell interaction to EVD pathogenesis⁶², which further corroborates the importance of future investigations on DC-T cell interactions. This model could be expanded to studying the contribution of specific DC subsets to pathogenesis and the role of cross-presentation. Also, the possible contribution of EVs as important mediators of cell-cell communication should be addressed with newer and more elaborated methods. Currently, in our lab efforts are put on the translation of our findings from murine to human DCs. For that, we are deriving different DC subsets from human stem cells with similar methods as described in the present study. Despite the fact that murine DCs are a good model system to study DC functionality, definite conclusions about the role of different DC subsets in human EVD can only be drawn from studies with human DCs. Yet, our findings provide a strong foundation for these future investigations.

References

1. Kuhn, J. H. *et al.* ICTV Virus Taxonomy Profile: Filoviridae. *Journal of General Virology* **100**, 911–912 (2019).
2. Biedenkopf, N. *et al.* Renaming of genera Ebolavirus and Marburgvirus to Orthoebolavirus and Orthomarburgvirus, respectively, and introduction of binomial species names within family Filoviridae. *Arch Virol* **168**, 220 (2023).
3. WHO. Ebola haemorrhagic fever in Zaire, 1976. *Bull World Health Organ* **56**, 271–293 (1978).
4. WHO. Ebola haemorrhagic fever in Sudan, 1976. *Bull World Health Organ* **56**, 247–270 (1978).
5. CDC. History of Ebola Disease Outbreaks. <https://www.cdc.gov/vhf/ebola/history/chronology.html> (2023).
6. Wamala, J. F. *et al.* Ebola Hemorrhagic Fever Associated with Novel Virus Strain, Uganda, 2007–2008. *Emerging Infectious Disease journal* **16**, 1087 (2010).
7. Kratz, T. *et al.* Ebola Virus Disease Outbreak in Isiro, Democratic Republic of the Congo, 2012: Signs and Symptoms, Management and Outcomes. *PLoS One* **10**, e0129333- (2015).
8. Formenty, P. *et al.* Human Infection Due to Ebola Virus, Subtype Côte d’Ivoire: Clinical and Biologic Presentation. *J Infect Dis* **179**, S48–S53 (1999).
9. Diego, C., Arran, H., Martin, M., N, W. M. & S, R. J. Risks Posed by Reston, the Forgotten Ebolavirus. *mSphere* **1**, 10.1128/msphere.00322-16 (2016).
10. Goldstein, T. *et al.* The discovery of Bombali virus adds further support for bats as hosts of ebolaviruses. *Nat Microbiol* **3**, 1084–1089 (2018).
11. Forbes, K. M. *et al.* Bombali virus in mops condylurus bat, kenya. *Emerg Infect Dis* **25**, 955–957 (2019).
12. CDC. Ebola Disease Distribution Map: Cases of Ebola Disease in Africa Since 1976. <https://www.cdc.gov/vhf/ebola/history/distribution-map.html> (2023).
13. Leroy, E. M. *et al.* Fruit bats as reservoirs of Ebola virus. *Nature* **438**, 575–576 (2005).
14. Swanepoel, R. *et al.* Experimental Inoculation of Plants and Animals with Ebola Virus. *Emerg Infect Dis* **2**, 321–325 (1996).
15. Riesle-Sbarbaro, S. A. *et al.* Selective replication and vertical transmission of Ebola virus in experimentally infected Angolan free-tailed bats. *Nat Commun* **15**, 925 (2024).

References

16. Leroy, E. M. *et al.* Human Ebola Outbreak Resulting from Direct Exposure to Fruit Bats in Luebo, Democratic Republic of Congo, 2007. *Vector-Borne and Zoonotic Diseases* **9**, 723–728 (2009).
17. Towner, J. S. *et al.* Isolation of Genetically Diverse Marburg Viruses from Egyptian Fruit Bats. *PLoS Pathog* **5**, e1000536- (2009).
18. McCormick, J. B. Ebola Virus Ecology. *J Infect Dis* **190**, 1893–1894 (2004).
19. Pigott, D. M. *et al.* Mapping the zoonotic niche of Ebola virus disease in Africa. *Elife* **3**, e04395 (2014).
20. Den Boon, S. *et al.* Ebola Virus Infection Associated with Transmission from Survivors. *Emerging Infectious Disease journal* **25**, 240 (2019).
21. Keita, A. K. *et al.* Resurgence of Ebola virus in 2021 in Guinea suggests a new paradigm for outbreaks. *Nature* **597**, 539–543 (2021).
22. Jacob, S. T. *et al.* Ebola virus disease. *Nat Rev Dis Primers* **6**, 13 (2020).
23. Muñoz-Fontela, C. & McElroy, A. K. Ebola Virus Disease in Humans: Pathophysiology and Immunity. *Curr Top Microbiol Immunol* **411**, 141–169 (2017).
24. The PREVAIL II Writing Group for the Multi-National PREVAIL II Study Team. A Randomized, Controlled Trial of ZMapp for Ebola Virus Infection. *New England Journal of Medicine* **375**, 1448–1456 (2016).
25. Sabue, M. *et al.* A Randomized, Controlled Trial of Ebola Virus Disease Therapeutics. *New England Journal of Medicine* **381**, 2293–2303 (2019).
26. Rijal, P. & Donnellan, F. R. A review of broadly protective monoclonal antibodies to treat Ebola virus disease. *Curr Opin Virol* **61**, 101339 (2023).
27. Woolsey, C. & Geisbert, T. W. Current state of Ebola virus vaccines: A snapshot. *PLoS Pathog* **17**, e1010078- (2021).
28. Xu, D. *et al.* Design of universal Ebola virus vaccine candidates via immunofocusing. *Proceedings of the National Academy of Sciences* **121**, e2316960121 (2024).
29. Heinz, F., Armand, S. & W, G. T. Ebola. *New England Journal of Medicine* **382**, 1832–1842 (2020).
30. Moller-Tank, S. & Maury, W. Ebola Virus Entry: A Curious and Complex Series of Events. *PLoS Pathogens* vol. 11 Preprint at <https://doi.org/10.1371/journal.ppat.1004731> (2015).

References

31. Beniac, D. R. *et al.* The Organisation of Ebola Virus Reveals a Capacity for Extensive, Modular Polyploidy. *PLoS One* **7**, e29608- (2012).
32. ViralZone SIB Swiss Institute of Bioinformatics. Orthoebolavirus. <https://viralzone.expasy.org/207> (2023).
33. Lee, J. E. & Saphire, E. O. Ebolavirus glycoprotein structure and mechanism of entry. *Future Virol* **4**, 621–635 (2009).
34. Alvarez, P. *et al.* C-Type Lectins DC-SIGN and L-SIGN Mediate Cellular Entry by Ebola Virus in cis and in trans. *J Virol* **76**, 6841–6844 (2002).
35. Perez-Zsolt, D. *et al.* Anti-Siglec-1 antibodies block Ebola viral uptake and decrease cytoplasmic viral entry. *Nat Microbiol* **4**, 1558–1570 (2019).
36. Brunton, B. *et al.* TIM-1 serves as a receptor for Ebola virus in vivo, enhancing viremia and pathogenesis. *PLoS Negl Trop Dis* **13**, e0006983- (2019).
37. Aleksandrowicz, P. *et al.* Ebola Virus Enters Host Cells by Macropinocytosis and Clathrin-Mediated Endocytosis. *J Infect Dis* **204**, S957–S967 (2011).
38. Salata, C. *et al.* Ebola virus entry: From molecular characterization to drug discovery. *Viruses* **11**, (2019).
39. Fang, J. *et al.* Spatial and functional arrangement of Ebola virus polymerase inside phase-separated viral factories. *Nat Commun* **14**, 4159 (2023).
40. Xu, W. *et al.* Ebola virus VP30 and nucleoprotein interactions modulate viral RNA synthesis. *Nat Commun* **8**, 15576 (2017).
41. Mohan, G. S., Li, W., Ye, L., Compans, R. W. & Yang, C. Antigenic Subversion: A Novel Mechanism of Host Immune Evasion by Ebola Virus. *PLoS Pathog* **8**, e1003065- (2012).
42. Masfique, M. *et al.* A New Ebola Virus Nonstructural Glycoprotein Expressed through RNA Editing. *J Virol* **85**, 5406–5414 (2011).
43. Dolnik, O. *et al.* Ectodomain shedding of the glycoprotein GP of Ebola virus. *EMBO J* **23**, 2175-2184–2184 (2004).
44. Ahad, A., Mahnoor, S., Zaid, M., Ali, M. & Afzal, M. S. Ebolavirus: Infection, Vaccination and Control. *Molecular Genetics, Microbiology and Virology* **36**, S55–S64 (2021).
45. Mühlberger, E. Filovirus replication and transcription. *Future Virol* **2**, 205–215 (2007).

References

46. Martines, R. B., Ng, D. L., Greer, P. W., Rollin, P. E. & Zaki, S. R. Tissue and cellular tropism, pathology and pathogenesis of Ebola and Marburg viruses. *J Pathol* **235**, 153–174 (2015).
47. Geisbert, T. W. *et al.* Pathogenesis of Ebola Hemorrhagic Fever in *Cynomolgus* Macaques Evidence That Dendritic Cells Are Early and Sustained Targets of Infection. *American Journal of Pathology* vol. 163 (2003).
48. Crowe, S. J. *et al.* Prognostic indicators for Ebola patient survival. *Emerg Infect Dis* **22**, 217–223 (2016).
49. Prescott, J. B. *et al.* Immunobiology of Ebola and Lassa virus infections. *Nature Reviews Immunology* vol. 17 195–207 Preprint at <https://doi.org/10.1038/nri.2016.138> (2017).
50. Bray, M. *The Role of the Type I Interferon Response in the Resistance of Mice to Filovirus Infection.* *Journal of General Virology* vol. 82 (2001).
51. Lüdtke, A. *et al.* Ebola virus infection kinetics in chimeric mice reveal a key role of T cells as barriers for virus dissemination. *Sci Rep* **7**, 1–10 (2017).
52. Escudero-Pérez, B. *et al.* Comparative pathogenesis of Ebola virus and Reston virus infection in humanized mice. *JCI Insight* **4**, (2019).
53. Bray, M. & Geisbert, T. W. Ebola virus: The role of macrophages and dendritic cells in the pathogenesis of Ebola hemorrhagic fever. *International Journal of Biochemistry and Cell Biology* vol. 37 1560–1566 Preprint at <https://doi.org/10.1016/j.biocel.2005.02.018> (2005).
54. Bosio, C. M. *et al.* Ebola and Marburg Viruses Replicate in Monocyte-Derived Dendritic Cells without Inducing the Production of Cytokines and Full Maturation. *The Journal of Infectious Diseases* vol. 188 <https://academic.oup.com/jid/article/188/11/1630/862409> (2003).
55. Liu, D. X. *et al.* Ebola Virus Disease Features Hemophagocytic Lymphohistiocytosis/Macrophage Activation Syndrome in the Rhesus Macaque Model. *Journal of Infectious Diseases* **228**, 371–382 (2023).
56. Rogers, K. J. & Maury, W. The role of mononuclear phagocytes in Ebola virus infection. *Journal of Leukocyte Biology* vol. 104 717–727 Preprint at <https://doi.org/10.1002/JLB.4RI0518-183R> (2018).
57. Jin, H. *et al.* The VP35 protein of Ebola virus impairs dendritic cell maturation induced by virus and lipopolysaccharide. *Journal of General Virology* **91**, 352–361 (2010).

References

58. Lubaki, N. M. *et al.* The Lack of Maturation of Ebola Virus-Infected Dendritic Cells Results from the Cooperative Effect of at Least Two Viral Domains. *J Virol* **87**, 7471–7485 (2013).
59. Osvaldo, M. *et al.* Ebola Virus Exploits a Monocyte Differentiation Program To Promote Its Entry. *J Virol* **87**, 3801–3814 (2013).
60. McNab, F., Mayer-Barber, K., Sher, A., Wack, A. & O’Garra, A. Type I interferons in infectious disease. *Nat Rev Immunol* **15**, 87–103 (2015).
61. Yan, N. & Chen, Z. J. Intrinsic antiviral immunity. *Nat Immunol* **13**, 214–222 (2012).
62. Rottstegge, M. *et al.* Avatar Mice Underscore the Role of the T Cell-Dendritic Cell Crosstalk in Ebola Virus Disease and Reveal Mechanisms of Protection in Survivors. *J Virol* **96**, 1–15 (2022).
63. Barry, M. & Bleackley, R. C. Cytotoxic T lymphocytes: all roads lead to death. *Nat Rev Immunol* **2**, 401–409 (2002).
64. Kervevan, J. & Chakrabarti, L. A. Role of cd4⁺ T cells in the control of viral infections: Recent advances and open questions. *International Journal of Molecular Sciences* vol. 22 1–23 Preprint at <https://doi.org/10.3390/ijms22020523> (2021).
65. McElroy, A. K. *et al.* Human Ebola virus infection results in substantial immune activation. *Proc Natl Acad Sci U S A* **112**, 4719–4724 (2015).
66. Speranza, E. *et al.* T-Cell Receptor Diversity and the Control of T-Cell Homeostasis Mark Ebola Virus Disease Survival in Humans. *Journal of Infectious Diseases* **218**, S508–S518 (2018).
67. Ruibal, P. *et al.* Unique human immune signature of Ebola virus disease in Guinea. *Nature* **533**, 100–104 (2016).
68. Younan, P. *et al.* Ebola virus-mediated T-lymphocyte depletion is the result of an abortive infection. *PLoS Pathog* **15**, e1008068- (2019).
69. Iampietro, M., Amurri, L., Reynard, O. & Bukreyev, A. Interplay of Ebola Virus With Immune Cells Leading to Their Death by Diverse Mechanisms. *J Infect Dis* **228**, S582–S586 (2023).
70. Iampietro, M. *et al.* Ebola virus glycoprotein directly triggers T lymphocyte death despite of the lack of infection. *PLoS Pathog* **13**, e1006397- (2017).
71. Lu, L. L., Suscovich, T. J., Fortune, S. M. & Alter, G. Beyond binding: antibody effector functions in infectious diseases. *Nat Rev Immunol* **18**, 46–61 (2018).

References

72. Heath, W. R., Kato, Y., Steiner, T. M. & Caminschi, I. Antigen presentation by dendritic cells for B cell activation. *Curr Opin Immunol* **58**, 44–52 (2019).
73. Steinman, R. M. & Cohn, Z. A. IDENTIFICATION OF A NOVEL CELL TYPE IN PERIPHERAL LYMPHOID ORGANS OF MICE : I. MORPHOLOGY, QUANTITATION, TISSUE DISTRIBUTION. *Journal of Experimental Medicine* **137**, 1142–1162 (1973).
74. Cytlak, U. *et al.* Differential IRF8 Transcription Factor Requirement Defines Two Pathways of Dendritic Cell Development in Humans. *Immunity* **53**, 353-370.e8 (2020).
75. Segura, E. Human dendritic cell subsets: An updated view of their ontogeny and functional specialization. *Eur J Immunol* **52**, 1759–1767 (2022).
76. Nakano, H., Lyons-Cohen, M. R., Whitehead, G. S., Nakano, K. & Cook, D. N. Distinct functions of CXCR4, CCR2, and CX3CR1 direct dendritic cell precursors from the bone marrow to the lung. *J Leukoc Biol* **101**, 1143–1153 (2017).
77. Sichien, D., Lambrecht, B. N., Guilliams, M. & Scott, C. L. Development of conventional dendritic cells: from common bone marrow progenitors to multiple subsets in peripheral tissues. *Mucosal Immunol* **10**, 831–844 (2017).
78. Backer, R. A., Probst, H. C. & Clausen, B. E. Classical DC2 subsets and monocyte-derived DC: Delineating the developmental and functional relationship. *European Journal of Immunology* vol. 53 Preprint at <https://doi.org/10.1002/eji.202149548> (2023).
79. Waskow, C. *et al.* The receptor tyrosine kinase Flt3 is required for dendritic cell development in peripheral lymphoid tissues. *Nat Immunol* **9**, 676–683 (2008).
80. McKenna, H. J. *et al.* Mice lacking flt3 ligand have deficient hematopoiesis affecting hematopoietic progenitor cells, dendritic cells, and natural killer cells. *Blood* **95**, 3489–3497 (2000).
81. Bosteels, C. & Scott, C. L. Transcriptional regulation of DC fate specification. *Mol Immunol* **121**, 38–46 (2020).
82. Anderson, D. A., Dutertre, C.-A., Ginhoux, F. & Murphy, K. M. Genetic models of human and mouse dendritic cell development and function. *Nat Rev Immunol* **21**, 101–115 (2021).
83. Sulczewski, F. B. *et al.* Transitional dendritic cells are distinct from conventional DC2 precursors and mediate proinflammatory antiviral responses. *Nat Immunol* **24**, 1265–1280 (2023).
84. Goudot, C. *et al.* Aryl Hydrocarbon Receptor Controls Monocyte Differentiation into Dendritic Cells versus Macrophages. *Immunity* **47**, 582-596.e6 (2017).

References

85. Villar, J. & Segura, E. The More, the Merrier: DC3s Join the Human Dendritic Cell Family. *Immunity* vol. 53 233–235 Preprint at <https://doi.org/10.1016/j.immuni.2020.07.014> (2020).
86. Cabeza-Cabrerizo, M., Cardoso, A., Minutti, C. M., Pereira da Costa, M. & Reis Sousa, C. Dendritic Cells Revisited. *Annual Reviews of Immunology* **39**, 131–166 (2021).
87. Diao, J. *et al.* In Situ Replication of Immediate Dendritic Cell (DC) Precursors Contributes to Conventional DC Homeostasis in Lymphoid Tissue1. *The Journal of Immunology* **176**, 7196–7206 (2006).
88. Inaba, K. *et al.* Generation of large numbers of dendritic cells from mouse bone marrow cultures supplemented with granulocyte/macrophage colony-stimulating factor. *Journal of Experimental Medicine* **176**, 1693–1702 (1992).
89. Balan, S. *et al.* Large-Scale Human Dendritic Cell Differentiation Revealing Notch-Dependent Lineage Bifurcation and Heterogeneity. *Cell Rep* **24**, 1902-1915.e6 (2018).
90. Naik, S. H. *et al.* Cutting Edge: Generation of Splenic CD8 + and CD8 – Dendritic Cell Equivalents in Fms-Like Tyrosine Kinase 3 Ligand Bone Marrow Cultures . *The Journal of Immunology* **174**, 6592–6597 (2005).
91. Sadiq, B. A., Mantel, I. & Blander, J. M. A Comprehensive Experimental Guide to Studying Cross-Presentation in Dendritic Cells In Vitro. *Curr Protoc Immunol* **131**, (2020).
92. Ding, J. *et al.* Murine hepatoma treatment with mature dendritic cells stimulated by *Trichinella spiralis* excretory/secretory products. *Parasite* **27**, (2020).
93. Hou, L. *et al.* CD11c regulates neutrophil maturation. *Blood Adv* **7**, 1312–1325 (2023).
94. Lu, L. *et al.* Differential expression of CD11c defines two types of tissue-resident macrophages with different origins in steady-state salivary glands. *Sci Rep* **12**, 931 (2022).
95. Gurka, S., Hartung, E., Becker, M. & Kroczeck, R. A. Mouse Conventional Dendritic Cells Can be Universally Classified Based on the Mutually Exclusive Expression of XCR1 and SIRP α . *Front Immunol* **6**, (2015).
96. Scott, C. L. *et al.* The transcription factor Zeb2 regulates development of conventional and plasmacytoid DCs by repressing Id2. *Journal of Experimental Medicine* **213**, 897–911 (2016).
97. Heger, L. *et al.* XCR1 expression distinguishes human conventional dendritic cell type 1 with full effector functions from their immediate precursors. *Proceedings of the National Academy of Sciences* **120**, e2300343120 (2023).

References

98. Williams, M. *et al.* Unsupervised High-Dimensional Analysis Aligns Dendritic Cells across Tissues and Species. *Immunity* **45**, 669–684 (2016).
99. Hongo, D. *et al.* Identification of Two Subsets of Murine DC1 Dendritic Cells That Differ by Surface Phenotype, Gene Expression, and Function. *Front Immunol* **12**, (2021).
100. Collin, M. & Bigley, V. Human dendritic cell subsets: an update. *Immunology* **154**, 3–20 (2018).
101. Reizis, B. Plasmacytoid Dendritic Cells: Development, Regulation, and Function. *Immunity* vol. 50 37–50 Preprint at <https://doi.org/10.1016/j.immuni.2018.12.027> (2019).
102. Schlitzer, A. *et al.* Identification of cDC1- and cDC2-committed DC progenitors reveals early lineage priming at the common DC progenitor stage in the bone marrow. *Nat Immunol* **16**, 718–728 (2015).
103. Keller, H. R. *et al.* The molecular basis and cellular effects of distinct CD103 expression on CD4 and CD8 T cells. *Cellular and Molecular Life Sciences* **78**, 5789–5805 (2021).
104. Chen, J. *et al.* The role of CD11b in phagocytosis and dendritic cell development. *Immunol Lett* **120**, 42–48 (2008).
105. Wu, J., Wu, H., An, J., Ballantyne, C. M. & Cyster, J. G. Critical role of integrin CD11c in splenic dendritic cell capture of missing-self CD47 cells to induce adaptive immunity. *Proceedings of the National Academy of Sciences* **115**, 6786–6791 (2018).
106. Sharygin, D., Koniaris, L. G., Wells, C., Zimmers, T. A. & Hamidi, T. Role of CD14 in human disease. *Immunology* **169**, 260–270 (2023).
107. Zhang, X., Yu, C., Liu, J.-Q. & Bai, X.-F. Dendritic cell expression of CD24 contributes to optimal priming of T lymphocytes in lymph nodes. *Front Immunol* **14**, (2023).
108. Breton, G., Lee, J., Liu, K. & Nussenzweig, M. C. Defining human dendritic cell progenitors by multiparametric flow cytometry. *Nat Protoc* **10**, 1407–1422 (2015).
109. Nimmerjahn, F. & Ravetch, J. V. Fcγ receptors as regulators of immune responses. *Nat Rev Immunol* **8**, 34–47 (2008).
110. Lin, H.-H. *et al.* The macrophage F4/80 receptor is required for the induction of antigen-specific efferent regulatory T cells in peripheral tolerance. *Journal of Experimental Medicine* **201**, 1615–1625 (2005).
111. Li, Y. *et al.* Occurrences and Functions of Ly6Chi and Ly6Clo Macrophages in Health and Disease. *Front Immunol* **13**, (2022).
112. Rock, K. L., Reits, E. & Neefjes, J. Present Yourself! By MHC Class I and MHC Class II Molecules. *Trends Immunol* **37**, 724–737 (2016).

References

113. Blasius, A. L. & Colonna, M. Sampling and signaling in plasmacytoid dendritic cells: the potential roles of Siglec-H. *Trends Immunol* **27**, 255–260 (2006).
114. Barclay, A. N. & Van Den Berg, T. K. The interaction between signal regulatory protein alpha (SIRP α) and CD47: Structure, function, and therapeutic target. *Annual Review of Immunology* vol. 32 25–50 Preprint at <https://doi.org/10.1146/annurev-immunol-032713-120142> (2014).
115. Kroczek, R. & Henn, V. The role of XCR1 and its ligand XCL1 in antigen cross-presentation by murine and human dendritic cells. vol. 3 Preprint at <https://doi.org/10.3389/fimmu.2012.00014> (2012).
116. Li, D. & Wu, M. Pattern recognition receptors in health and diseases. *Signal Transduct Target Ther* **6**, 291 (2021).
117. Bosteels, C. *et al.* Inflammatory Type 2 cDCs Acquire Features of cDC1s and Macrophages to Orchestrate Immunity to Respiratory Virus Infection. *Immunity* **52**, 1039-1056.e9 (2020).
118. Broeke, T. ten, Wubbolts, R. & Stoorvogel, W. MHC class II antigen presentation by dendritic cells regulated through endosomal sorting. *Cold Spring Harb Perspect Biol* **5**, (2013).
119. Muntjewerff, E. M., Meesters, L. D. & van den Bogaart, G. Antigen Cross-Presentation by Macrophages. *Front Immunol* **11**, 1–12 (2020).
120. Embgenbroich, M. & Burgdorf, S. Current concepts of antigen cross-presentation. *Front Immunol* **9**, (2018).
121. Curtsinger, J. M. & Mescher, M. F. Inflammatory cytokines as a third signal for T cell activation. *Curr Opin Immunol* **22**, 333–340 (2010).
122. Cibrián, D. & Sánchez-Madrid, F. CD69: from activation marker to metabolic gatekeeper. *European Journal of Immunology* vol. 47 946–953 Preprint at <https://doi.org/10.1002/eji.201646837> (2017).
123. Lewis, D. A. & Ly, T. Cell Cycle Entry Control in Naïve and Memory CD8⁺ T Cells. *Front Cell Dev Biol* **9**, (2021).
124. Bhat, P., Leggatt, G., Waterhouse, N. & Frazer, I. H. Interferon- γ derived from cytotoxic lymphocytes directly enhances their motility and cytotoxicity. *Cell Death Dis* **8**, e2836–e2836 (2017).
125. Zhan, Y., Carrington, E. M., Zhang, Y., Heinzl, S. & Lew, A. M. Life and Death of Activated T Cells: How Are They Different from Naïve T Cells? *Front Immunol* **8**, (2017).

References

126. Brusko, T. M. *et al.* Influence of Membrane CD25 Stability on T Lymphocyte Activity: Implications for Immunoregulation. *PLoS One* **4**, e7980- (2009).
127. Shah, K., Al-Haidari, A., Sun, J. & Kazi, J. U. T cell receptor (TCR) signaling in health and disease. *Signal Transduct Target Ther* **6**, 412 (2021).
128. Mørch, A. M., Bálint, Š., Santos, A. M., Davis, S. J. & Dustin, M. L. Coreceptors and TCR Signaling – the Strong and the Weak of It. *Front Cell Dev Biol* **8**, (2020).
129. Baaten, B. J. G., Li, C.-R. & Bradley, L. M. Multifaceted regulation of T cells by CD44. *Commun Integr Biol* **3**, 508–512 (2010).
130. Mohammed, R. N. *et al.* L-selectin Is Essential for Delivery of Activated CD8⁺ T Cells to Virus-Infected Organs for Protective Immunity. *Cell Rep* **14**, 760–771 (2016).
131. Ruhland, M. K. *et al.* Visualizing Synaptic Transfer of Tumor Antigens among Dendritic Cells. *Cancer Cell* **37**, 786-799.e5 (2020).
132. Buzas, E. I. The roles of extracellular vesicles in the immune system. *Nature Reviews Immunology* vol. 23 236–250 Preprint at <https://doi.org/10.1038/s41577-022-00763-8> (2023).
133. Pleet, M. L. *et al.* Ebola VP40 in exosomes can cause immune cell dysfunction. *Front Microbiol* **7**, (2016).
134. Pleet, M. L. *et al.* Ebola Virus VP40 Modulates Cell Cycle and Biogenesis of Extracellular Vesicles. in *Journal of Infectious Diseases* vol. 218 S365–S387 (Oxford University Press, 2018).
135. Clarke, S. Rm. *et al.* Characterization of the ovalbumin-specific TCR transgenic line OT-I: MHC elements for positive and negative selection. *Immunol Cell Biol* **78**, 110–117 (2000).
136. Barnden, M. J., Allison, J., Heath, W. R. & Carbone, F. R. Defective TCR expression in transgenic mice constructed using cDNA-based α - and β -chain genes under the control of heterologous regulatory elements. *Immunol Cell Biol* **76**, 34–40 (1998).
137. Olal, C. A. Dendritic cell- and T cell-based Immune Therapies against Ebola Virus Infection. (University of Lübeck, Lübeck, 2023).
138. Carette, J. E. *et al.* Ebola virus entry requires the cholesterol transporter Niemann-Pick C1. *Nature* **477**, 340–343 (2011).
139. Dersh, D., Yewdell, J. W. & Wei, J. A SIINFEKL-based system to measure MHC class I antigen presentation efficiency and kinetics. in *Methods in Molecular Biology* vol. 1988 109–122 (Humana Press Inc., 2019).

References

140. Liao, L. E. *et al.* Quantification of Ebola virus replication kinetics in vitro. *PLoS Comput Biol* **16**, 1–15 (2020).
141. Honda, K. *et al.* Selective contribution of IFN- α/β signaling to the maturation of dendritic cells induced by double-stranded RNA or viral infection. *Proceedings of the National Academy of Sciences* **100**, 10872–10877 (2003).
142. Le Bon, A. *et al.* Cross-priming of CD8⁺ T cells stimulated by virus-induced type I interferon. *Nat Immunol* **4**, 1009–1015 (2003).
143. Ali, S. *et al.* Sources of type I interferons in infectious immunity: Plasmacytoid dendritic cells not always in the driver's seat. *Frontiers in Immunology* vol. 10 Preprint at <https://doi.org/10.3389/fimmu.2019.00778> (2019).
144. Na, Y. R., Jung, D., Gu, G. J. & Seok, S. H. GM-CSF Grown Bone Marrow Derived Cells Are Composed of Phenotypically Different Dendritic Cells and Macrophages. *Mol Cells* **39**, 734–741 (2016).
145. Xu, Y., Zhan, Y., Lew, A. M., Naik, S. H. & Kershaw, M. H. Differential Development of Murine Dendritic Cells by GM-CSF versus Flt3 Ligand Has Implications for Inflammation and Trafficking. *The Journal of Immunology* **179**, 7577–7584 (2007).
146. Zhang, W. *et al.* Bone marrow-derived inflammatory and steady state DCs are different in both functions and survival. *Cell Immunol* **331**, 100–109 (2018).
147. Kirkling, M. E. *et al.* Notch Signaling Facilitates In Vitro Generation of Cross-Presenting Classical Dendritic Cells. *Cell Rep* **23**, 3658-3672.e6 (2018).
148. Lewis, K. L. *et al.* Notch2 Receptor Signaling Controls Functional Differentiation of Dendritic Cells in the Spleen and Intestine. *Immunity* **35**, 780–791 (2011).
149. Lu, L., Tanaka, Y., Ishii, N., Sasano, T. & Sugawara, S. CD103⁺CD11b⁻ salivary gland dendritic cells have antigen cross-presenting capacity. *Eur J Immunol* **47**, 305–313 (2017).
150. Langlet, C. *et al.* CD64 Expression Distinguishes Monocyte-Derived and Conventional Dendritic Cells and Reveals Their Distinct Role during Intramuscular Immunization. *The Journal of Immunology* **188**, 1751–1760 (2012).
151. Sun, L. *et al.* GM-CSF Quantity Has a Selective Effect on Granulocytic vs. Monocytic Myeloid Development and Function. *Front Immunol* **9**, (2018).
152. Musumeci, A., Lutz, K., Winheim, E. & Krug, A. B. What Makes a pDC: Recent Advances in Understanding Plasmacytoid DC Development and Heterogeneity. *Front Immunol* **10**, (2019).

References

153. Bohnen, C. *et al.* Vaccination with recombinant modified vaccinia virus Ankara prevents the onset of intestinal allergy in mice. *Allergy* **68**, 1021–1028 (2013).
154. El-Gogo, S. *et al.* Recombinant murine gammaherpesvirus 68 (MHV-68) as challenge virus to test efficacy of vaccination against chronic virus infections in the mouse model. *Vaccine* **25**, 3934–3945 (2007).
155. Garulli, B., Di Mario, G., Sciaraffia, E., Kawaoka, Y. & Castrucci, M. R. Immunogenicity of a recombinant influenza virus bearing both the CD4⁺ and CD8⁺ T cell epitopes of ovalbumin. *J Biomed Biotechnol* **2011**, (2011).
156. Marchingo, J. M. *et al.* Antigen affinity, costimulation, and cytokine inputs sum linearly to amplify T cell expansion. *Science (1979)* **346**, 1123–1127 (2014).
157. Kelly, E., Won, A., Refaeli, Y. & Van Parijs, L. IL-2 and Related Cytokines Can Promote T Cell Survival by Activating AKT1. *The Journal of Immunology* **168**, 597–603 (2002).
158. Silvin, A. *et al.* Constitutive resistance to viral infection in human CD141⁺ dendritic cells. *Sci Immunol* **2**, (2017).
159. Ribeiro, C. M. S. *et al.* Receptor usage dictates HIV-1 restriction by human TRIM5 α in dendritic cell subsets. *Nature* **540**, 448–452 (2016).
160. Leung, L. W., Martinez, O., Reynard, O., Volchkov, V. E. & Basler, C. F. Ebola virus failure to stimulate plasmacytoid dendritic cell interferon responses correlates with impaired cellular entry. *Journal of Infectious Diseases* **204**, (2011).
161. Lee, H. K., Lund, J. M., Ramanathan, B., Mizushima, N. & Iwasaki, A. Autophagy-Dependent Viral Recognition by Plasmacytoid Dendritic Cells. *Science (1979)* **315**, 1398–1401 (2007).
162. Hornung, V. *et al.* Replication-Dependent Potent IFN-Induction in Human Plasmacytoid Dendritic Cells by a Single-Stranded RNA Virus 1. *The Journal of Immunology* vol. 173 <http://journals.aai.org/jimmunol/article-pdf/173/10/5935/1185252/5935.pdf> (2004).
163. Jin, P. *et al.* Molecular signatures of maturing dendritic cells: Implications for testing the quality of dendritic cell therapies. *J Transl Med* **8**, (2010).
164. Yun, T. J. *et al.* Human plasmacytoid dendritic cells mount a distinct antiviral response to virus-infected cells. *Sci Immunol* **6**, (2021).
165. Lund, J., Sato, A., Akira, S., Medzhitov, R. & Iwasaki, A. Toll-like Receptor 9–mediated Recognition of Herpes Simplex Virus-2 by Plasmacytoid Dendritic Cells. *Journal of Experimental Medicine* **198**, 513–520 (2003).

References

166. Dreux, M. *et al.* Short-Range Exosomal Transfer of Viral RNA from Infected Cells to Plasmacytoid Dendritic Cells Triggers Innate Immunity. *Cell Host Microbe* **12**, 558–570 (2012).
167. Mahanty, S. *et al.* Cutting Edge: Impairment of Dendritic Cells and Adaptive Immunity by Ebola and Lassa Viruses. *The Journal of Immunology* **170**, 2797–2801 (2003).
168. Gamales Magalhaes Sebastian Amigorena, J., Andres Alloatti, addresses, Kotsias, F., Gamales Magalhaes, J. & Amigorena, S. *Dendritic Cell Maturation and Cross-Presentation: Timing Matters!* (2016).
169. Nan, F. L. *et al.* Newcastle Disease Virus Inhibits the Proliferation of T Cells Induced by Dendritic Cells In Vitro and In Vivo. *Front Immunol* **11**, 1–10 (2021).
170. Gurung, S., Perocheau, D., Touramanidou, L. & Baruteau, J. The exosome journey: from biogenesis to uptake and intracellular signalling. *Cell Communication and Signaling* vol. 19 Preprint at <https://doi.org/10.1186/s12964-021-00730-1> (2021).
171. Abels, E. R. & Breakefield, X. O. Introduction to Extracellular Vesicles: Biogenesis, RNA Cargo Selection, Content, Release, and Uptake. *Cellular and Molecular Neurobiology* vol. 36 301–312 Preprint at <https://doi.org/10.1007/s10571-016-0366-z> (2016).
172. Fu, C. *et al.* Plasmacytoid dendritic cells cross-prime naive CD8 T cells by transferring antigen to conventional dendritic cells through exosomes. *Proc Natl Acad Sci U S A* **117**, 23730–23741 (2020).
173. Tkach, M. *et al.* Qualitative differences in T-cell activation by dendritic cell-derived extracellular vesicle subtypes. *EMBO J* **36**, 3012–3028–3028 (2017).
174. Liangsupree, T., Multia, E. & Riekkola, M.-L. Modern isolation and separation techniques for extracellular vesicles. *J Chromatogr A* **1636**, 461773 (2021).
175. Wakim, L. M. & Bevan, M. J. Cross-dressed dendritic cells drive memory CD8⁺ T-cell activation after viral infection. *Nature* **471**, 629–632 (2011).
176. McNally, A., Hill, G. R., Sparwasser, T., Thomas, R. & Steptoe, R. J. CD4⁺CD25⁺ regulatory T cells control CD8⁺ T-cell effector differentiation by modulating IL-2 homeostasis. *Proceedings of the National Academy of Sciences* **108**, 7529–7534 (2011).
177. Malek, T. R. The Biology of Interleukin-2. *Annu Rev Immunol* **26**, 453–479 (2008).
178. Dudziak, D. *et al.* Differential antigen processing by dendritic cell subsets in vivo. *Science (1979)* **315**, 107–111 (2007).
179. Ohara, R. A. & Murphy, K. M. The evolving biology of cross-presentation. *Semin Immunol* **66**, 101711 (2023).

References

180. Mauvais, F.-X. & van Endert, P. Cross-presentation by the others. *Semin Immunol* **67**, 101764 (2023).
181. Pulendran, B., Tang, H. & Denning, T. L. Division of labor, plasticity, and crosstalk between dendritic cell subsets. *Curr Opin Immunol* **20**, 61–67 (2008).

List of Figures

Figure 1	Outbreaks caused by viruses within the <i>Orthoebolavirus</i> genus since 1976.	4
Figure 2	Ebola virus particle and genome organization.	7
Figure 3	Ebola virus life cycle.	8
Figure 4	Human dendritic cell ontogeny.	14
Figure 5	Murine dendritic cell morphology.	15
Figure 6	Dendritic cell – CD8 T-cell interaction.	20
Figure 7	The role of EVs in antigen-presentation.	23
Figure 8	Schematic showing the genome organization of EBOV-OVA.	24
Figure 9	Differentiation of murine DCs from bone marrow progenitors.	47
Figure 10	Extended characterization of the mixed DC culture.	49
Figure 11	EBOV-OVA infection of the mixed DC culture.	53
Figure 12	DC activation upon EBOV-OVA infection.	56
Figure 13	DC activation upon sOVA and LPS stimulation.	58
Figure 14	T-cell proliferation and activation induced by sOVA pulsed DCs.	60
Figure 15	T-cell proliferation and activation by EBOV-OVA infected DCs.	62
Figure 16	Isolation of cell debris and extracellular vesicles (EVs) from Vero E6 cells.	65
Figure 17	Activation of DC after stimulation with cell debris or EVs.	67
Figure 18	T-cell proliferation after cross-presentation of antigens from cell debris or EVs. .	70
Figure 19	Cross-presentation and activation of T-cell proliferation by cDC1 and cDC2.	71
Figure 20	Effect of EBOV infection on T-cell proliferation and activation via cross-presentation of cell debris.	73
Figure 21	T-cell proliferation and activation by cDC2:cDC1 co-cultures of different ratio. .	75
Figure 22	The role of cDCs in T-cell activation in EBOV infections.	88

List of Tables

Table 1	Species of the <i>Orthoebolavirus</i> genus.....	3
Table 2	Relevant murine DC markers and their functions	16
Table 3	Relevant T-cell markers and their functions.....	21
Table 4	List of mouse strains.....	26
Table 5	List of reagents	27
Table 6	List of consumables.....	28
Table 7	Recipes for buffers and media.....	28
Table 8	Dendritic cell antibody panel #1 (flow cytometry)	29
Table 9	Dendritic cell antibody panel #2 (extended) (flow cytometry)	29
Table 10	T-cell antibody panel (flow cytometry).....	30
Table 11	Antibodies for immunofocus assay	30
Table 12	Antibodies for western blot	30
Table 13	List of Kits.....	30
Table 14	List of machines and equipment.....	31
Table 15	List of computer programs and softwares	32
Table 16	EBOV-OVA infection rate in different DC subsets under various conditions.	53
Table 17	Cell viability and infection rate in mock infected and EBOV-OVA infected DC cultures (MOI 3) and EBOV-OVA infection rate in different DC subsets 1-3 days post infection (dpi).	54
Table 18	EBOV-OVA titer in samples throughout the EV isolation procedure.	66

List of Supplementary Data

Supplementary Figure 1 Expression of OVA in EBOV-OVA infected cells. 106

Supplementary Figure 2 DC activation by UV-inactivated EBOV-OVA..... 106

Supplementary Figure 3 Optimization of DC-T cell co-culture time and DC/T cell ratio.. 107

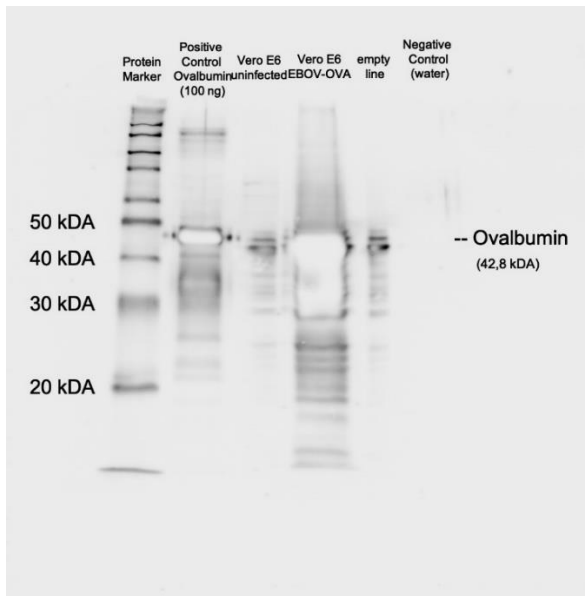
Supplementary Figure 4 T-cell activation by cell debris without DCs..... 107

Supplementary Figure 5 Cytokines in supernatants of DC-T cell co-cultures stimulated with cell debris..... 108

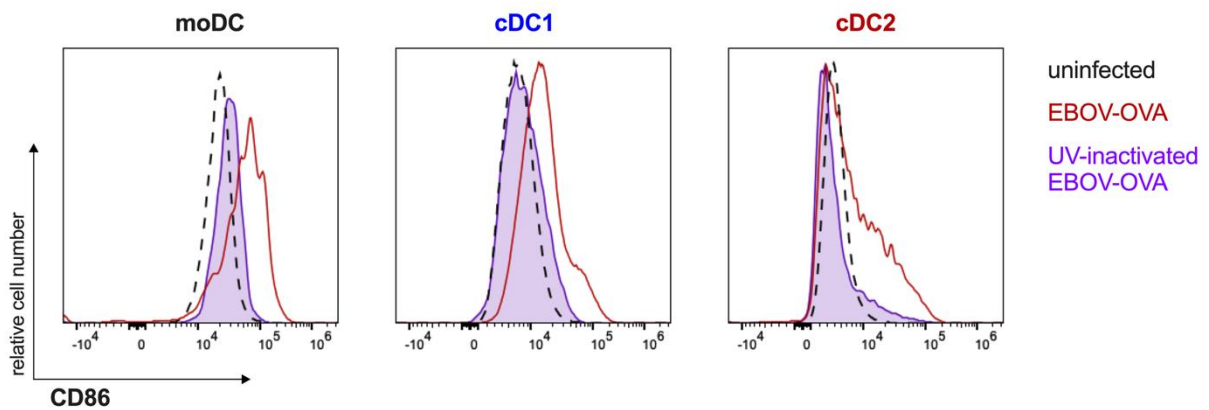
Supplementary Figure 6 Cytokines in supernatants of cDC2/cDC1/T-cell co-cultures infected with EBOV-OVA. 109

Supplementary Table 1 Parameters of T-cell proliferation induced by uninfected DCs or wt EBOV-infected DCs..... 107

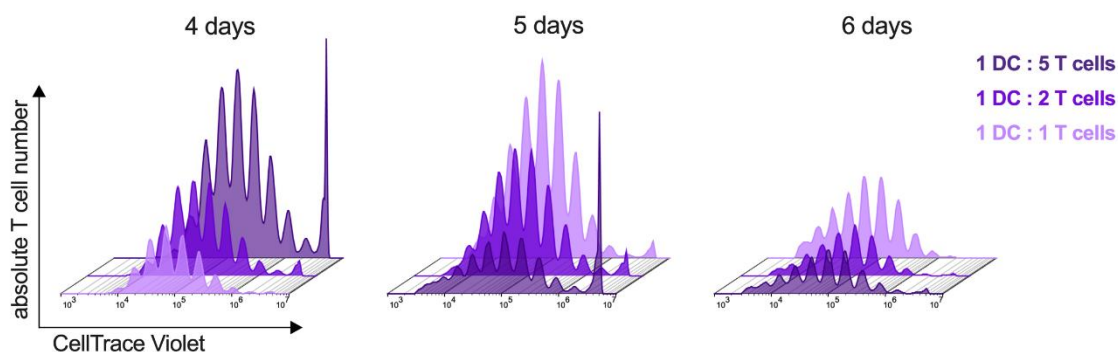
Appendix



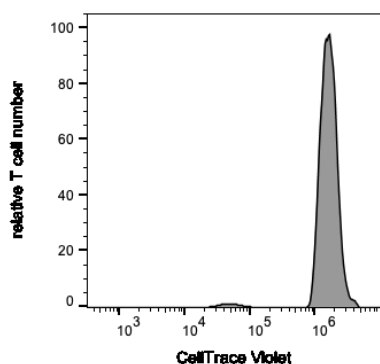
Supplementary Figure 1 Expression of OVA in EBOV-OVA infected cells. Vero E6 cells were infected with EBOV-OVA for 7 days or left uninfected. Presence of OVA (42,8 kDA) was determined by Western Blot analysis. From left to right: positive control (OVA, 100 ng), uninfected cells, EBOV-OVA infected cells, empty line, water (negative control).



Supplementary Figure 2 DC activation by UV-inactivated EBOV-OVA. Mixed DC cultures were infected with EBOV-OVA (red), UV-inactivated EBOV-OVA (purple) or left uninfected. Histograms show CD86 expression in moDCs, cDC1 and cDC2 (n=1). The DC activation upon EBOV-OVA seems to be replication dependent.



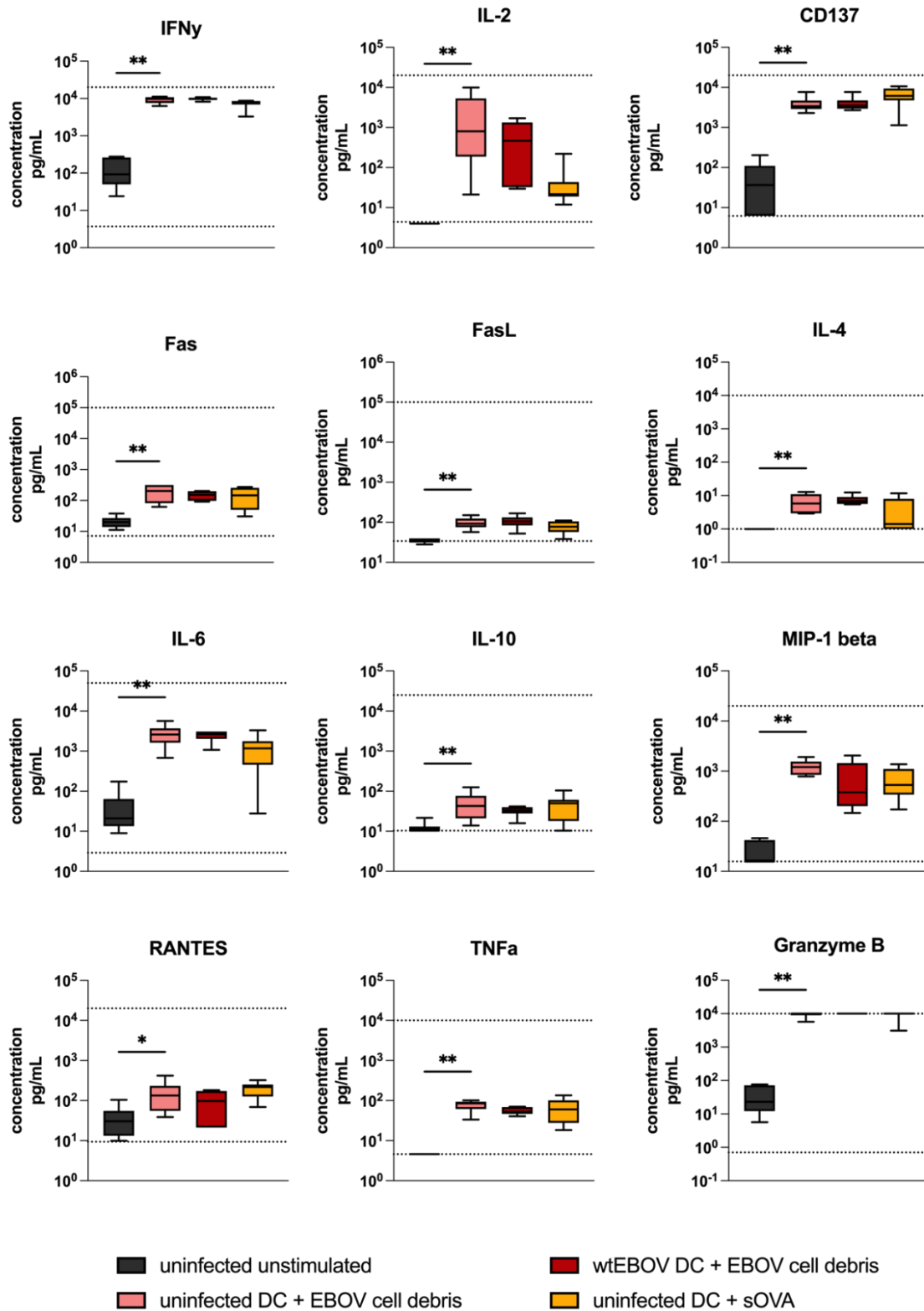
Supplementary Figure 3 Optimization of DC-T cell co-culture time and DC/T cell ratio. DCs were stimulated with 100 µg/mL sOVA and 100 ng/mL LPS and subsequently co-cultured with CellTrace Violet stained OT-1 CD8 T cells in different DC:T-cell ratios: 1:1, 1:2, 1:5 for 4-6 days. CD8 T-cell proliferation was analyzed as reduction of CellTrace Violet signal intensity upon cell division.



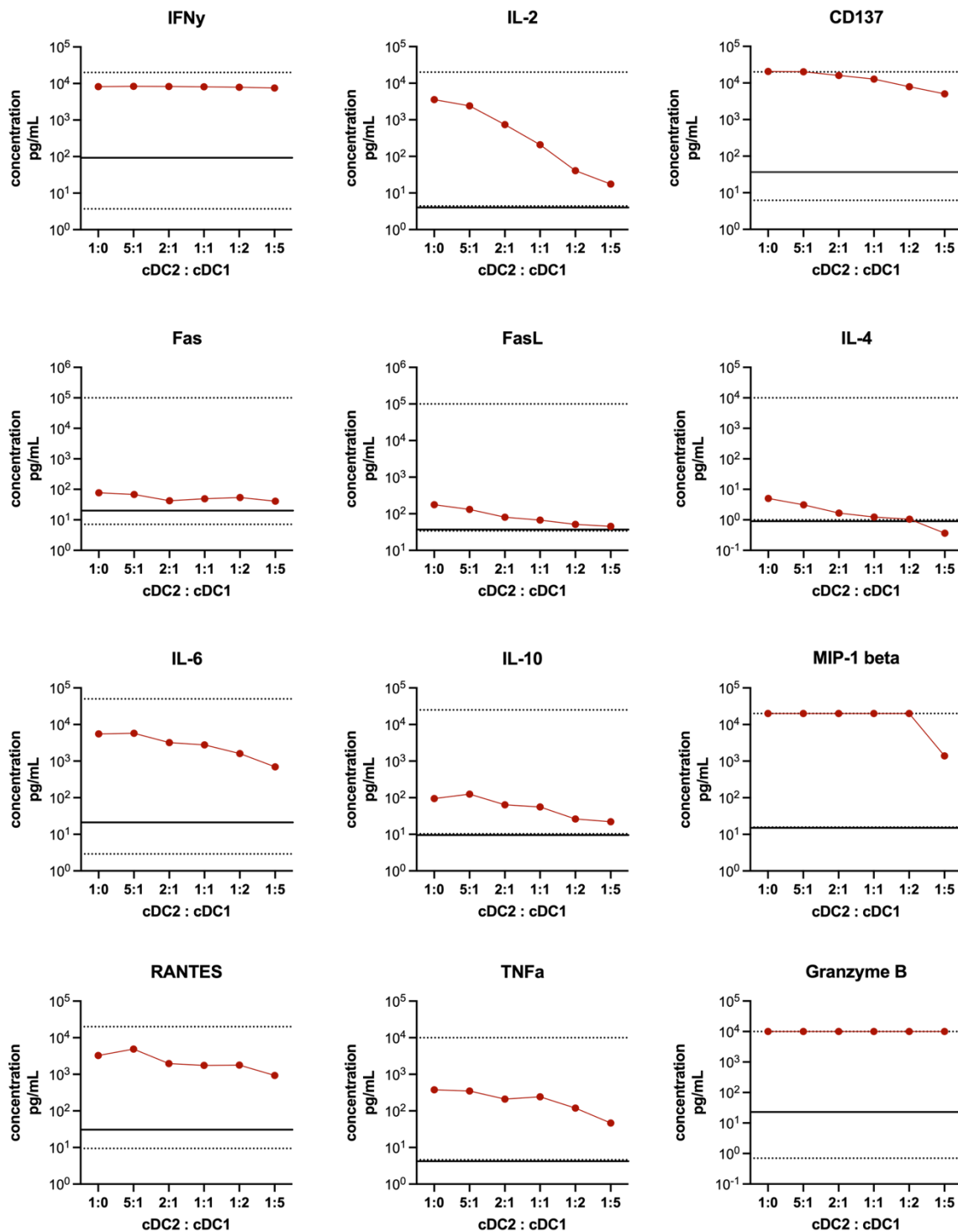
Supplementary Figure 4 T-cell activation by cell debris without DCs. Cell debris was harvested from EBOV-OVA infected Vero E6 and added to CellTrace Violet stained OT-1 CD8 T cells for 4 days. The co-culture did not include any DCs. T cells did not proliferate.

Supplementary Table 1 Parameters of T-cell proliferation induced by uninfected DCs or wt EBOV-infected DCs.

	Uninfected DCs		wt EBOV-infected DCs	
	% divided T cells	Absolute T-cell number	% divided T cells	Absolute T-cell number
#1	31.6	27040	63.45	26168
#2	51.3	15532	71.45	25937
#3	7.8	16642	50.7	44377
#4	7.6	16604	43.7	16562
#5	34.1	761	43.4	6220
#6	48.1	5743	58.3	4923



Supplementary Figure 5 Cytokines in supernatants of DC-T cell co-cultures stimulated with cell debris. DCs were infected with wt EBOV or left uninfected. 24 hours post infection DCs were stimulated with cell debris from EBOV-OVA infected Vero E6 (uninfected DC: pink, wt EBOV infected DCs: red) or left unstimulated (black). Stimulation of uninfected DCs with sOVA served as positive control (orange). Depicted are concentrations (in pg/mL) of different cytokines in each condition (n=6). Dotted lines mark detection range.



Supplementary Figure 6 Cytokines in supernatants of cDC2/cDC1/T-cell co-cultures infected with EBOV-OVA. cDC1 and cDC2 were sorted from the mixed DC culture. cDC2 were infected with EBOV-OVA (MOI 3) and then co-cultured with cDC1 at different ratios. 24 hours post-infection CellTrace Violet stained OT-1 CD8 T cells were added to the co-culture. The co-culture was incubated for 4 days. Depicted are the concentrations (in pg/mL) of different cytokines in the different ratios of cDC2/cDC1 co-cultures (n=1). Black line reflects negative control (unstimulated, uninfected, mixed DCs co-cultured with T cells). Dotted lines mark detection range.

Publication

Niemetz, L. *et al.* Ebola virus infection of Flt3-dependent, conventional dendritic cells and antigen cross-presentation leads to high levels of T-cell activation. *Journal of Infectious Diseases* (submitted May 2024)

Ich versichere, dass dieses gebundene Exemplar der Dissertation und das in elektronischer Form eingereichte Dissertationsexemplar (über den Docata-Upload) und das bei der Fakultät (zuständiges Studienbüro) zur Archivierung eingereichte gedruckte gebundene Exemplar der Dissertationsschrift identisch sind.

I, the undersigned, declare that this bound copy of the dissertation and the dissertation submitted in electronic form (via the Docata upload) and the printed bound copy of the dissertation submitted to the faculty (responsible Academic Office) for archiving are identical.

Hamburg, den 16.05.2024

